$5

QEX

INCLUDING: COMMUNICATIONS QUARTERLY

Forum for Communications Experimenters

July/August 2003
Issue No. 219

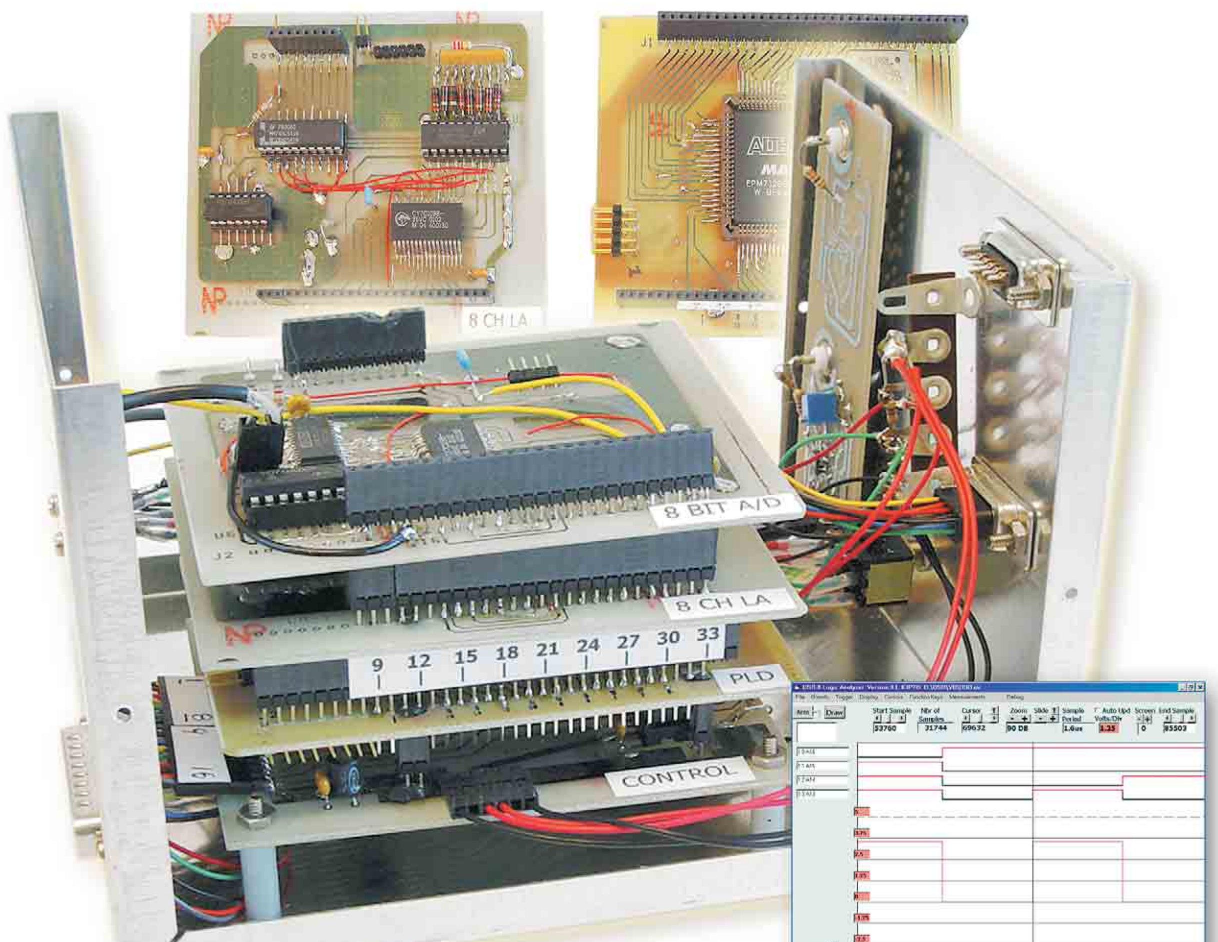

K3PTO's Digital Storage Scope *and* Logic Analyzer

ARRL The national association for AMATEUR RADIO
225 Main Street
Newington, CT USA 06111-1494

INCLUDING: COMMUNICATIONS QUARTERLY

QEX (ISSN: 0886-8093) is published bimonthly in January, March, May, July, September, and November by the American Radio Relay League, 225 Main Street, Newington CT 06111-1494. Periodicals postage paid at Hartford, CT and at additional mailing offices.

POSTMASTER: Send address changes to: QEX, 225 Main St, Newington, CT 06111-1494
Issue No 219

Offices
225 Main St, Newington, CT 06111-1494 USA
Telephone: 860-594-0200
Telex: 650215-5052 MCI
Fax: 860-594-0259 (24 hour direct line)
e-mail: **qex@arrl.org**

Subscription rate for 6 issues:

In the US: ARRL Member $24, nonmember $36;

US by First Class Mail: ARRL member $37, nonmember $49;

Elsewhere by Surface Mail (4-8 week delivery): ARRL member $31, nonmember $43;

Canada by Airmail: ARRL member $40, nonmember $52;

Elsewhere by Airmail: ARRL member $59, nonmember $71.

Members are asked to include their membership control number or a label from their *QST* when applying.

In order to ensure prompt delivery, we ask that you periodically check the address information on your mailing label. If you find any inaccuracies, please contact the Circulation Department immediately. Thank you for your assistance.

About the Cover

Larry Cicchinelli, K3PTD, offers a versatile test instrument. The article begins on p 13.

Features

Columns

July/Aug 2003 *QEX* Advertising Index

Empirical Outlook

Revenge of the Leptons

Hey, here's a ripper of an idea. Let's put radio transceivers on the power lines every few km and send lots of data over them. We think we can get all those electrons moving in the right direction at the right time over what looks like a rather high-impedance transmission line about 30 feet above ground. Oh, by the way, all that Part-15 stuff about not impressing RF onto the power grid—we might have to change it. We may not have known what we were thinking before.

Yes, we realize it's going to cause interference and we're not quite sure how to get round all those nasty transformers, the arcing, lightning, geomagnetic storms, Amateur Radio transmitters and the like. But gee whiz, that sure seems neat and it sure would be good to doubly exploit all that copper...

Does that sound more than a little touched? Drill down to the technical details and you'll discover just what a horror show it is. Try to fight it and you'll find yourself toe-to-toe with some big money, some of which has apparently made its impression on Michael Powell and your FCC.

Evidently, one argument advanced in support of Broadband over Power Line or BPL is that the necessary infrastructure already exists—the power lines—but that's not quite right. You still need to fit those transceivers every mile or so to make it work. That's because the transmission lines are "lossy." They're lossy partly because they radiate. They radiate because they weren't designed for RF in the first place. That's bad news for radio operators.

Even a cursory examination reveals the scheme to be financially flawed. A coaxial cable would carry much more data than a power line, more reliably and without interference. Were you to buy hundreds of miles of coax, you might pay a couple pennies per foot. Compare its cost and reliability per mile to that of even a very simple data transceiver and you will see what we mean.

Wireless Internet service providers are already exploiting vast microwave spectrum for broadband connections. Installed cost per mile beats coax in many cases, and it reaches remote areas. Is it really necessary to saturate the power grid with data, too, and risk destroying the rest of our bands? The answer is certainly no!

We say that much of the data being passed these days belong in a different public utility: the sewer. Regulators should concern themselves with *what* is being communicated rather than *how much*. Kill the spam-and-scam fiasco before it's too late!

Another of the second thousand points of light is still being pursued virulently by your would-be technological leaders: hydrogen fuel cells. Proponents say that the world has lots of hydrogen and we should make use of it. The trouble is that most of it is married to its cousins: oxygen, nitrogen and carbon. Separating them to get H_2 takes energy. Can you recover as much energy burning H_2 as you invested getting it?

Well, only just, and that makes the efficiency of the process quite low; but don't try to get your H_2 from H_2O because you will definitely spend more than you get in return. You're better off making electricity with your starting energy. Perhaps there's some other stuff to put into your fuel cell.

In This Issue

Bob Larkin, W7PUA, Larry Liljeqvist, W7SZ, and Ernest P. Manly, W7LHL, bring us a detailed look at tropospheric scattering on the microwave bands. Larry Cicchinelli, K3PTO, brings us a PC-based digital storage oscilloscope that functions as a logic analyzer, too.

John Gibbs, KC7YXD, starts a three-part series on D-STAR, the new JARL system for digital voice, data and video over VHF/UHF. Check it out. Chris Trask, N7ZWY, returns to *QEX* with the first part of two on active-loop antennas for HF reception. Grant Bingeman, KM5KG, discusses the use of 45° networks in impedance matching. I contribute a piece of what I learned about energy transformation in capacitors. Some of the answers may surprise you. In *RF*, Zack Lau, W1VT, details a homebrew 2-meter transmitter—73, *Doug Smith, KF6DX,* **kf6dx@arrl.org**.

Microwave Propagation in the Upper Troposphere

Amateur microwave work need not be restricted to operation from hilltop locations. Let's explore the use of scattering in the upper regions of the troposphere, which offers the possibility of communications over highly obstructed paths.

By Bob Larkin, W7PUA; Larry Liljequist, W7SZ, and Ernest P. Manly, W7LHL

The selection of propagation modes for amateur microwave stations is often progressive. Most of us start with simple equipment and the contacts are usually by line-of-sight propagation. Longer distances are then accomplished by going to high locations. As equipment gets better, the use of various objects for reflections and scattering becomes a possibility. Hills, mountains, water tanks are attractive, since they are generally available at any time. Aircraft are also attractive reflectors when they are at high altitudes.[1] Scatter from raindrops can be effective and many stations have used this propagation mode.[2]

[1]Notes appear on page 11.

Bob Larkin, W7PUA
2982 NW Acacia Pl
Corvallis, OR 97330
boblark@proaxis.com

Larry Liljequist, W7SZ
2804 SE 347th Ave
Washougal, WA 98671
LLL@pacifier.com

Ernest P. Manly, W7LHL
PO Box 1307
Graham, WA 98338-1307
epmanly@ispwest.com

Better-equipped stations are able to work others beyond their horizon by use of the propagation mode called *tropospheric scattering*. This mode occurs to some degree at all times. It involves reflection in multiple directions (scattering) of the microwave signal using irregularities in the material of the troposphere. Most definitions of this mode do not make a distinction of the particular material. This allows inclusion of variations in the water content, water or ice particles, dust, insects or possibly other materials. This scattering is strongest in the lower portions of the troposphere, but can occur throughout the region.

The troposphere starts at the Earth's surface and includes all portions of the atmosphere where convection caused by changes in the air temperature is a major effect. This is the region of weather production. The top of this layer varies between about 6 and 15 km (20,000 to 50,000 feet), depending on the region of the world and the local weather conditions. The best opportunity for tropospheric scatter is generally in the lower portion, where the air density is greatest; however, because of the Earth's curvature and local terrain blockage, this region may not be available for propagation. To extend our range of contacts, we must use the upper portions of the troposphere. In a sense, we are doing the reverse of going to the mountaintops to work over the horizon. We stay at home and scatter the signals from the material high in the troposphere. This

Fig 1—Map of the station locations in Washington and Oregon. The Cascade Mountains extend north and south through the area and portions of these are directly north of W7SZ.

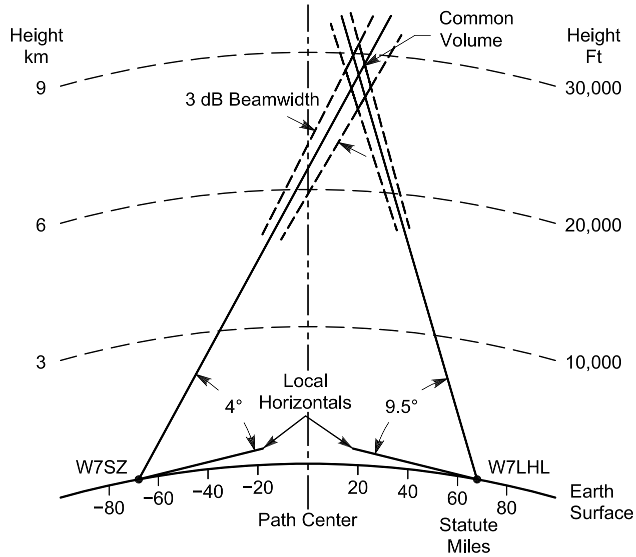

Fig 2—Close-in hills at each end obstruct the path between W7LHL and W7SZ, setting minimum usable elevation angles of 9.5° and 4°, as shown. This plot has very different scales for the height above ground and the horizontal distance. This makes the small angles look very large and distorts the scaling between the angles. The commonly viewable volume is at a height of about 8.5 km (28,000 feet). The beamwidths are only about 0.7°, making the common volume about 1.5 km (5000 feet) in height. The total path length is 159 km (99 statute miles).

article will discuss our measurements of tropospheric scattering from locations where the terrain restricts the path to the regions above about 4.5 km (15,000 feet).

All modes that can scatter or reflect from high regions are attractive for amateur microwave operation since they can be exploited from home locations. In many parts of the country, this can add six months or more to the microwave season! It also allows many more hours of operation than is practical using portable equipment. This attracted us to this type of operation, as the terrain in the Pacific Northwest is mountainous and thus far from line-of-sight as well as inaccessible for much of the year.

We began trying to make contacts between home stations on 10 GHz over some very mountainous paths. This was surprisingly successful, and most often, the propagation mode was determined not to be from aircraft or rain scatter. After finding that microwave contacts were possible, we started making measurements of the signal strengths and signal spectra, trying to correlate this to the weather conditions. We also extended the measurements to 1296 MHz. We found almost certain indications that the signals were being scattered by material in the upper troposphere. The nature of the material is still uncertain. Neither do we know how well our results would apply to other parts of the world. This report is to let other operators know about our observations

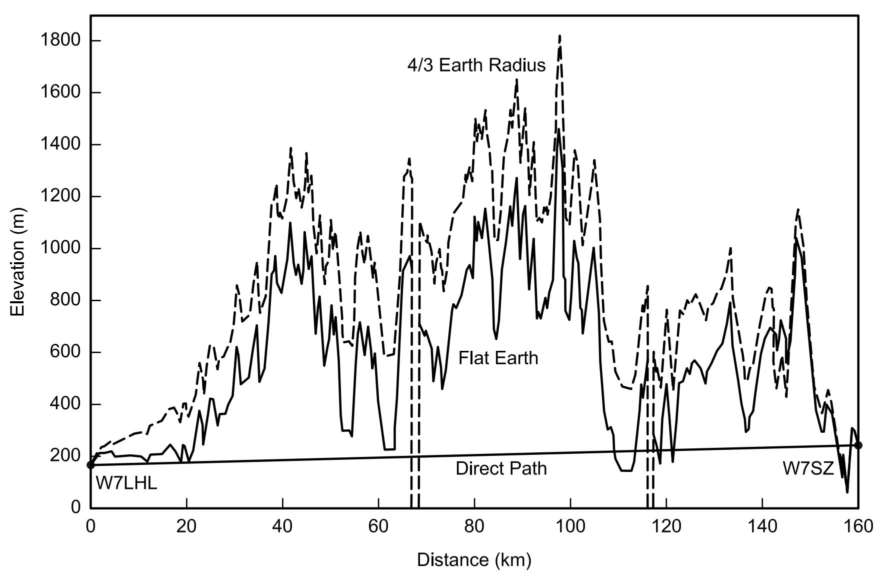

Fig 3—Cross section of the terrain between W7LHL and W7SZ. It is far from a direct path. The tallest peak, shown at about 100 km from the W7LHL end, is the side of Mt St Helens. The upper trace shows the effect of the Earth's curvature, including a 4/3 correction for refraction. The "Flat-Earth" trace is about 400 meters lower in the center of the path. (Plot by KB1VC; users.rcn.com/acreilly/los_form.html)

Table 1—Path Summary

Stations 1 - 2	*Distance (km)*	*Take-off Angle 1 (°)*	*Take-off Angle 2 (°)*	*Common-Volume Height (km/kft)*
W7LHL-W7SZ	159	9.5	4	8.6/28
KD7TS-W7SZ	198	1	4	4.1/13
W7SZ-W7PUA	138	4	3	4.5/15

Fig 4—The 10-foot parabolic-dish antenna used for both 1296 MHz and 10 GHz by W7LHL. This is a surplus TVRO antenna. The RF equipment is mounted at the center feedpoint.

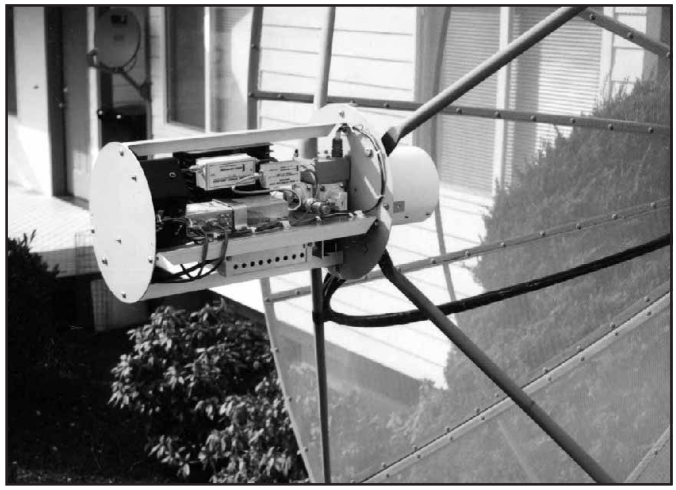

Fig 5—This photo shows W7LHL's 10-GHz equipment that is mounted at the feed for the parabolic dish shown in Fig 4. A DB6NT transverter, along with an MKU-101B receive preamplifier (0.8-dB noise figure), a driver amplifier and an MKU-102XL output amplifier (all from Kuhne Electronic) are at the feed. A waveguide TR switch minimizes losses at the feed horn. A frequency-reference signal comes from the shack on a coaxial cable to phase-lock the crystal oscillator in the transverter.

Table 2—Equipment Used

Station	*Dish (m)*	*Power (W)*
KD7TS	1.0	1
W7LHL	3.0	5
W7SZ	3.0	10
W7PUA	1.2	9

Fig 6—W7SZ with his dish antenna used on 10 GHz. The microwave equipment is mounted at the focus of the antenna. Equipment for 10 GHz is similar to that used by W7LHL except that the transmitter power amplifier uses a TWT (traveling-wave tube).

and encourage further exploration of microwave paths.

Tropospheric-scatter propagation modes have utility because they may be available when modes like airplane reflections, mountain-bounce and rain scatter are not. In addition, the associated Doppler shift is considerably less than that from either airplane reflections or rain scatter, allowing the efficient use of narrow-band modulation, such as CW or some computerized modes such as JT44 or PUA43.

The Propagation Paths

The work reported here was between home locations as shown in Fig 1, a general map of the area. The geometry of the path between W7LHL and W7SZ is shown in Fig 2. The distances and take-off angles are in Table 1. The take-off angle is the lowest angle that the station can view clear sky, measured from the local horizon. This angle is in all cases determined by local obstructions, within a few kilometers of the station. The common volume height (lowest altitude that is mutually visible between the two stations) is set by the take-off angles and the Earth's curvature.

The heights shown do not include atmospheric refraction; this has only a small effect. Fig 3 shows more detail of the mountainous path between W7LHL and W7SZ.

All three paths of Table 1 have been explored to varying degrees, but the most intensive data collection was for the path from W7LHL to W7SZ. This path is interesting since not only are the take-off angles poor but almost in the middle is Mt St Helens, with a post-eruption height of over 8500 feet. W7LHL and W7SZ are at 650 and 750 feet, respectively.

Equipment Used

Table 2 summarizes the equipment used on 10 GHz, portions of which can be seen in Figs 4, 5 and 6.

All contacts and measurements described in this article used equipment capable of very accurate measurements of the frequency spectrum. The conversion oscillators in the transverters were phase-locked to 10-MHz frequency standards that, in turn, were phase-locked to the GPS system using W5OJM controllers.[3] The IF radios used were DSP-10s that were again phase-locked to the frequency standards.[4] This system allows accuracy and resolution to a few hertz, even at an operating frequency of 10 GHz. In turn, it is possible to make accurate spectrum measurements, which imply the movement of scattering material.[5]

The only 1296-MHz measurements described are for the W7LHL/W7SZ path. On that band, W7SZ used 20 W and a 3.7-meter (12-foot) parabolic dish while W7LHL used 40 W and a 3-meter (10-foot) dish. The 1296-MHz transverters were again phase-locked to the station frequency references.

All stations had sensitive receivers. For the terrestrial paths, the system noise temperature includes quite a bit of ground-noise contribution.

Microwave scattering from moving media results in a Doppler-shifted spectrum in the received signal. By measuring this spectrum, it is possible to learn much about the path. The tool used for these measurements was the DSP-10 transceiver. The spectral resolution of the DSP-10 could be set to 2.3, 4.7 or 9.4 Hz. Provision was made for averaging of the received signal-plus-noise power over long periods of time to increase the apparent sensitivity. The resulting spectra were displayed either as amplitude-versus-frequency traces or as a waterfall display where the intensity of the display represents received power plotted against both time and frequency.

Observations—10 GHz

In February 2001, W7SZ and W7PUA exchanged signals on the first attempt at 10 GHz. The signals were weak, but adequate for an easy contact using digital modes. The signal had a few hertz of spectral broadening to it, and both stations observed an upward frequency shift of about 45 Hz. The night sky was clear and and there was an ice-crystal halo around the Moon. The frequency shift was consistent with Doppler shift from a decreasing path length, such as would occur with a scattering medium that was falling. (See the sidebar "Doppler Shift from Moving Media.") Other observations were made on later days and the signal was found to vary in both amplitude and amount of Doppler shift.

In July 2001, W7SZ and W7LHL were pleasantly surprised to find they could exchange signals on 10 GHz. As discussed above, this 159-km path is highly obstructed. The signals were present for long periods and possessed none of the Doppler spectra associated with aircraft and rain. Enhanced signals from aircraft over this same path confirmed the differences in the spectra.

KD7TS and W7SZ found similar success on 10 GHz in August 2001. Local terrain blocks this 198-km path, particularly on the southern end. Signal-to-noise ratios of around 7 dB in a 4.7-Hz bandwidth allowed them to easily complete a digital-mode contact (see Fig 7). Signals again showed broadening by about 20 Hz and the Doppler shift from the moving media was about +15 Hz, corresponding to a net shortening of the path. The weather was clear.

Beginning in November 2001, W7LHL and W7SZ conducted a series of experiments at 10 GHz. This path has a major local obstruction at the W7LHL end. Some tries produced no measur-

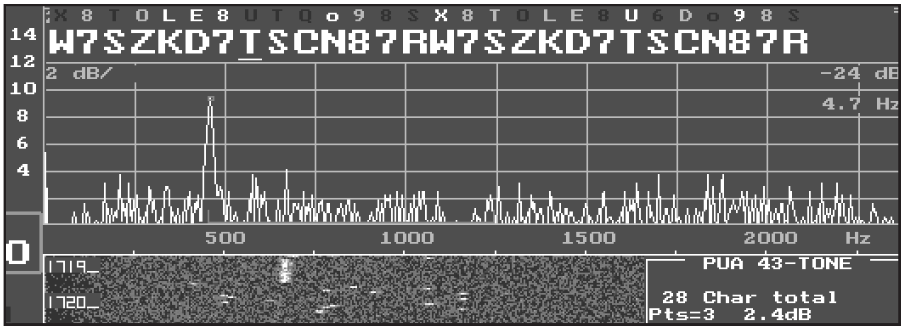

Fig 7—Partial screen shot of KD7TS's 10-GHz signal being received at W7SZ. The top lines of text show the most likely (large letters) and the second most likely characters being received in PUA43 mode. Below the letters is the latest spectrum of the multitone FSK signal. A portion of the waterfall display appears at the bottom.

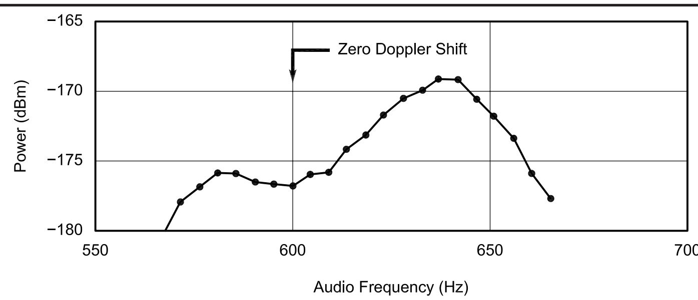

Fig 8—Frequency spectrum of W7SZ's 10-GHz signal, as received at W7LHL on 10 February 2002. The resolution bandwidth, or "bin size" is 4.7 Hz. This small bandwidth shows the details of the spectrum but makes the peak power appear to be 10 dB less than the total received power. The main spectral peak shows a Doppler shift of 37 Hz. This data has been processed to remove the noise power, based on measurements taken outside the spectrum of the signal. The double-humped response was observed frequently and would seem to represent two types of scattering material as is discussed in the text.

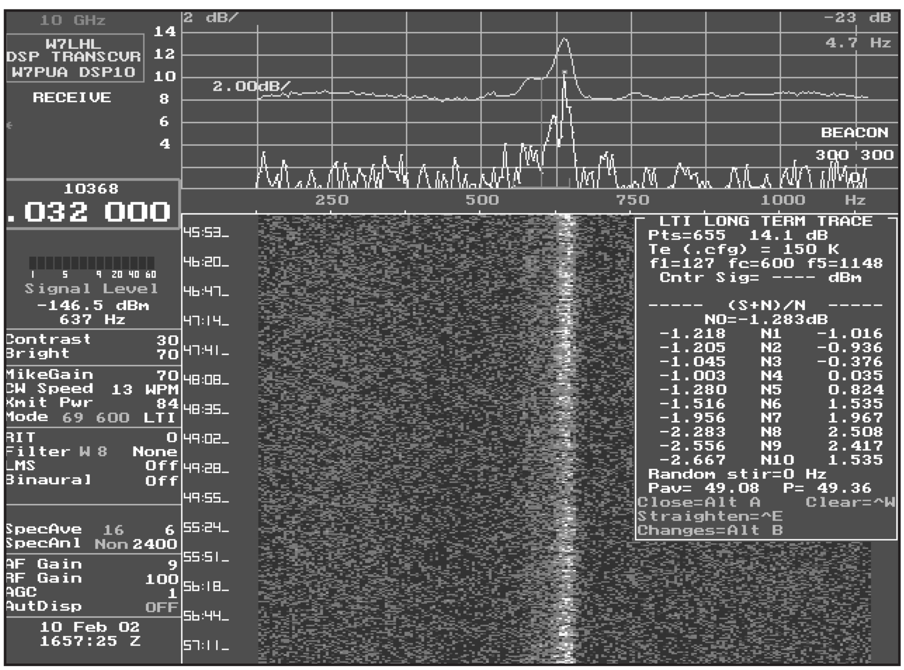

Fig 9—DSP-10 screen shot of W7LHL's 10-GHz signal being received at W7SZ over a 159-km mountainous path. The upper trace in the top spectral graph is the average spectrum being received. The lower trace in the same graph is the last received spectrum. The waterfall in the lower-right display shows many of the received spectra with time going from top to bottom. Brighter areas are stronger signals. The strongest (S+N)/N is about 7 dB, which occurs at 637 Hz. This is a Doppler shift of about 37 Hz to the high side of the transmitted frequency, corresponding to an approaching velocity of 1.1 m/s. The second, weaker peak is about 20 Hz to the low-frequency side. The total received power over the entire signal spectrum is about –155 dBm.

able signals other than from infrequent airplane reflections, which are easily identified by their characteristic high-to-low Doppler shift. Most tries produced weak signals on direct headings that would persist for hours. Over a period of 38 tests on different days during the winter and spring, measurable signals were observed on about 80% of the tests. Fig 8 is typical of the observed spectrum. The received power was –157 dBm, corresponding to a path loss of 291 dB between isotropic antennas. This is about 134 dB below the free-space loss and 70 dB above that predicted for a tropospheric scatter path.[6]

The antenna beamwidth for both stations was less than a degree, allowing some exploration of the scattering medium in azimuth and elevation. In all cases, the antennas needed to be elevated to clear the local hills. Past that, signals would most often drop off with increasing elevation angles. Both stations could move their antennas to the western side of the direct path by several degrees and still receive signals, but the strength dropped. Moving to the eastern side was less productive, probably because of increased local hills at W7SZ's location. Moving to the sides showed Doppler shift that was consistent with the prevailing upper winds. Spectral spreading, as can be seen in the figure, was always observed; but this is far less than occurs with rain scatter.

On many occasions, the 10-GHz signal between W7LHL and W7SZ had a spectrum that suggested two different scattering media. A hint of this effect was seen in Fig 9, but Fig 10 makes this spectral pattern very obvious. The waterfall display shows one signal at about 600 Hz and a second signal at about 55 Hz higher in frequency. The first signal has very little Doppler shift, whereas the second represents a path shortening of about 1.6 m/s. Both signals tend to fade at the same time but not entirely. There are times when only the first or second signal is present.

As the W7LHL/W7SZ experiments progressed, there was speculation about the propagation media involved. One candidate for 10 GHz is scattering by ice particles. KD7TS suggested the use of aircraft icing plots, prepared by NOAA. These didn't seem to correlate, but they led to our discovery of the GOES IR3 water-vapor plots that are updated on a regular basis and available over the Internet.[7] Considerable assistance in understanding the nature of the IR3 data was provided to us by Don Hillger, WDØGCK, of Colorado State University. The IR3 plots, such as Fig 11, indicate the radiation temperature for the highest levels of water vapor or clouds. The areas of the plots with lower temperatures are often associated with higher elevations.[8] The only common volume on the propagation path was at the upper levels of the troposphere, so it is not surprising that water content at these heights could be important.

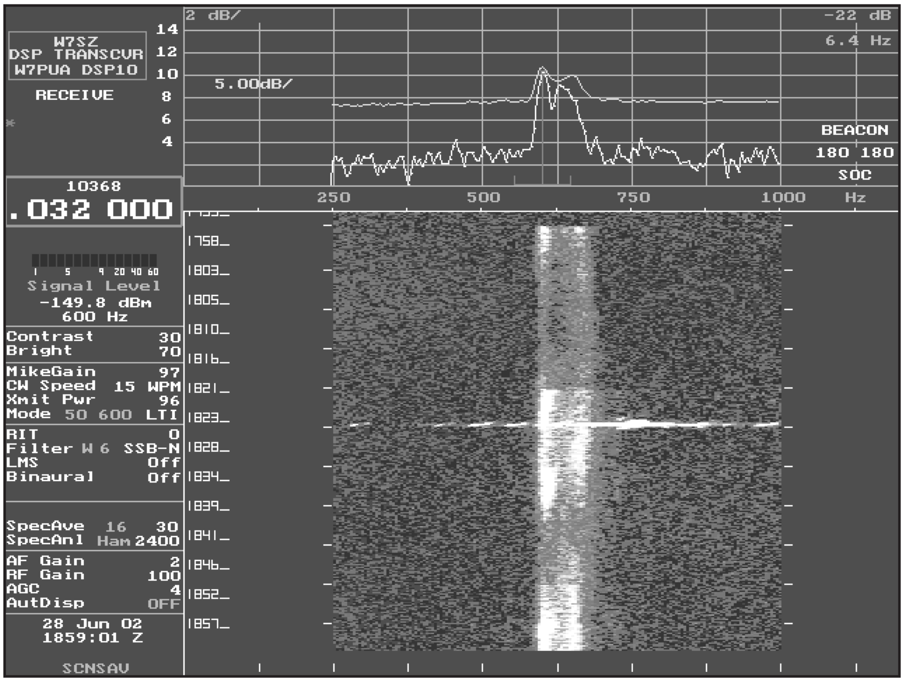

Fig 10—Screen shot of W7LHL's signal on 10 GHz as received by W7SZ. The waterfall display in the lower right portion of the screen shows the spectrum of the signal over a period of about an hour, as indicated by the times on the left. The two stations were transmitting in alternate three-minute periods and causing the abrupt changes in the displayed spectrum. Stronger signals are shown as brighter colors in the waterfall. As set up here, the weakest signal discernible on the waterfall is about –175 dBm. The strongest signals shown are about –150 dBm. The horizontal trace at about 1833 is from an airplane flying through the common volume.

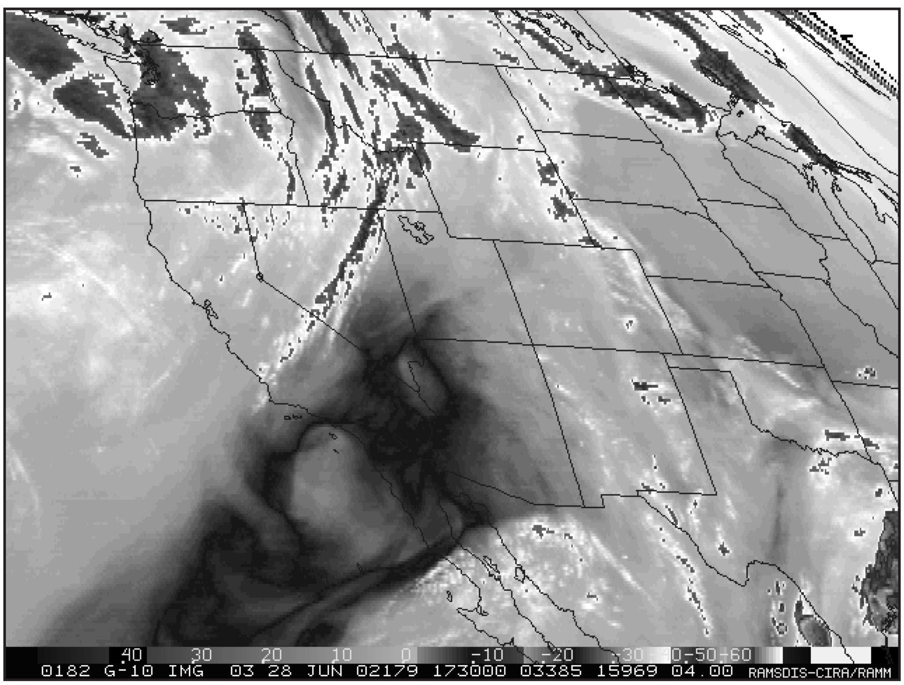

Fig 11—A view of the western United States from the GOES10 satellite. This is the IR3 channel (water vapor) at an infrared wavelength of about 6.7 micrometers. Since this wavelength is absorbed by water vapor, the radiation temperature is close to that of the highest cloud layer. The temperature scale is indicated at the bottom. The Internet pictures are in color, making interpretation easier. For this picture, the dark areas, over western Washington, are in the magenta range, indicating a temperature of –40 to –50°C.

The GOES-10 IR3 temperatures showed correlation with the 10-GHz signal strengths. Fig 12 shows the results of 19 measurements taken between 10 Feb and 28 March 2002. The signal strengths were estimated from the appearance of the waterfall by comparing with known levels. A "relative signal" of zero in the plot indicates that no sign of a signal was found. This means the strength was –175 dBm or less. Above this level, the estimates were made in roughly 5-dB steps, shown as relative signal values from 1 to 6. Most notable is that anytime the GOES IR3 temperature was –40°C or colder, the 10-GHz signal was strong enough to measure. The trend line on the plot generally shows an increase of almost 1 dB in signal for each 1°C of cooling. Of course, the colder temperature is probably not the direct cause of the signal changes, but rather it indicates the presence of water vapor at greater height.

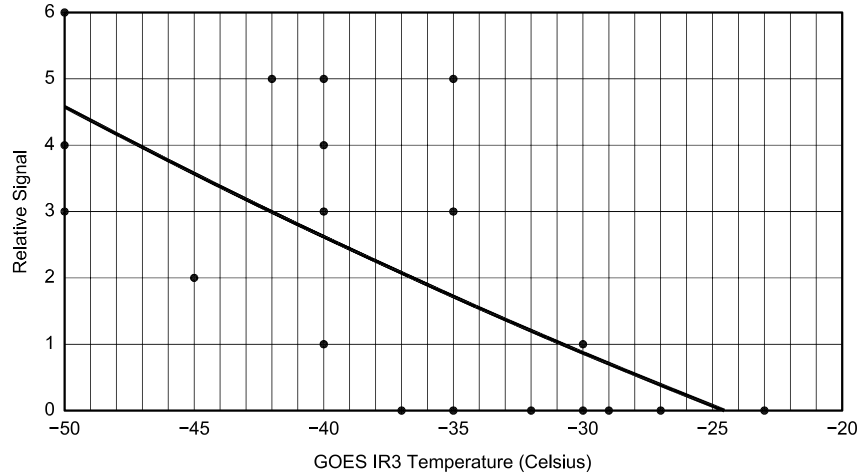

Fig 12—This plot shows the correlation between the GOES-10 IR3 temperature and the received 10-GHz signal strength over the W7LHL/W7SZ path. See the text for the meaning of the relative signal strength. Each of the 19 dots represents a different day's measurement. The straight line in the plot is a linear curve fit to the data, showing the trend between temperature and signal strengths.

Observations—1296 MHz

At this point, our interest moved to 1296 MHz. We thought that an eightfold increase in wavelength might help us to learn more about the scattering media. Tests between W7LHL and W7SZ at 1296 MHz ran for several months starting in April of 2002. Signals proved strong enough to be observed on most days, even without the most obvious feature of frequent strong aircraft reflections. Seeing more aircraft than at 10 GHz was not surprising, since the wider antenna beamwidths produced a higher probability of an aircraft being in the common volume.

We soon determined that, as at 10 GHz, signals associated with tropospheric air masses were present. Signal strengths would vary from day to day, but generally the levels were in the range of –145 to –160 dBm. Like the 10-GHz signals, these showed broadened spectra, typically 10 to 20 Hz at the –3-dB points. Generally, there was only a single peak to the spectrum; but on at least one occasion (4 May 2002), double peaks were observed with a spacing of about 8 Hz. The GOES IR3 was indicating a very cold top cloud layer (below –40°C) at the time, and this may be related. This double peak was of particular interest as it had been seen many times at 10 GHz.

Experiments were run with the antennas moved in azimuth at both ends of the path, as had been done at 10 GHz. Again, the signal strength dropped off to the sides; but the main feature observed was a shift in center frequency. An example of this is Fig 13, showing the signal at the southern end of the path.

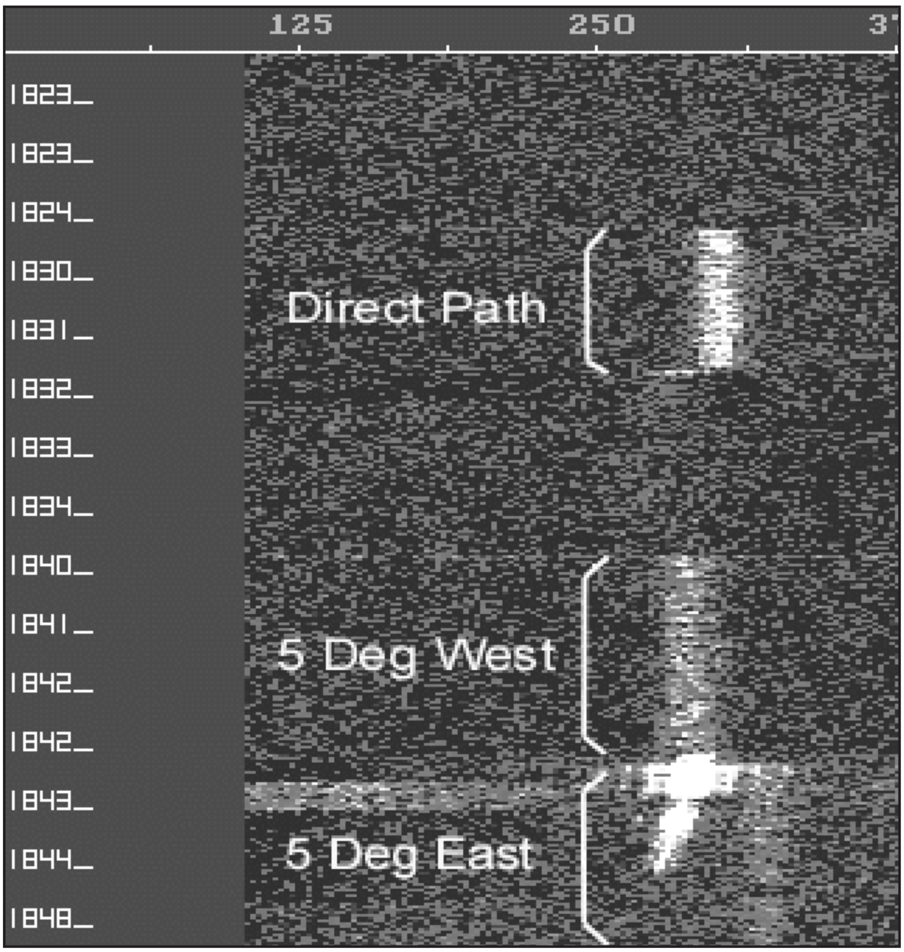

Fig 13—A spectral waterfall plot of the 1296-MHz signal being received at W7SZ, showing the variation in received frequency with azimuth angle. The frequency scale is at the top, and time (to the nearest minute) is on the left. The top segment marked "Direct Path" is for both antennas pointed at one another. This works out to be very close to a north-south path. The two lower segments correspond to azimuthal shifts of 5° east or west. The corresponding change in frequency is ±15 Hz. One probable explanation for this behavior is that the scattering media is in motion with these winds. The bright areas on the left at about 1843 are from an aircraft, and thus irrelevant.

Always in search of data correlation, we looked at the GOES-10 IR3 temperature that seemed to show correlation at 10 GHz. This was quite unsuccessful! Fig 14 is an example of the observed correlation. On that plot, both the strongest and weakest signals were found at a temperature of –30°C. The nine measurements show very little correlation. This agreed with the impressions that we gained from the many measurements. We explored correlation with other measures, generally with poor success. We looked at water-vapor content in the upper troposphere, wind speed and the product of wind speed and water-vapor content. The latter measure showed some correlation, but there were also contrary indications, so more data is needed to see if this is a valid measure of the propagation.

One problem in finding correlation with tropospheric conditions is the scarcity of atmospheric data. The best sources of data are weather balloons. In our area, these are launched twice a day—at 0000 and 1200 UTC. The locations available for our area are Salem, Oregon, and Quillayute, Washington, which are not generally at the center of a propagation path. We are left trying to correlate with data measured at the wrong time or place! Fortunately, the upper-air features generally change slowly. Sometimes, features may change quite rapidly, and this alone could cause poor correlation. In contrast, the GOES IR-3 data are frequently updated, which is beneficial when those data can be used.

Signal Strengths

Although not strong, signals scattered from the upper regions of the troposphere are within the range of many amateur microwave stations. We wanted to try to quantify the losses for this type of propagation. Fortunately, the DSP-10 radio provides an estimate of the received power. (See the sidebar "Total Received Power.") The path between W7LHL and W7SZ will be used as an example, as illustrated in Fig 2.

The density of scattering material can be estimated by looking upon the measurements as a "bistatic" radar,[9] where the transmitter and receiver are geographically separated. The equation for the received power is:

$$P_r = \frac{P G_t G_r \lambda^2 \sigma}{(4\pi)^3 R_t^2 R_r^2} \qquad \text{(Eq 1)}$$

where
P_r = received power in watts
P = transmitted power in watts
G_t = transmitter antenna power gain as a ratio
G_r = receiver antenna power gain as a ratio
λ = wavelength in meters
σ = bistatic radar cross section in meters, discussed below
R_t = distance from the transmitter to the scattering particles in meters
R_r = distance from the receiver to the scattering particles in meters

Radar cross-section, σ, refers to the size of a hypothetical reflector that returns all the energy it intercepts. Jet aircraft cross sections are commonly 10 to 100 m^2. For the path from W7LHL to W7SZ, a received signal of –150 dBm at 10 GHz corresponds to a cross section of about 0.001 m^2. We will now try to put this into perspective.

It seems reasonable to assume that the scattering is coming from material distributed throughout the commonly visible volume. Some layering might occur that would produce more scattering at one height than at another; however, it is informative to estimate the density of scattering material and for this purpose, we will assume the density is uniform. One might envision that the first particles encountered would shadow those further away. As we will see, the densities are so low that this would be most unlikely.

The volume of the two intersecting beams is approximately the area of the smaller beam times the width of the larger beam divided by the sine of A, the angle between the beams. For the W7LHL/W7SZ case, the smaller beam is from W7LHL, as the common volume is closer to that station. For short paths, this angle is the sum of the elevation angles of the two stations, or in our case, about 13.5°. Thus the common volume is about

$$\mathit{Common\ Volume} \approx \frac{\pi (B_t R_t)^2 B_r R_r}{4 \sin A} \qquad \text{(Eq 2)}$$

where B_t and B_r are the transmit and receive beamwidths in radians (degrees $\times \pi / 180$). This assumes that the transmit path has a smaller beam area; else the transmit and receive subscripts should be reversed.

For the W7LHL/W7SZ case, the common volume at 10 GHz is about 1.7 km^3 or 1,700,000,000 m^3. This is the volume required to provide a scattering cross section of about 0.001 m^2 (about 1.5 $inch^2$). In terms of scattering signals, it is obviously a sparsely occupied volume!

If the scattering is nearly uniform throughout the common volume, it suggests that smaller antennas may result in only modest decreases in signals. If both stations were to cut their antenna size by half, the antenna gain would drop by 6 dB at each end—or 12 dB over the total path. The common volume would increase by $2^3 = 8$, or 9 dB, and make up for all but 3 dB of the antenna's reduced gain. We have not experimentally measured this scaling, but it should encourage those with smaller antennas to explore these scattering mechanisms.

Possible Scattering Media

Part of the fun of these experiments has been postulation about scattering media. The RF signal strength and spectrum measurements provide only indirect indications of the nature of

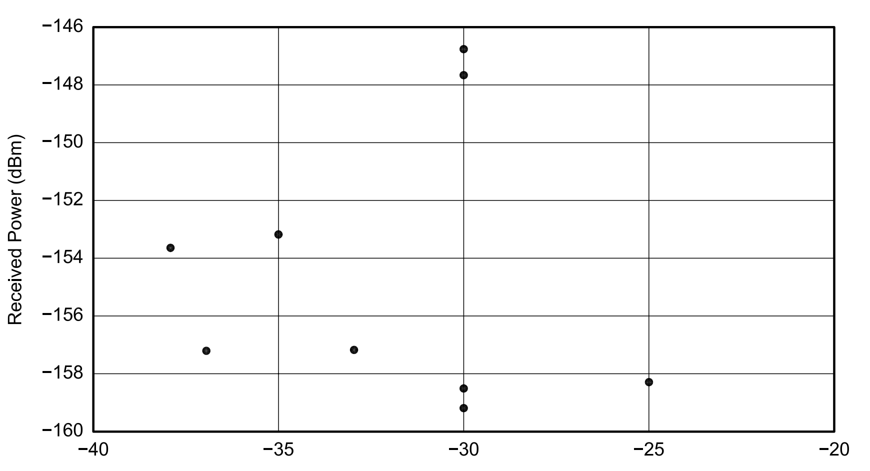

Fig 14—1296-MHz signal strength of W7LHL received at W7SZ is plotted here as a function of the observed GOES10 IR3 temperature. The correlation at this lower frequency is much less than observed at 10 GHz. That is seen here as randomness in the positions of the data points.

the media. Likewise, only limited data are available for the amount and character of the water vapor in the upper troposphere. One must search for an explanation that is consistent with both types of observations. In the following, we will explore several possibilities. Any scattering that occurs in the troposphere might be included in the term "tropospheric scattering," and so we are attempting here to be more specific about the media involved.

The location of the scattering media in the upper troposphere seems highly probable. If earthbound features such as mountains or sharp rocky edges were involved, there should not be a Doppler shift. Yet, Doppler measurements show a net movement of the scattering media that correlates with weather-balloon measurements of the winds in the common scattering volume. The Doppler shift consistently varies with the antenna direction. Pointing the antennas towards the wind source causes positive Doppler shifts while pointing away from the source causes negative shifts.

Rain scatter is precluded for two reasons: The signals are present on many occasions when no rain exists, either as observed by the station operators or as would be expected from the weather conditions. In addition, on paths where rain scatter is observed (never on the W7LHL/W7SZ path), the spectrum is much broader—often by hundreds of Hertz—than has been observed for upper-tropospheric scattering. This spectral broadening is associated with the noisy sound that operators report on rain scatter, sometimes making these signals difficult to copy with the ear. A net incoming (positive) Doppler shift is observed as a result of falling rain.

Aircraft scatter produces strong signals that are readily identified on the spectral display from the Doppler changes. Aircraft following a straight course will always start with a positive Doppler shift and end with a negative shift. These signals have often been observed on the paths such as W7LHL to W7SZ or W7SZ to W7PUA. For situations where aircraft are frequently present and where the changing Doppler shift is tolerable, these reflectors can be a major aid to communication. They were not our objects of primary interest, though, and we have consistently selected data where aircraft were not present.

This leaves the upper troposphere as our scattering material. Two possibilities have been identified: ice particles and water-vapor boundaries.[10]

Under certain conditions in the upper troposphere, water vapor can produce ice. Ice particles would be small compared to either of our wavelengths. This type of scattering object, called Rayleigh scattering, produces a scattering cross section that varies inversely with the fourth power of the wavelength. On a per-particle basis, the 1296-MHz signals would be about 36 dB below those at 10 GHz.[11] The larger beamwidths of the lower frequency would, however, have a larger number of particles in the common volume, making up most of the difference. Ice particles can have sufficient mass and volume to cause them to fall vertically. This could be responsible for some of the Doppler shifts observed.

Water-vapor irregularities produce boundaries of changing dielectric constant. These boundaries are continually altered by turbulence in the troposphere. This effect has generally been considered the dominant cause of tropospheric scatter.[12] Gannaway published a summary of this propagation mechanism, along with a model for the expected signal strengths.[13] This model gives poor results for the paths that we have been exploring, underestimating the signal strengths of the W7LHL/W7SZ path by 50-70 dB and overestimating the W7SZ/W7PUA path by 20-30 dB. The fading rates reported by Gannaway are in general agreement with our observations, though.

One would expect the water-vapor boundaries to be swept along with the winds, much as a cloud travels across the sky. The average movement causes fixed Doppler shift while the turbulence around the boundaries causes broadening of the spectrum. This is all consistent with the observations.

Our observations of two separate signal spectra suggest that two different scattering materials might be involved. Our current speculation is that these are ice particles and turbulent water-vapor boundaries.

Further Exploration

Amateur Radio allows one to explore areas such as propagation at will. Our experiments over the last year and a half have led to more questions than answers! There are many opportunities

Doppler Shift from Moving Media

The upper levels of the troposphere are windy. Wind speeds are seldom less than 50 km/hr. At times, jet-stream speeds over 150 km/hr are common and they can sometimes be twice that value. When the scattering media are moving with this wind, there will be Doppler frequency shifts on the received signals, depending on the details of the geometry.

The propagation paths that we have used are essentially north-and-south. The prevailing winds are at right angles to these paths, or west-to-east, as shown in Fig A. For this geometry, the Doppler shift is zero when the two stations point directly at one another. With the antennas shifted to either side of the direct path, however, there is a Doppler shift that is proportional to the beam angle, as shown in the figure. Comparisons between this Doppler shift and the radiosonde balloon wind-velocity data is good confirmation that the scattering is from the moving medium. [For θ from 1° to 58°, sin θ ≈ θ in radians —*Ed.*]

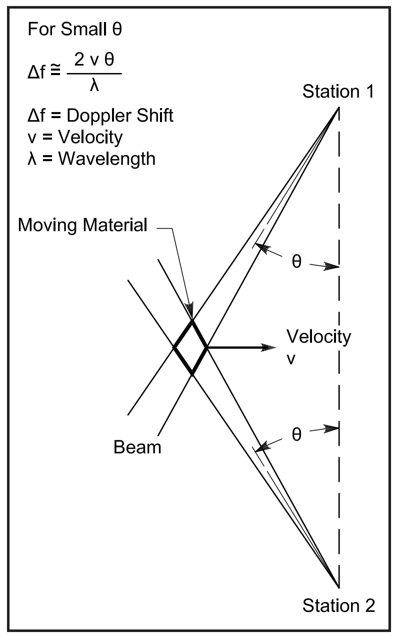

Fig A—Geometry for observing the Doppler shift on a signal that has been scattered by a moving media. The antenna beams have been shifted off the direct path. Angles are in radians, which are about 0.01745 times the angle in degrees. The distance units for velocity and wavelength should be the same and the velocity should be in distance units per second. Then the Doppler frequency shift will be in hertz. This geometry is specific to a path at right angles to the moving media.

for others to add to our knowledge of tropospheric propagation.

For instance, all of our work has been done in the maritime climate of the US Pacific Northwest. Other regions may exhibit different properties. We have had very little opportunity for working with cumulonimbus thunderstorm systems. Those should be interesting sources of scattering.

Multiple types of scattering have been observed, but we feel these are not fully understood. What is the role of ice particles and turbulent water-vapor boundaries? Are other factors, such as dust or insects involved? Our experiments have only involved the two frequencies of 1296 and 10,368 MHz. Further work at other frequencies is likely to show interesting results. The common-volume concept suggests diminishing returns for increasing antenna sizes. This area could lend itself to considerable exploration.

Besides what we have listed here, there must be many more interesting areas of exploration in the troposphere. Every answer found seems to suggest a new list of questions!

Conclusion

Microwave signals have been exchanged over several obstructed paths in the US Pacific Northwest. This includes the 159-km path between W7LHL and W7SZ that would seem to be so obstructed as to preclude any sort of knife-edge refraction or reflection from mountains. The local horizons for this path are about 9.5° and 4°. The lowest mutually visible volume is in the troposphere at about 28,000 feet above the Earth's surface.

Using DSP-10 radios, along with phase-locked transverters for 1296 MHz and 10,368 MHz, it was possible to measure the Doppler shift on the path and from this, to determine that the scattering media were moving. By movement of the parabolic dish antennas to either side of the shortest path, it was possible to make rough estimates of the scattering-object speed and direction. This was found to correlate reasonably well with the velocity vectors at this height above the Earth, as determined by radiosonde balloon measurements.

In addition, it was found at 10 GHz that the signal-strength level increased with the height of the top of any cloud layer. GOES-10 IR3 infrared data was used to estimate the height of the cloud top. This effect was so strong on 10 GHz that signals often became too weak to measure when the top of the cloud layer was below the height of the commonly viewable volume. At 1296 MHz, the variations in signal strength were not as great and signals were found on most days, regardless of the cloud top height.

It is reasonable to associate this signal propagation with scattering from some suitable medium. Scattering stands in contrast to refraction. Refraction bends an RF wave in layers of varying dielectric constants. Scattering refers to re-radiation from some medium that is being excited by an incident wave. With antennas at both ends of the path off the direct heading, the ability to propagate signals is associated with scattering.

For the paths we explored, signals were being propagated by scattering in the upper levels of the troposphere from about 4.5 km (15,000 feet) to 9 km (30,000 ft), or higher. We tried to deduce the details of the scattering medium. The cirrus clouds associated with the stronger signals were typically at –40°C. Any condensed water vapor would be in the form of ice. A second possible scattering medium would be rapid changes in water-vapor content, such as small vortices that have been claimed to be responsible for some tropospheric scattering. Frequently on 10 GHz—and rarely on 1296 MHz—there is Doppler evidence that two different scattering media are involved, each moving with a different velocity. We have been unable to be specific about the scattering media.

In summary, we have been able to communicate over some difficult microwave paths between home stations. Scattering in the upper troposphere has been successful for this purpose. The signals are not strong, but this propagation mode has allowed us to communicate over paths when other modes were not available. We are still learning about the scattering media involved. We encourage others to join us in this endeavor. The study of propagation can be a fun and rewarding activity that extends beyond the making of conventional contacts. In addition, the signals being exchanged are sufficient for making contacts and represent a challenge for the better-equipped stations.

This has been a learn-as-you-go experience for us. We received assistance in understanding the multiple disciplines involved in this project from many helpful individuals. We would especially like to thank Don Hillger, WDØGCK, of Colorado State University for help with the GOES IR3 data and Mike Reed, KD7TS, for important measurements as well as leads to many useful weather data sources; and Matt Reilly, KB1VC, for supplying the path-profile plots. Thanks to Beb Larkin, W7SLB, for help with coordination of the measurements.

Notes

[1]See, for example, E. Pocock, W3EP, "Chapter 3, UHF and Microwave Propagation," *The ARRL UHF/Microwave Experimenter's Manual,* (Newington, Connecticut: ARRL, 1990).

[2]T. Williams, WA1MBA, "10 GHz—A Nice Band for a Rainy Day," *CQ VHF*, Feb 1997.

Total Received Power

The spectral display of the DSP-10 is an estimate of the signal-plus-noise (S+N) power at each of many frequency bands. These bands are narrow and have selectable spacings of 2.3, 4.7 or 9.4 Hz. At microwave frequencies, the signals' total spectral width is often wider than a single band, because of the propagation-path modulation. The total received power, measured across all the spectral signal bands, is often the quantity of interest. This quantity is calculated as follows.

First, the noise power in each band is found and referenced to the antenna input. This is the sum of the noise powers from the receiver and external noise sources. For the experiments described here, the latter quantity is dominated by Earth noise when the antenna beam is along the horizon. If the total receiver noise power were expressed in kelvins as the system noise temperature,* T_s, the noise power in a band of B Hz would be $n = K\ T_s\ B$ W, where K is Boltzmann's constant or 1.38×10^{-23} joule/kelvin.

By observing the average spectrum at frequencies where signals are absent, the receiver power response for noise, n, can be found. If the $S+N$ power response were divided by this noise power, we would have $(S+N)/N$.

At this point, we would have removed the effect of the receiver gain, since we would be using the same signal path for both $S+N$ and N. The signal-to-noise ratio could now be found: $(S+N)/N = 1+(S/N)$. Knowing N, we could calculate S. So the process of finding signal power involves starting with $(S+N)/N$ (as a power ratio, not in decibels), subtracting 1 and multiplying by the noise power, in watts.

*Bob Atkins, KA1GT, "Estimating Microwave System Performance," in Chapter 7 of *The ARRL UHF/Microwave Experimenter's Manual,* (ARRL, 1990).

[3]E. B. Shera, W5OJM, "A GPS-Based Frequency Standard," *QST*, July 1998, pp 37-44.

[4]The DSP-10 transceiver project was originally described in a three-part article by Bob Larkin, W7PUA, "The DSP-10: An All-Mode 2-Meter Transceiver Using a DSP IF and PC-Controlled Front Panel," *QST*, Sep, Oct and Nov 1999. See also **www.proaxis.com/~boblark/dsp10.htm**.

[5]P. Martinez, G3PLX, "Narrow-Band Doppler Spectrum Techniques for Propagation Study," *QEX*, Sep/Oct 1999, pp 45-51. This paper demonstrates the use of Doppler-spectrum measurements to imply changes in the propagation media at HF. Although the media are different from that explored in this paper, the measurement principles are the same.

[6]See Note 1.

[7]See **www.cira.colostate.edu/ramm/rmsdsol/ROLZIP.HTML** with links from there to specific images. The temperature at the upper levels of the clouds is indicated by the IR3 wavelength as viewed by the GOES satellites.

[8]For North America, information about the atmosphere can be obtained from the weather-balloon data linked from the Web site **www.rap.ucar.edu/weather/upper/**. The balloons measure dry and wet bulb temperatures and barometric pressure.

[9]The conventional radar "range equation" is for a co-located transmitter and receiver. A similar equation exists for a separated transmitter and receiver. See, for example, David K. Barton, *Radar System Analysis*, (Englewood Cliffs, New Jersey: Prentice-Hall, 1964) Section 4.3.

[10]Insects and dust are sometimes offered as scattering material. Because of both the height of the common volumes and having the prevailing winds from the Pacific Ocean, we suspect that insects are unlikely. We have been unable to quantify the possibilities of dust scattering, but we should have a relatively poor area of the Earth for such material.

[11]Assuming that the antenna sizes, receiver sensitivities and transmitter powers are kept constant.

[12]A summary of tropospheric scattering is in "Radio Transmission by Ionospheric and Tropospheric Scatter," *Proceedings of the IRE*, Jan 1960, pp 5-44.

[13]J. N. Gannaway, G3YGF, "Tropospheric Scatter Propagation," *QST*, Nov 1983, pp 43-48. Essentially the same material was first published under the same title in the RSGB *Radio Communications,* Aug 1981. It is also in M. W. Dixon, G3PFR, Editor, *Microwave Handbook,* Vol 1, (Radio Society of Great Britain, 1989), section 3.2.4.

Bob Larkin, W7PUA, has been active in Amateur Radio since he was first licensed in 1951 as WN7PUA. He received a BS in EE from the University of Washington and an MSEE from New York University. He is a consulting engineer for communications companies. His current interests are VHF through microwave propagation and weak signal techniques using DSP.

Larry Liljequist, W7SZ, has been a licensed for 46 years, previously holding calls WF8C, G4BIR and W7EKI. He has a BSME from Oregon State University (1959), and is retired from Caterpillar Inc.

Ernie Manly, W7LHL, was licensed in 1947. He is no stranger to the pages of ARRL publications. His article, "A Two-Meter Transverter," appears in the Sep 1963 QST. *He co-authored "Crystal Control on 10,000 Megacycles" with L. F. Garrett, W7JIP (*QST, *Nov 1963). He and W7JIP set world distance records on 10 GHz in 1959 and 1960. For a history of 10-GHz activity, browse to* **www.g3pho.free-online.co.uk/microwaves/history.htm**. □□

A PC-Based Digital Storage Oscilloscope and Logic Analyzer

Build this handy multipurpose instrument for your test bench.

By Larry Cicchinelli, K3PTO

I believe that most Amateur Radio operators today will agree that our hobby is somewhere in the middle of the "digital revolution." As such, we are using digital techniques more and more in our daily communications. The rapid growth and acceptance of PSK31 may be considered an indicator of this revolution. Those of us who like to "roll our own" and experiment with our equipment recognize the importance of having good test equipment.

The device described in this article is a combination Digital Storage Oscilloscope (DSO) and Logic Analyzer (LA). It interfaces to a PC via a parallel (printer) port and is built using several printed-circuit boards. The system is designed such that it allows for six input cards. Each card can be either eight logic-analyzer channels or a single analog channel (8-bit resolution).

119 River Run Cir
Sacramento, CA 95833
k3pto@arrl.net

I am considering designing a serial interface for the device—if there is enough interest from readers. However, I have not yet decided on the exact mechanism yet. It will probably be based on a microprocessor. The current parallel-port interface can access the 130 kbytes of data in about 1 second per board. Unless the PC and microprocessor serial ports can achieve 920k baud it will be somewhat slower. A serial interface would make this device available for use on those operating systems that do not allow direct access to the parallel port.

A previous article (*QEX*, Jan 2000) describes an eight-channel LA that I built and have used quite a bit. The knowledge and experience gained in its development were instrumental in the development of this project. The original intent was to build a DSO only; however, it soon became obvious that most of the design was also useful for implementing a logic analyzer (see Fig 1). I used many of the ideas from the original LA in the design of this combination device. My main goals for the DSO/LA were:

- Ease of construction—use printed circuit boards
- Two analog channels
- Minimum 20-MHz sample rate
- LA channels
- Selectable pre-trigger count
- Trigger selection to allow any combination of analog, digital and LA signals

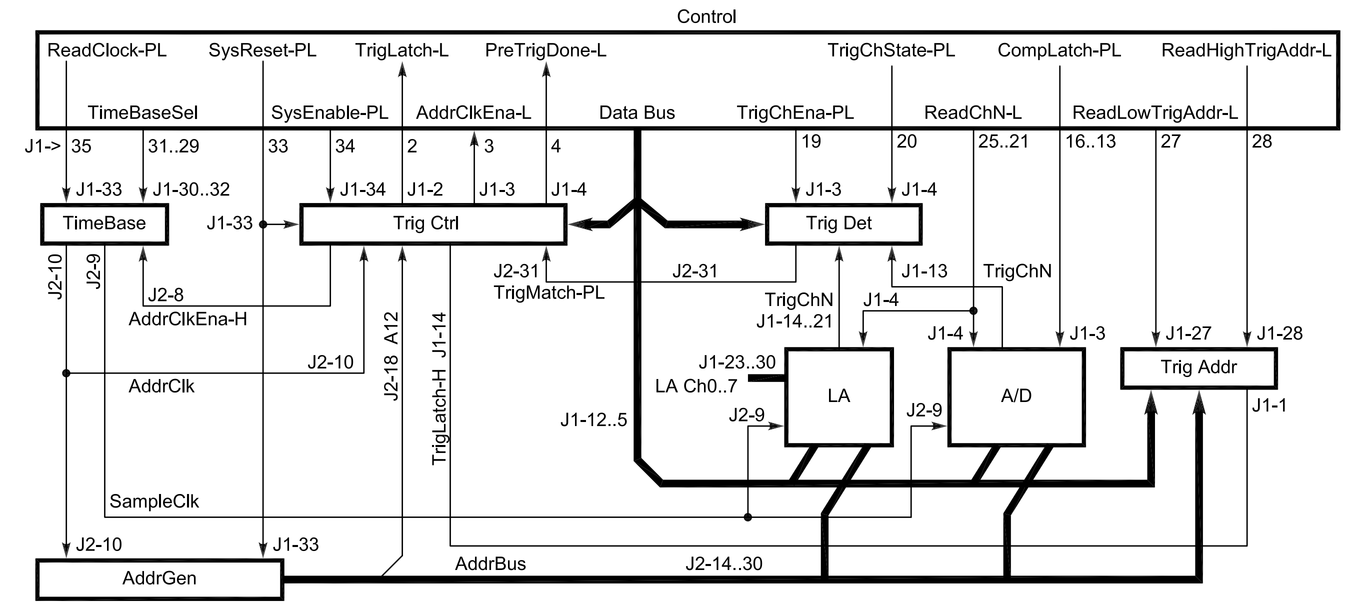

Fig 1—A block diagram of the DSO/LA project as separate boards. (This diagram should be used for reference only—the PLD implementation combines several of these boards onto one.)

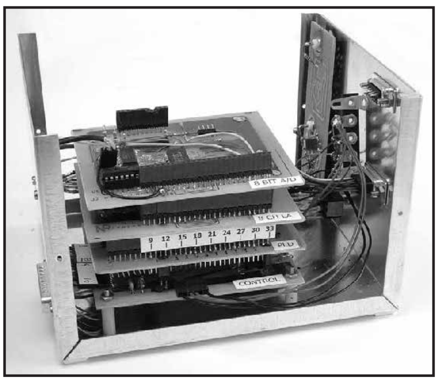

Fig 2—A picture of my "sandwich" construction before I converted several circuits to PLDs.

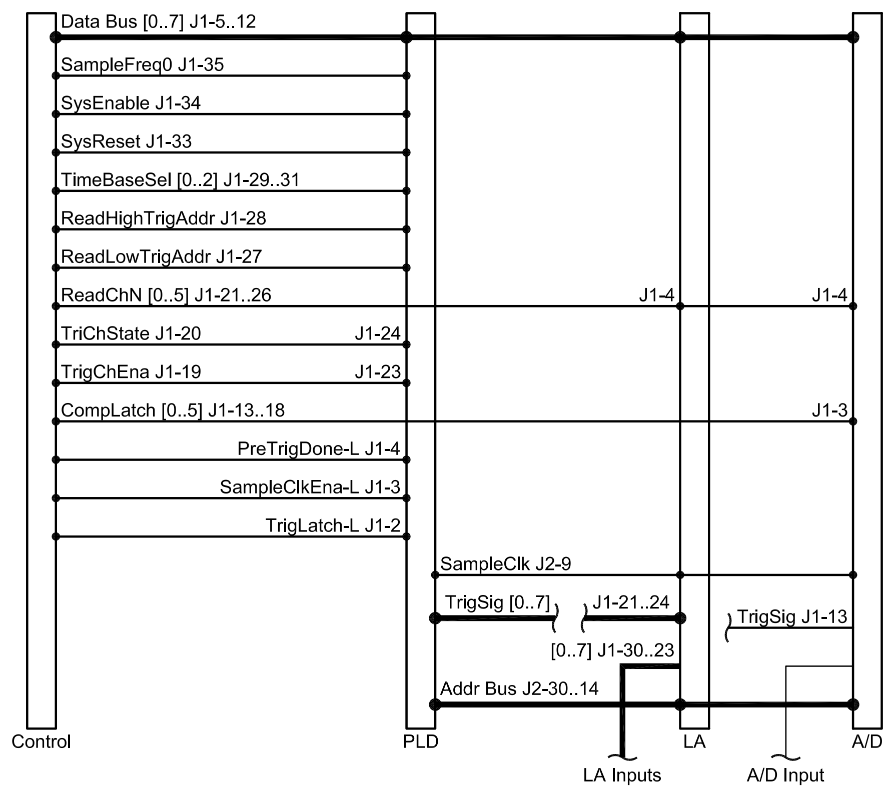

Fig 3—A wiring diagram of the connections between boards.

- An initialization file (referred to in the text as the INI file) that allows the user to define almost all of the operating parameters

The design consists of circuit boards that stack one upon another (see Fig 2). They are connected together via "board stacking" connectors (see Figs 3 and 13). This method allows me to design a system that is easy to modify, expand and customize. It allows the builder to implement up to 48 LA channels (in multiples of eight) or a maximum of six analog channels and any combination thereof. The resulting assembly is fairly close to a 4.5-inch cube with two analog cards and one LA card. Great care was taken in the design of the circuit boards in order to achieve this modularity. A template board having just the inter-board connectors was designed first. It was then used as the basis for all the boards.

I wanted to achieve a 20-MHz sample rate so that the analog channels would be useful to 10 MHz. The A/D converter selected (ADS820) is specified to a 20-MHz sample rate, a 60-MHz bandwidth and has 10-bit resolution. Since the circuit uses only the most significant eight bits, some errors of the A/D can be ignored. A higher-frequency A/D IC is available, and it is pin compatible with the unit I selected, but I doubt my ability to implement a circuit board that would allow the additional band-width. The circuit appears in Fig 4.

Major Circuits

- Control—interfaces to the printer port, source for all the static control signals.
- Trigger Address—stores the address at which the trigger occurs.
- Trigger Control—develops most of the dynamic control signals, pre/post trigger count.
- Trigger Detect—detects the trigger condition.
- Address Generator—17-bit address = 132 k.
- Time Base—generates the sample clock frequencies.
- LA—CMOS levels, eight channels, 132 k memory depth.
- A/D Converter—+0.5 to +4.5 V, 8-bit resolution using a 10-bit A/D and 132 k memory depth.

Design History

During the various phases of building and debugging the circuits, I developed several versions of some circuits. Initially, the above circuits were built on seven circuit boards. I managed to implement the Address-Generator and the Trigger-Address circuits on opposite sides of the same board. I used this implementation to get the initial hardware and software design working. The completed assembly was an approximately 4.5-inch cube with one LA and one A/D board. Since I do not have through-hole construction capability, there were quite a few hand-wired jumpers on the various boards.

I then decided to try my hand at using *programmable logic devices* (PLDs). Design number two combined the Time-Base and Address-Generator circuits into a single PLD and the Trigger-Control and Trigger-Detect circuits into another PLD. The PLDs are on opposite sides of the same circuit board. I had never used PLDs before, so this was a learning experience. Getting the software to work with this design was relatively easy, since I was able to keep the design essentially the same, with only some minor changes. This design has five circuit boards.

Design three combines the following circuits into a single PLD: Trigger Address (Fig 5), Trigger Control (Fig 6), Trigger Detect (Fig 7), Address Generator and Time Base (Fig 8). This yields a much more compact system that requires only two circuit boards more than the desired input boards. Additional wiring is shown in Fig 9.[1]

I would like to encourage any of you designing logic circuits to consider PLDs. My experience was most satisfactory. The free software is very easy to use, especially since I had already debugged my initial circuitry. It was only necessary to translate my schematics to functions available in the PLD design software. The "larger" functions I needed were available as library elements. To give you a better idea of the ease of use of PLDs (programmable logic devices), I will expand on the 17-bit counter example.

The address generator requires a 17-bit (131,072 count) synchronous counter. A synchronous counter is required so that all the address bits change at the same time, synchronously. The discrete circuit I initially implemented is shown in Fig 10. Notice that it uses five ICs. Even though I use only one stage of the fifth device, it is required to maintain synchronous operation.

The PLD implementation is quite a bit simpler (see Fig 8). I needed to select the synchronous counter from a list of device models, select and define the needed parameters and place it in my schematic. A complete list of possible parameters appears as Table 2. The only inputs I needed were *aclr* and *clk*, the only output was *q[]* and the parameters I specified were direction and width.

Once the part was placed, I then needed to "wire" the I/O ports to the appropriate circuits or I/O pins. See the AddrClock circuit of the Time Base and Address Generator schematic.

When the schematic entry has been completed, the next step is to "compile" it. This basically assigns the schematic elements to the internal circuit blocks of the PLD and determines whether or not the circuit fits. If the circuit does not fit, there are several options available that can be used to reduce the amount of resources used. Some of these are:

1. Disabling JTAG (Joint Test Action Group) capability.
2. Disabling globally assigned signals such as clocks and clears.

Once this stage of compilation is complete, the pin assignments must be made. This can be done automatically or manually. I always chose manually, because I wanted the PLD I/O to allow the easiest printed circuit board layout. The manual method is really quite easy. I had previously determined the signal-to-pin assignments based on the PC board layout. The PLD software presents a list of signals as well as a "picture" of the PLD. All I had to do was "drag and drop" each signal onto the desired pin.

Now the final compilation phase can be executed. This phase attempts to "fit" the circuit into the PLD with the pin assignments. The software I used does several iterations to complete the fitting process. I have seen up to 20 iterations. If it is successful, a file is created that is used to program the PLD. If the process is not successful, some pin reassignment will be necessary.

Finally, it is time to program the PLD. A programming device or equivalent circuit is required. I was able to obtain a programmer from the PLD manufacturer; but, since the circuit consists of a common IC and a few resistors, it would not be difficult to build one. The PLD I selected is capable of in-system programming. This requires only that I implement the appropriate connector on the circuit board with four connections to specific PLD pins. These four pins can be used for I/O, but I chose to not do that. The programmer connects to the printer port of the PC and the connector on my board. Once the PC software programmed the PLD, I removed the programming cable from the board.

The circuit is now ready for the "smoke" test! Since it is impossible to probe the internal circuit points, I strongly suggest that test points be designed into the PLD circuit. At one point of my design cycle, I had three of them. These allowed me to 'scope some of the critical timing points. Because I had previously implemented identical circuits using discrete logic, my debugging was minimal, so I did not need many test points. Untested circuits will probably require more. I

Table 1—Printer Port Signal Usage

Output Control Bits

Pin	Printer Port Name	Usage
1	/C0: Strobe	RegSel 0
14	/C1: Auto-Linefeed	RegSel 1
16	C2: Initialize	RegSel 2
17	/C3: Select-Printer	Strobe

Input Control Bits

Pin	Printer Port Name	Usage
10	S6: Ack	PreTrigDone-L
11	/S7: Busy	
12	S5: Paper-Out	AddrClockEna-L
13	S4: Select	Trigger Latch-L
15	S3: Error	

Data Bits

Pin	Printer Port Name	Usage
2 - 9	D0 - D7	Data
18	Ground	

[1]A package containing additional details of the PLD connections and PC-board etching patterns is available from *ARRLWeb.* You can download this package at **http://www.arrl.org/qexfiles/**. Look for 0307CICC.ZIP.

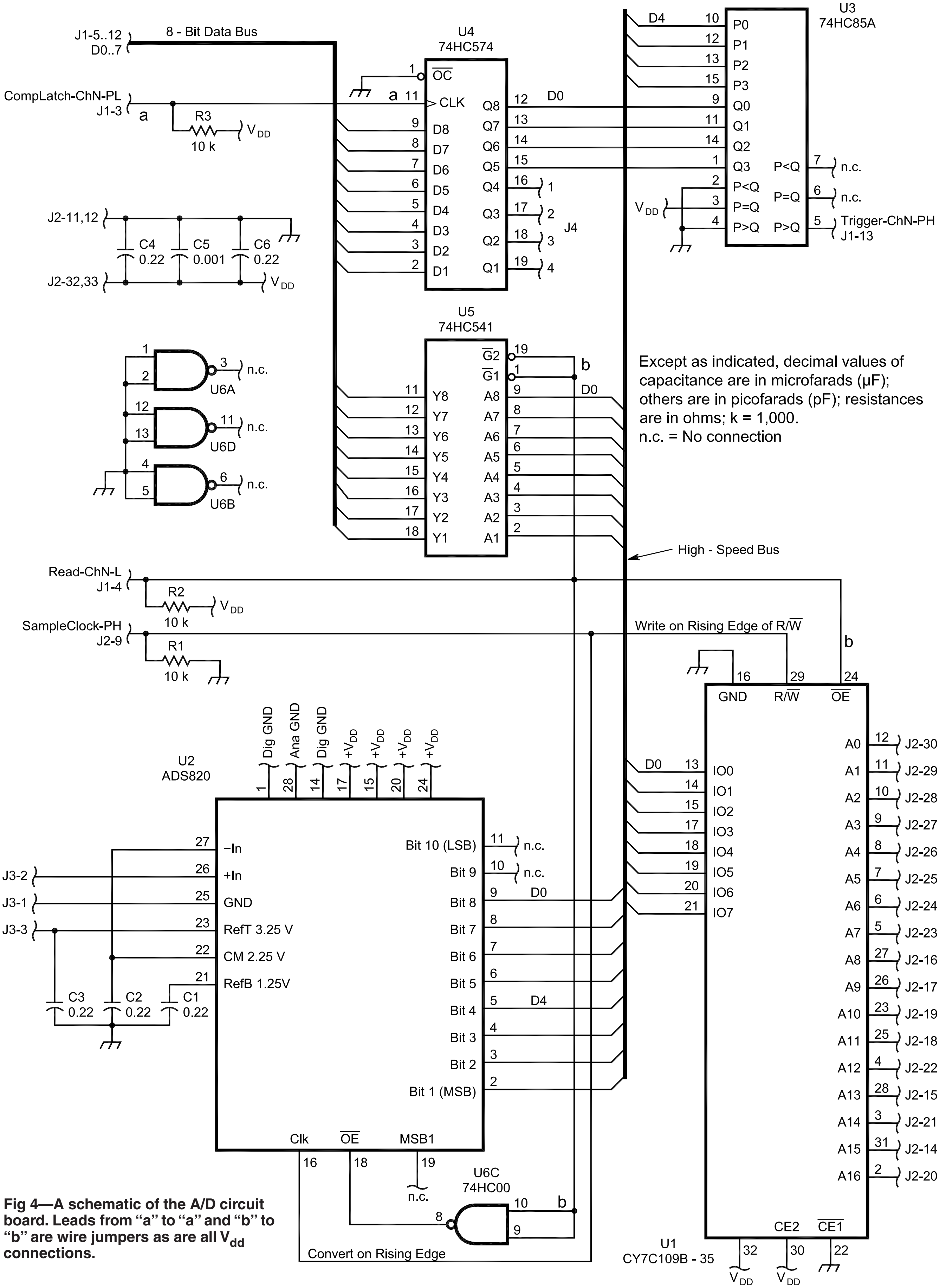

Fig 4—A schematic of the A/D circuit board. Leads from "a" to "a" and "b" to "b" are wire jumpers as are all V_{dd} connections.

recommend that outputs be buffered so that external loading of the I/O pins does not adversely affect system operation.

This was my first attempt at using PLDs, and I found it to be much easier than expected. The free software, downloaded from the Web, is fairly intuitive and comes with a tutorial. I ran the tutorial through the first dozen or so steps; then, like a typical engineer and ham, went off on my own. I was able to go from starting with no previous experience to a finished product within a few weeks working an hour or so several evenings a week. Table 2 shows a complete list of the possible I/O signals and parameters that may be used to define the operation of the counter; Table 3 lists the parts used in each board.

Circuit Descriptions

I have followed a naming convention for the signal names to more easily determine their operation and make the schematics and other documentation easier to follow:

1. Dynamic signals have a "PL" or "PH" suffix, indicating "pulse low" or "pulse high."
   Example: *SysReset-PL*.
2. Static signals have an "H" or "L" suffix indicating a "High" true or "Low" true state.
   Example: *Read-Ch0-L*.
3. Static signals, which are neither high nor low true, do not have a suffix.
   Example: *TimeBaseSel0*

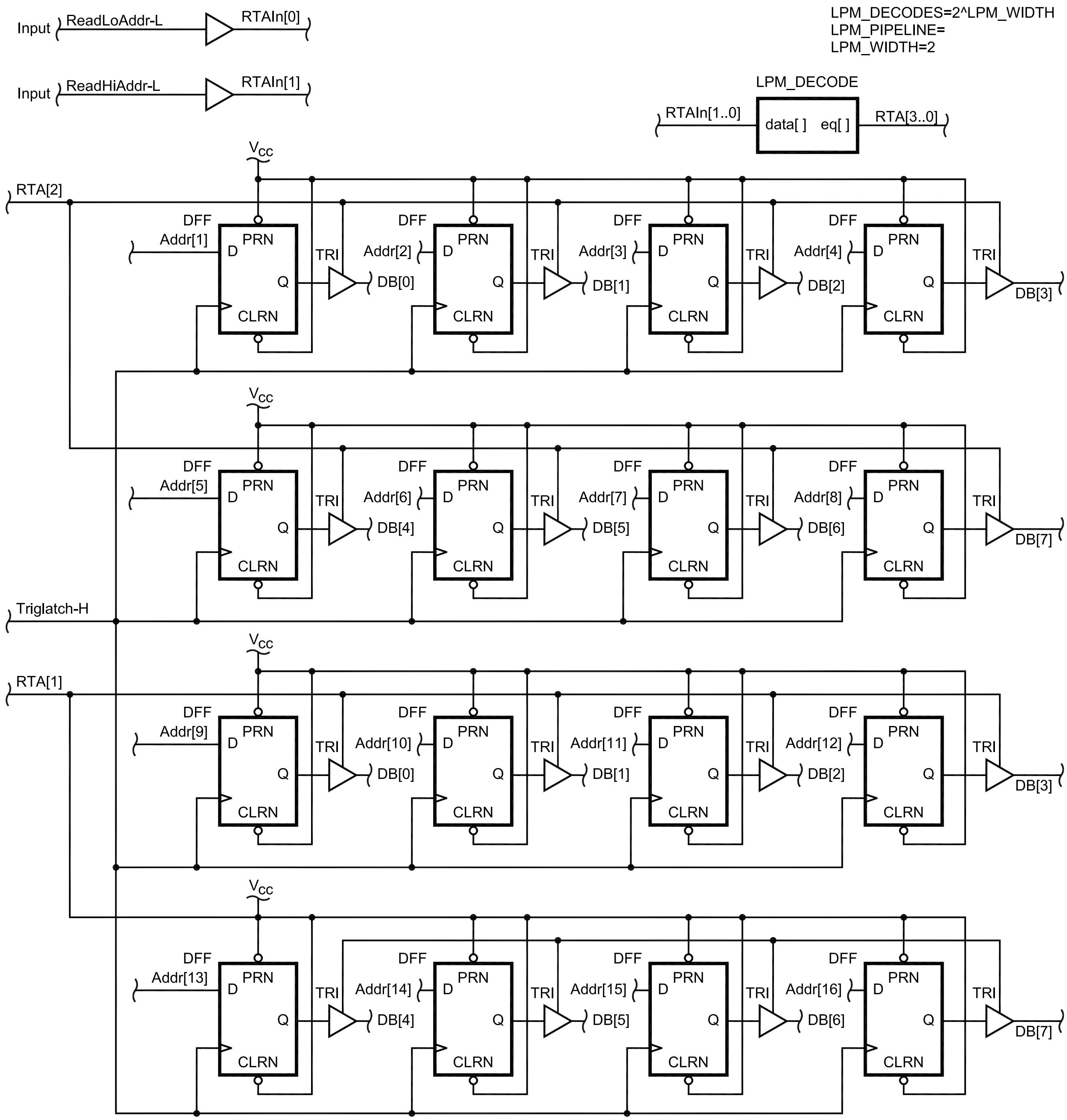

Fig 5—A schematic of the PLD Trigger Address Latch circuit.

In general, I have labeled only signals that go between circuits.

Control Circuit

The main purposes of the Control Circuit (Fig 12 and 13) are to provide the interface to the PC (parallel port) and develop the static signals used to control the remaining circuits. The printer-port control bits are used to control the primary-decoder (U1) function. The functions performed by the primary decoder are:

- System Reset
- System Enable
- Secondary Decoder and Time Base Select Strobe—U2
- Read Clock and Secondary Decoder Read Strobe—U5
- Secondary Decoder Write Strobe—U4

Except for the Time Base Select signals, all of the signals generated by this circuit are low-true pulses.

There is also a bus transceiver (U3) that controls the direction of data flow between the PC and the DSO/LA. It uses the *ReadClock* to determine the data direction. When *ReadClock* is low, read from the DSO/LA; when it's high, write to DSO/LA. Although many of the circuits allow for customization, this one does not, since the software is written to correspond with the functions it performs.

Time Base

The operation of the Time Base is rather straightforward (see Fig 8). There are three control bits (with possible expansion to four) that come from the Control Circuit (*TimeBaseSel*). These bits control a multiplexer that is used to select from among eight signals that can clock the Address Generator (*AddrClk-PH*). Seven of these are also the Sample Clock signal for both the A/D and LA circuits (*SampleClock-PH*). The eighth signal is for advancing the Address Generator when the program needs to read the data from the A/D and LA RAMs. The 20-MHz oscillator and Sample Clock are enabled by a signal from the Trigger Control Circuit (*SampleClockEna-H*).

Notice that the signal driving the Address Generator goes through three inverters, while the signal that drives the Sample Clock only goes through a single gate. There are two reasons for this configuration:

1. The Sample Clock should be disabled when reading from the A/D and LA Circuits.

2. The Address Clock is delayed

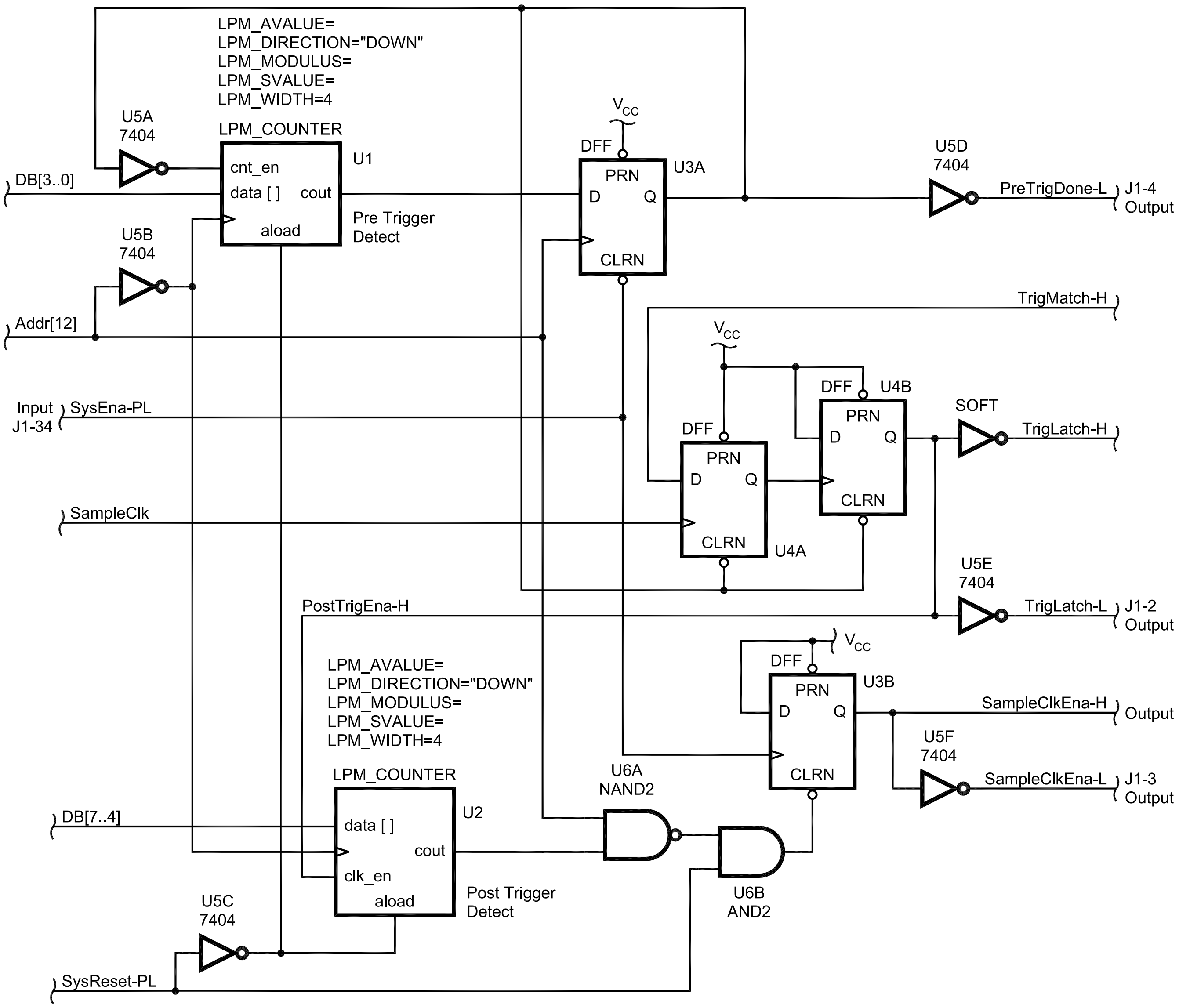

Fig 6—A schematic of the PLD Trigger Control circuit.

slightly so that the input signals are sampled a short time (two gate delays) before the address bus is incremented. This allows the input signals and address bus to settle for almost a full clock period before the data is sampled and is really only significant at the highest sample rate but is necessary to meet the access time specification of the RAM.

I elected to make the sample rate/period circuit as simple as possible. I have used binary dividers to generate the various sample rates. Starting with a 20-MHz clock the next rate is 10 MHz, followed by 5 MHz and so on. The sample periods with this circuit are: 50 ns, 100 ns, 200 ns, 400 ns, 800 ns, 1.6 µs and 3.2 µs. These may seem like strange values, but it really does not make any practical difference in the interpretation of the displayed signals. Since the software allows you to measure the time between cursors, it accounts for the sample period. Also, the software allows you to set the time scale.

The design of the system is flexible, so if you prefer to use sample periods different from what I have chosen, the circuit can be redesigned to implement the ones you like. I will be more than happy to customize the PLD for anyone building this system. The sample periods must be defined in the INI file. Simply relate the decoder input value to the sample period as follows: SELECT_<decode value:1..15> = <sample period>. For example: SELECT_1 = 50 ns. The program will correctly interpret nanoseconds, microseconds and milliseconds as units of time.

Address Generator

This is a 17-bit synchronous binary counter that yields 2^{17} = 131,072 addresses (see Fig 8). It is driven by the Address Clock from the Time Base Circuit. The counter outputs are all set to zero by the *SysReset-PL* signal from the Control Circuit. Because of the way the Pre and Post Trigger circuits operate, the full count is not utilized. This will be explained further in the discussion of the Trigger Control circuit.

The original design of the circuit called for 74HC161 binary counters that are specified to 25 MHz with a 5-V supply. When more than two units are cascaded, however, there is a glitch. I had not thoroughly read the details of the specification and missed the information on the glitch. I thought that since they were rated to 25 MHz, I would not have a problem since I was only going up to 20 MHz. The glitch occurs because of internal delays when using the Ripple Carry Out. This limits the upper frequency to 17 MHz when cascading. The solution was relatively simple: use 74AC161 devices instead. They are rated at a much higher frequency but draw quite a bit more current. Since I have now converted the circuit to a PLD, the above situation is no longer applicable, but I thought it worth mentioning since it was part of my learning experience.

Trigger Detect

Those of you who have used commercial LAs will recognize that the triggering available with this design is very limited. These units will usually have quite a few possibilities

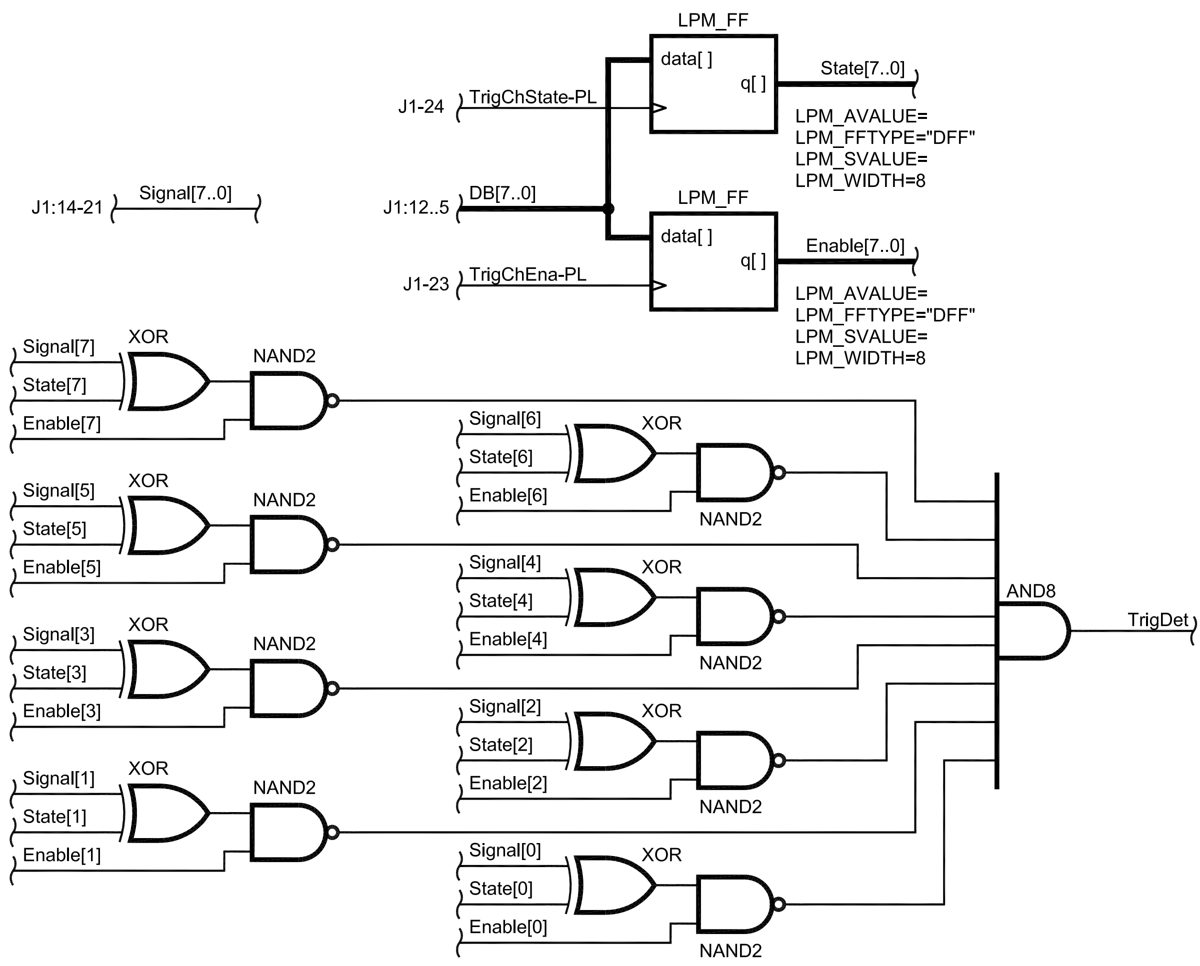

Fig 7—A schematic of the PLD Trigger Detect circuit.

for triggering such as:

- High level
- Low level
- Low to high transition
- High to low transition
- Either transition
- Various logic combinations of selected signals

My circuit implements only these three:

- High level
- Low level
- Ignore the signal

This circuit compares the current state of the trigger inputs to those that have been selected by the operator. The circuit operates as an 8-bit **AND** gate (see Fig 7). Each of the eight input signals can be enabled or disabled and inverted or not inverted. The source for each of the eight inputs is up to you. I have mine set up so that the first six signals are channels 0 through 5 of the first LA board. The remaining two inputs are from the two A/D boards. This is one area where the system is not very flexible. You cannot dynamically select from among all the possible inputs. You must predetermine which eight signals you will use as possible triggers. If this is not flexible enough for your applications, you will need to implement a switch of some kind. I am certainly open to suggestions about how to make this function more flexible.

Each exclusive-or gate is used as programmable inverter. When its control input is low, the output follows the input. When the control input is high,

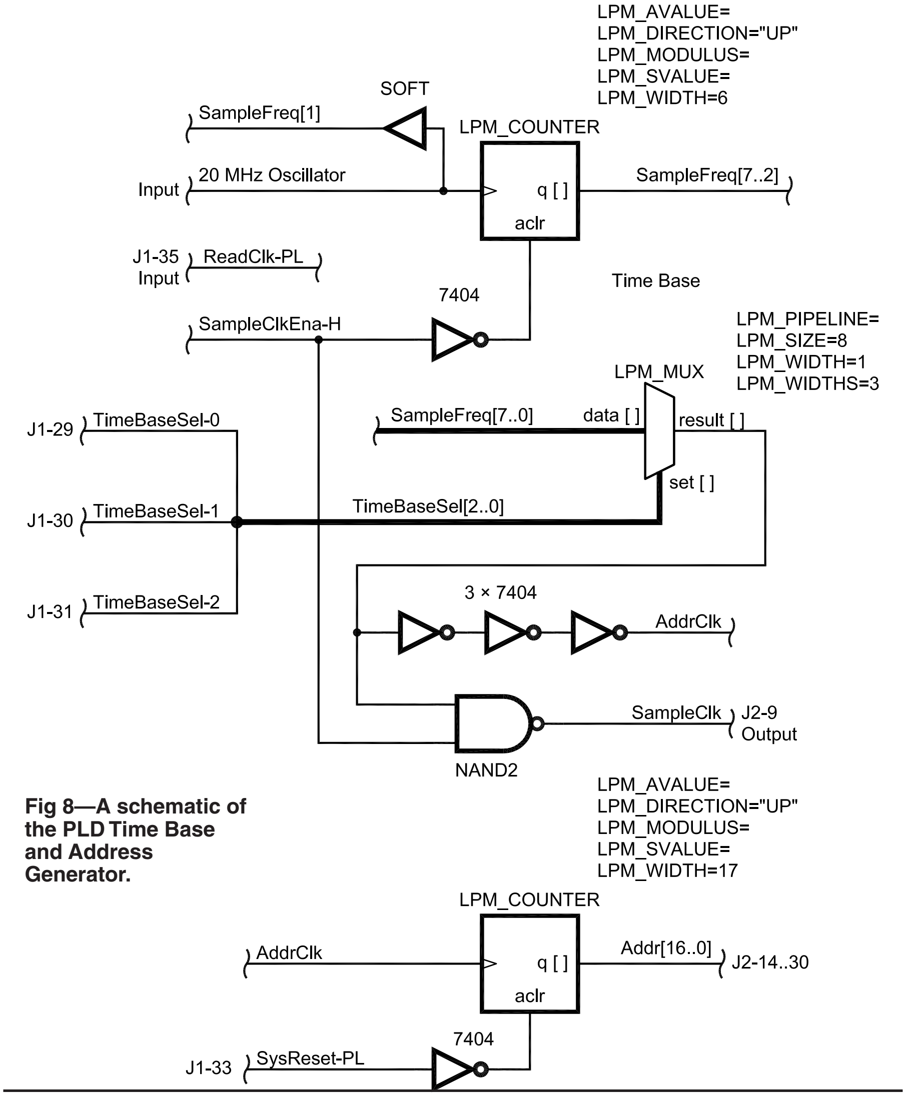

Fig 8—A schematic of the PLD Time Base and Address Generator.

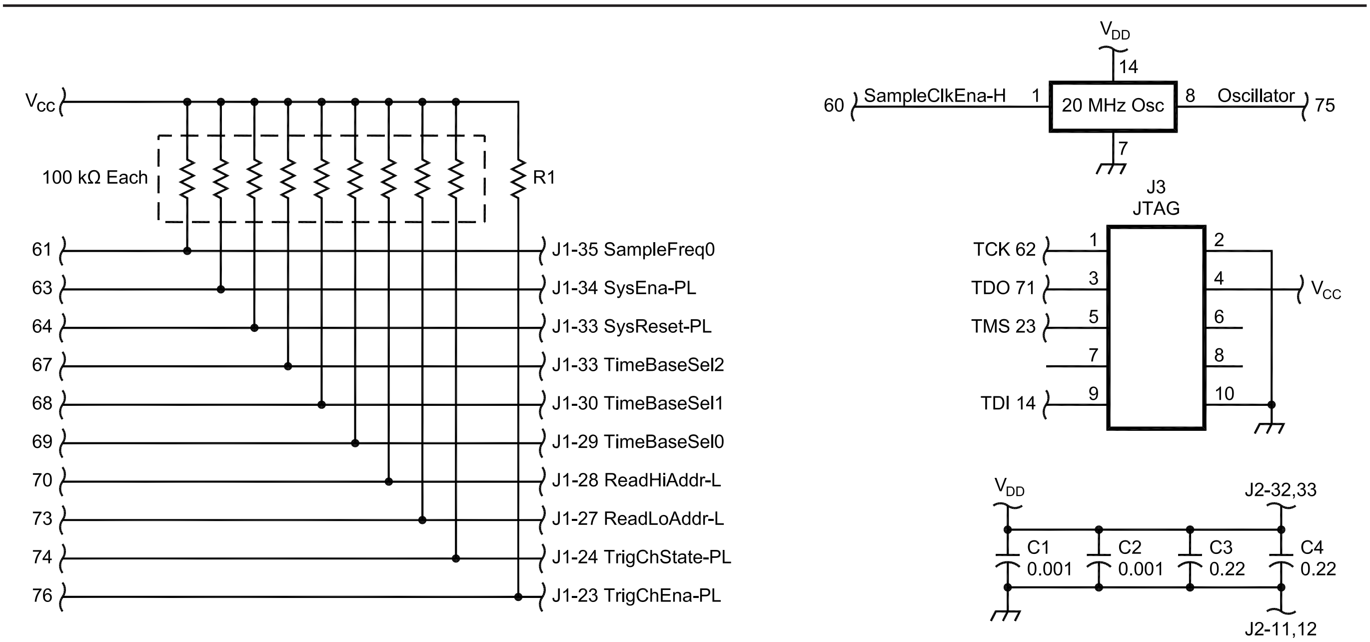

Fig 9—A schematic of the PLD board. Numbers without connector designations (J1 or J2) are on the PLD (EPM7128SLC84). See Table 2 for most signal connections.

the output will be the inversion of the input. The following **AND** gate is used to enable/disable the input signal. When its control signal is low, the output is forced high, independent of the input signal. This basically creates a match condition for the final eight-input **AND** gate. If all the signal inputs are disabled, there will be a continuous match condition.

The original, discrete-logic version of the circuit was quite different. The 8-bit latches were 74HC574s, very similar to the PLD implementation. However, the enable/disable circuit used tri-state buffers (74HC126) and the output **AND** gate was actually an 8-bit comparator (74HC688). The circuit required five ICs. If I were to implement the circuit I designed for the PLD as discrete ICs, it would require seven. Since the circuit is now in a PLD, I can probably modify it to meet some other requirements.

Trigger Control

The Trigger Control (Fig 6) was perhaps the most difficult circuit to design and get working as I wanted. My goal was to have a programmable pre-trigger capability—unlike my original LA, which has a fixed amount of pre-trigger. I have added "U" numbers to the schematic of the PLD circuit to make it easier to reference the different parts of the circuit. Both U1 (the pre-trigger counter) and U2 (the post-trigger counter) are 4-bit down counters. They are clocked by the inverted A12 signal. As such, they decrement every 8192 samples.

You can set the pre-trigger count to any value between 0 and 14. The number of pre-trigger samples can be determined by this formula: pre-trigger samples = (pre-trigger count × 8192) + 4096. The post-trigger count is set by the system as follows: post-trigger count = 15 – pre-trigger count. The total number of samples is (15 × 8192) + 4096 = 126976 = 2^{17} – 4096.

Once the system is "armed," the pre-trigger counter starts counting down to 0. When it reaches 0, the output of U3A will go high on the next positive transition of A12 (4096 samples later). This enables a Trigger Match to be detected. A Trigger Match will then cause the *Q* outputs of U4A and U4B to go high, thus enabling the post-trigger counter. When it reaches 0, the sample clock will be disabled and the system will stop sampling.

Three status signals are monitored by the program that allow it to determine the state of the system:

- *PreTrigDone-L*
- *TrigLatch-L*
- *SampleClockEna-L*

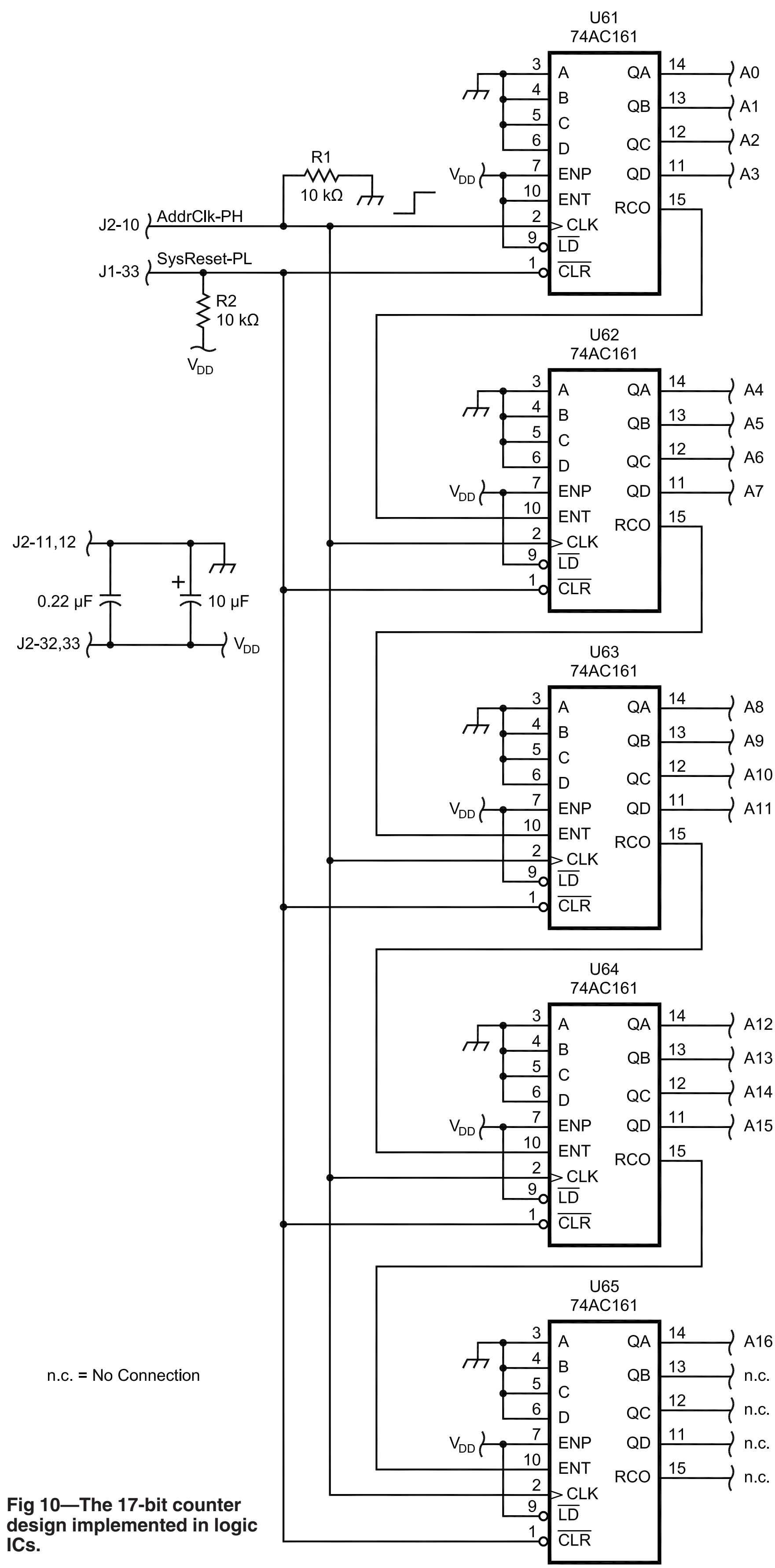

Fig 10—The 17-bit counter design implemented in logic ICs.

A message is displayed as the system waits for each of these signals. Please notice that each of these signals is derived from signals used internally by the Trigger Circuit. However, I have buffered them via sections of U5 so that the wiring associated with getting them to the PC does not interfere with the circuit operation.

The PLD version of the circuit is almost identical to the discrete version. I would like to detail some of the differences for those of you who wish to convert a circuit to a PLD.

The carry out of PLD counters is true when high and becomes active as soon as the count reaches 0 or 15, de-

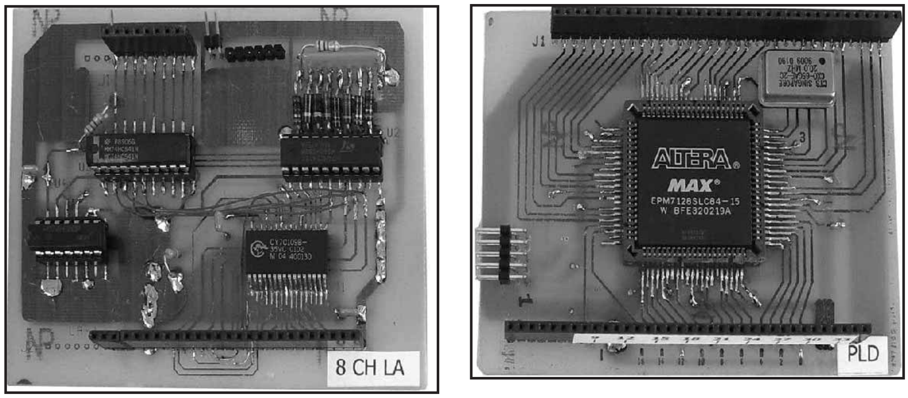

Fig 11—The 8-channel LA board and the PLD board. Notice the two board-stacking connectors on the PLD board.

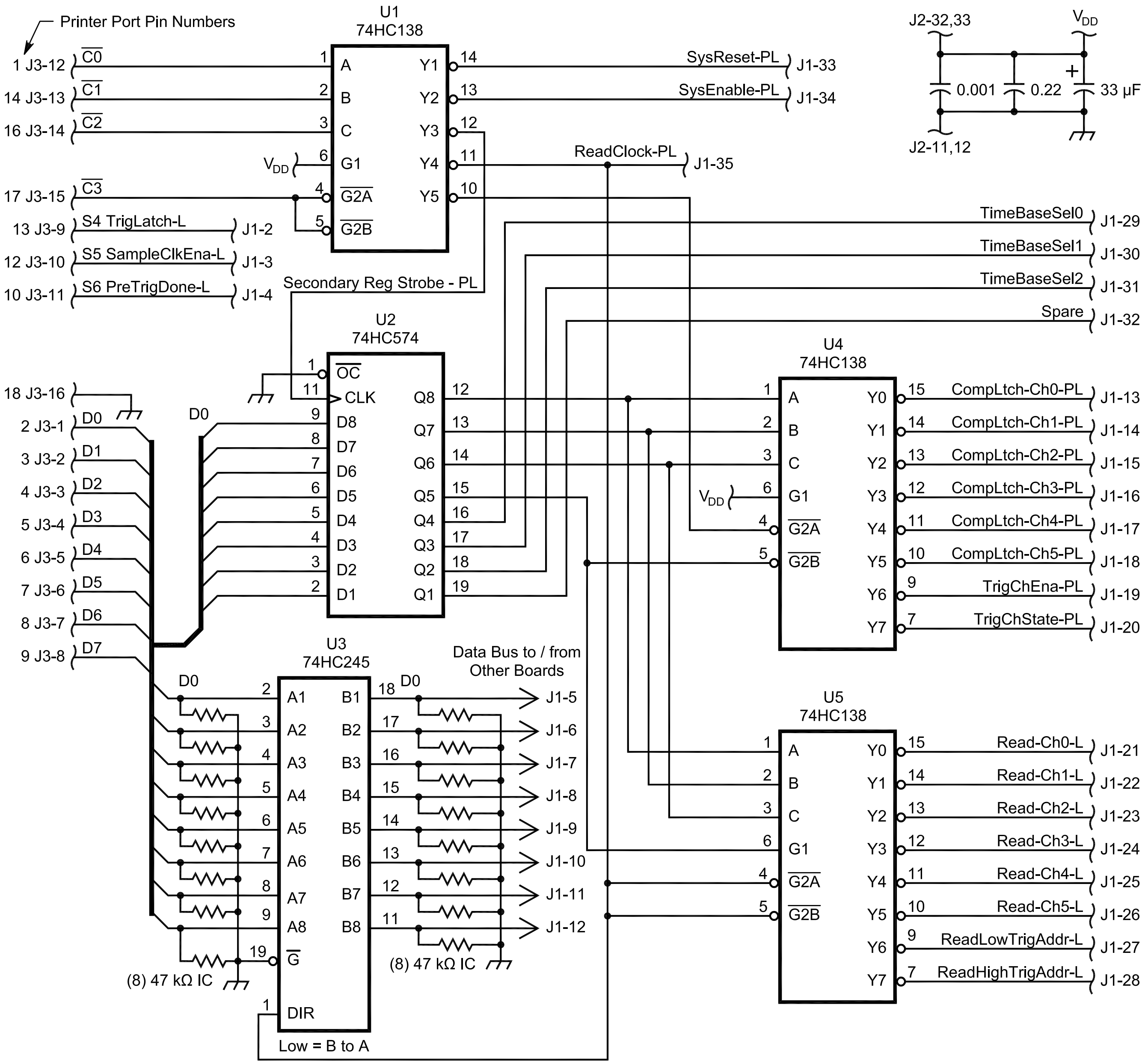

Fig 12—A schematic of the DSO/LA control board.

pending on the count direction. The discrete device I used is a 74HC191. Its carry out is true when low and is gated with the clock so that it goes true during the second half of the end count.

Both counter-control inputs, Count Enable and Load, are true when high for the PLD but are true when low for the '191.

The discrete version required an **AND** function so I used a 74HC00 as a **NAND** and then followed it with another section to invert it. This is certainly not necessary in a PLD, since it has built-in **AND** blocks.

LA

This is another relatively simple circuit (see Fig 14). All it must do is apply eight input signals to the data bus of the RAM and allow the data bus to be read back by the PC. There are two resistor networks in the input circuit. One insures that the input-switch device has no floating inputs. The other limits current in case of excessive applied signal voltage. As can be seen on the schematic, U2 and U3 create an eight-pole, two-position switch controlled by the *Read-ChN-L* signal. When *Read-ChN-L* is high, the RAM data bus is connected to the input signals, and the *SampleClock-PH* signal writes the data to the RAM on its rising edges. The *SampleClock* signal is high during the read operation. When *Read-ChN-L* is low, the RAM data bus is connected to the system data bus, which is eventually read by the PC. Each LA board has its own *Read-ChN-L* from the Control circuit.

Please note that the address bits driving the RAM are "scrambled." This was done in order to make the circuit-board layout easier. It was much easier to route the address signals to the RAM from J2 using this technique as opposed to routing the address lines to their "correct" pins. This is a common technique in industry. The RAM really does not care which signal from the address generator is connected to which address input. I have seen many RAM devices that do not assign specific address bits to their address inputs.

A/D

The circuit is somewhat similar in operation to the LA except that the eight data bits come from an A/D channel instead of individual digital sources (see Fig 4). The *ReadChN-L* signal is used to determine whether the circuit is sampling A/D data or transferring it to the PC. U5 is used to connect the RAM data to the system data bus when *ReadChN-L* is low. When this signal is high it allows the *SampleClock-PH* signal to clock the A/D and write data to the RAM.

The A/D I selected (ADS820) requires a single 5-V power supply and has a maximum 20-MHz sample rate and a full power bandwidth of 65 MHz. There are faster pin-compatible versions available, but I did not feel that I could adequately implement the circuits for higher frequencies. There is nothing in the system design, however, that would prohibit you from implementing a faster A/D if you desire. The RAM (CY7C109B-35) is good up to about 28 MHz but has faster versions. The -20 is a 50-MHz part.

When sampling the input signal, the rising edge of *SampleClock-PH* initiates an A/D conversion and writes A/D data to the RAM. These types of A/D converters have a pipeline architecture. In the ADS820, this causes a six-cycle latency between when a signal is sampled and when the converted data is available on its output bus. In my design, this means that I need to account for the latency in the software so that I store the data in the correct place.

There are two additional functions on this card:

- Digital comparator
- Four-bit latch for controlling the A/D buffer

The digital comparator allows the user to set a trigger level that can then be used to trigger the system. On the schematic, notice that I have labeled the RAM data bus as "High Speed Bus." I tried to be as careful as possible in routing these signals in order to maintain signal integrity. The comparator is operating on the A/D samples at the sample rate, as high as 20 MHz. When the digitized signal value is greater than the comparison value stored in the upper four bits of U4, the **P>Q** output of U3 will go high. This signal can be used to trigger the system. I have implemented a four-bit comparator so the resolution is only 1 part in 16 (6.25%). I felt this was a reasonable compromise so that I could use the remaining four bits to control the A/D buffer.

The timing requirements for writing

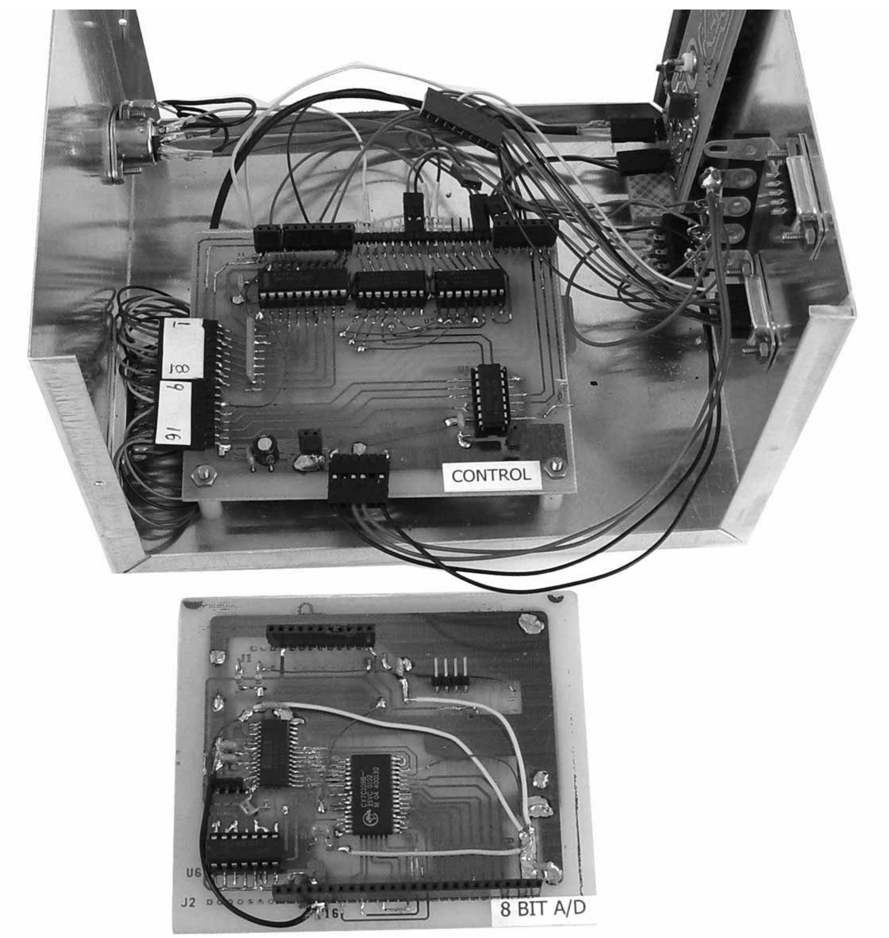

Fig 13—A photo of the Control circuit board and one 8-bit A/D board. Two of the five jumpers are there to "fix" broken traces. The other three are designed-in because I could not route them. There is one IC mounted on the underside.

A/D data to the RAM can cause problems if the circuit design is not carefully considered. A careful inspection of the A/D timing shows a "dead" time on its data bus immediately following the positive transition of the clock. Note that writing to the RAM also occurs on the rising edge. At first I thought this might cause a problem. However, the A/D specifications show that the data is good for a minimum of 3.9 ns after the rising edge, while the RAM specifications show a 0 ns input hold time for the data. Although 3.9 ns does not seem like very much, it is sufficient for the circuit to operate properly.

A/D Buffer

This circuit (see Fig 15) is built on a board that is not part of the "stack" forming the main body of the instrument. I wanted it as close as possible to the signal source, so I designed a small board that mounts directly to the front of the LA/DSO housing and has the input (BNC) connector mounted to the board. This keeps the shortest possible signal path to the buffering op-amp. This is a simple dual op-amp circuit that has three basic functions:

1. Buffer the signal, which may be up to 10 MHz.
2. Input attenuator to allow a –5 to +5 V input span.
3. Condition the signal to the 4-V span of the A/D converter.
4. Offset adjustment to center the signal about 2.5 V.

This particular op amp has relatively high input and offset voltages and currents so its dc characteristics are not the best. Nonetheless, it is fast enough to handle 10-MHz signals as long as you do not require the full 8-bit accuracy. There are op amps

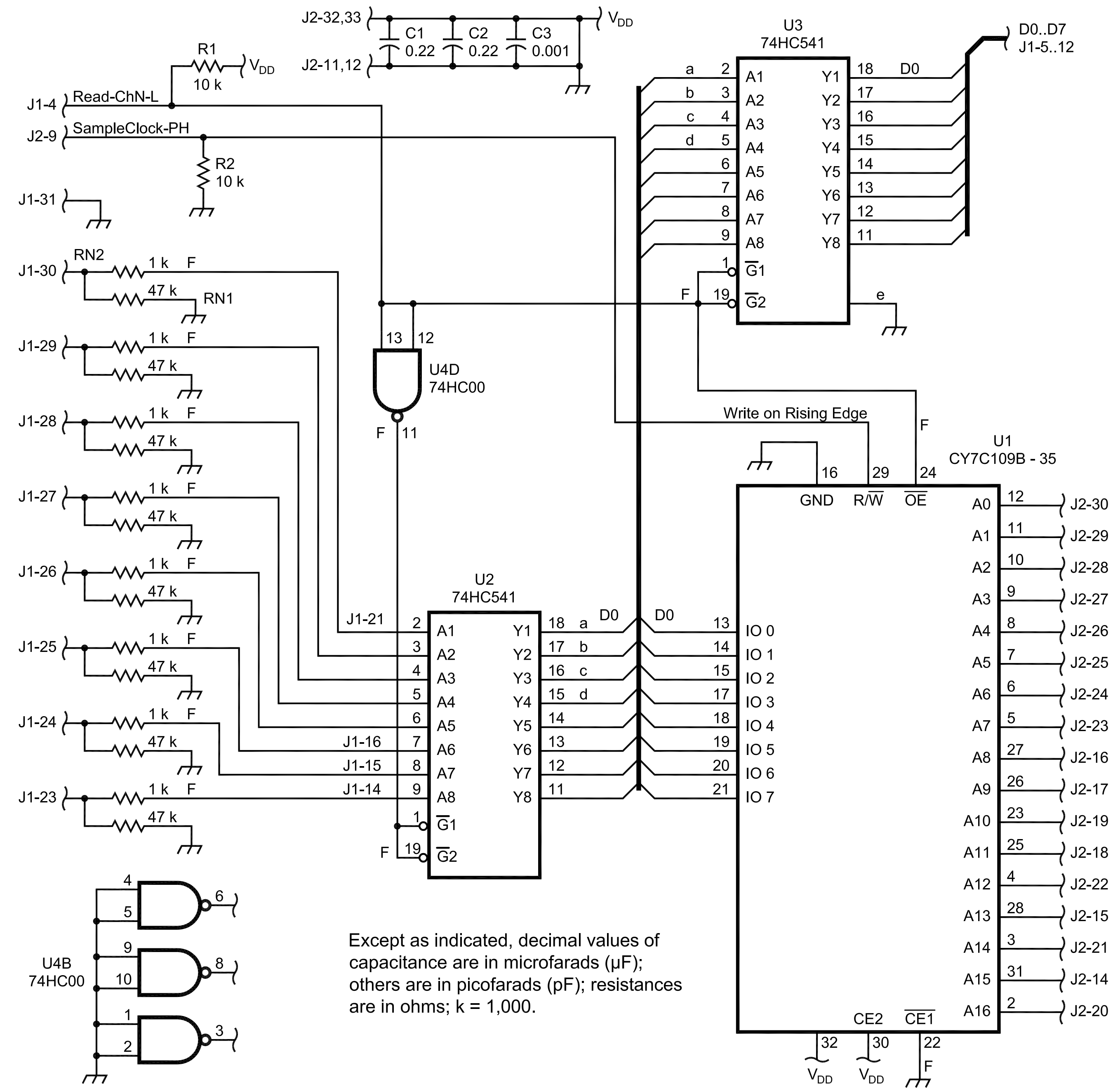

Fig 14—A schematic of a logic-analyzer circuit board. Wires labeled "a," "b," "c," "d" and "e" are jumpers. Letters "F" indicate a connection between the two copper layers of the circuit board.

available that would be better, but they are probably more expensive and this great expense was not one of my primary design goals.

The circuit I designed does not use the four control bits available from the A/D card. I did not want to add this complexity to my circuit for the first design. This means that the basic input level is –5 to +5 V. I use attenuator probes to extend the range as required. I will be designing a programmable attenuator board sometime in the near future and will post it on my Web site (**www.qsl.net/k3pto/**). The input ranges are completely flexible, and you can make them whatever you want. The INI file allows you to specify the ranges associated with the four control bits (16 values) coming from the A/D circuit.

Trigger Address

This is perhaps the simplest of the circuits. It is simply a 16-bit latch that is triggered by the output of the Trigger Detect Circuit via the Trigger Control Circuit. This was done so that only a single trigger event will cause the address to be latched. I used a 16-bit latch, implemented via two 8-bit latches, because I did not want to build the necessary additional circuitry for the 17th bit. The program will read the upper 16 bits and then determine if the data actually meets the trigger criteria. If it does not, then it must be the next higher address. This little bit of extra programming saved me several ICs in the circuit design. However, now that I am using a PLD, I may go back and revisit this as I work on improving the system.

System Operation

The operation of the DSO/LA is fairly intuitive. You can get the basics simply by seeing the pictures that follow. There will be a complete Help file available, which explains each of the controls as well as the contents of the INI file. Here is a brief explanation of each of the menu items:

- File—typical file operations for reading and writing both INI and data files.
- Boards—define the board for each of the six channels.
- Trigger—define trigger conditions, including the pre-trigger/post-trigger values.
- Display—select Time Base, Zoom factor, Slide factor and so on.
- Cursors—enable the four time-measurement cursors.
- Function Keys—list the applicable function keys.
- Debug—some hardware-debugging aids as well as some dummy data so you can “play” with the display.

Future Enhancements

I am in the process of redesigning the layout of both the A/D and Logic Analyzer boards to make them easier to build. Both will probably have a PLD to replace the logic devices. This will also make it easier to lay out. These new boards will be totally backward compatible with the current designs so that they can be installed in my current system.

As indicated at the beginning of the article, I am considering a serial interface. If I design one it will probably have Ethernet capability also. I have not completely thought this through yet, but with an Ethernet interface it is easy to operate the unit over the Internet.

Once the data has been captured, it can be analyzed in many ways. Currently, I simply display it. I plan to add several measurement capabilities by the time this article is printed. Some possibilities are:

1. Count the number of logic transitions between cursors.
2. Decode an ASCII bit stream.
3. Decode SPI—synchronous data with a clock.
4. Decode I^{2}C—more difficult than SPI but still a possibility.
5. Perform some limited math operations on both the LA and A/D data.
6. Possibly even a limited spectrum analysis—if I can develop or obtain some code.

Suggestions from anyone who builds a system are welcome.

Some Suggestions for Making PC Boards

Make the traces as wide as possible. Most of the boards started out with 20-mil traces. After completing the design I went back and made each trace as wide as possible. If necessary, I narrowed the trace where it passes between IC or connector pins. The undercutting of traces during etching has minimal effect on wide traces.

Make the ground traces even wider to minimize the resistance of ground leads. I routed signal traces and grounds first, ignoring the +V leads. Since this was my first effort at double-sided printed circuit boards and I do not have the ability to implement plated-through holes, I felt it better to use wire jumpers for the +V leads than for signals. This allowed me to use relatively heavy wires for the power leads.

Implement ground fill where possible. This reduces the amount of copper that must be etched as well as giving more ground area.

Use a scrap piece of perforated board as a drilling template for the connector holes. I had some unused circuit boards from RadioShack with 0.1-inch-spaced holes. I lined up the board holes with holes to be drilled and taped the perf board to my circuit board. Viewing the boards with a 50-W lamp behind them made this relatively easy.

I have no drill press, but an attachment for my electric drill allows it to operate as a drill press. Without this

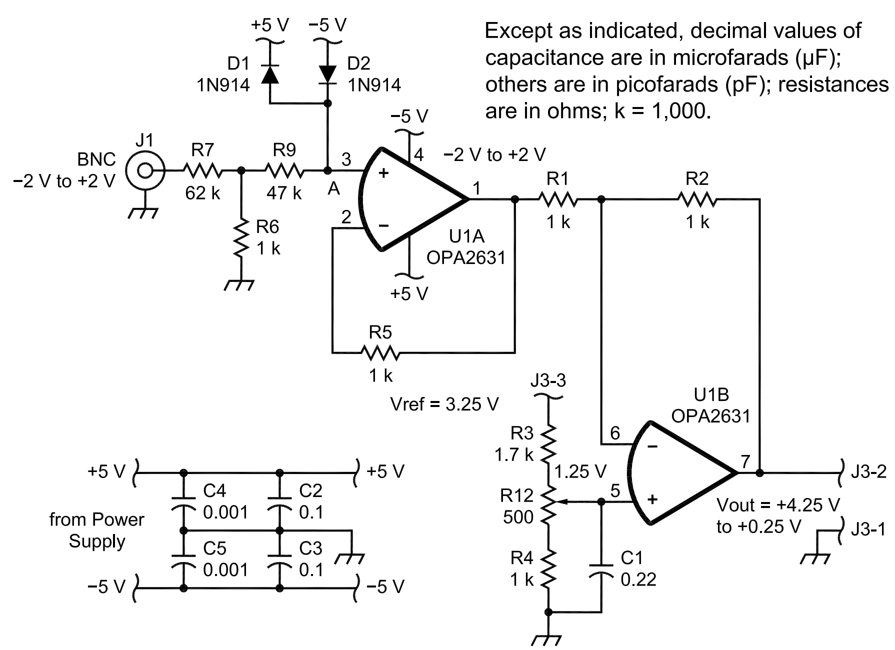

Fig 15—A schematic of the A/D input buffer and conditioning circuits.

device I could not have drilled the circuit boards.

I had a relatively bad experience with drill bits with thickened shanks. The ones I purchased broke rather easily. In order to use the small bits in my drill I wrap thin packaging tape around the upper part of the shank. This worked quite well as long as I wrap the tape carefully.

For those holes that are not on 0.1-inch centers I used a center punch to mark the hole. I modified my punch by cutting off some of the spring so that it makes a smaller dent in the circuit-board material.

Check every connection for both continuity and soldering integrity. I was able to minimize troubleshooting by finding several assembly problems before installing ICs in their sockets and applying power. I also tested every printed wiring trace for continuity after installing all components except ICs.

If the etchant instructions suggest etching at an elevated temperature,

Table 2—Possible I/O Signals and Parameters to define the Operation of the PLD Counter

INPUTS

Port Name	*Required*	*Description / Comments*
data[]	No	Parallel data input to the counter. Input port LPM_WIDTH wide. Uses load or sload.
clock	Yes	Positive-edge-triggered Clock.
clk_en	No	Clock Enable input. Enables all synchronous activities. Default = 1 (enabled).
cnt_en	No	Count Enable input. Disables the count when low (0) without affecting sload, set, or sclr. Default = 1 (enabled).
updown	No	Controls the direction of the count. High (1) = count up. Low (0) = count down. Default = up (1). If the LPM_DIRECTION parameter is used, the updown port cannot be connected. If LPM_DIRECTION is not used, the updown port is optional.
cin	No	Carry-in to the low-order bit. If omitted, the default is 0.
aclr	No	Asynchronous Clear input. Default = 0 (disabled). If both aset and aclr are used and asserted, aclr overrides aset.
aset	No	Asynchronous set input. Default = 0 (disabled). Sets q[] outputs to all 1's, or to the value specified by LPM_AVALUE. If both aset and aclr are used and asserted, aclr overrides aset.
aload	No	Asynchronous load input. Asynchronously loads the counter with the value on the data input. Default = 0 (disabled). If aload is used, data[] must be connected.
sclr	No	Synchronous Clear input. Clears the counter on the next active Clock edge. Default = 0 (disabled). If both sset and sclr are used and asserted, sclr overrides sset.
sset	No	Synchronous set input. Sets the counter on the next active Clock edge. Default = 0 (disabled). Sets q outputs to all 1's, or to the LPM_SVALUE value. If both sset and sclr are used and asserted, sclr overrides sset.
sload	No	Synchronous load input. Loads the counter with data[] on the next active Clock edge. Default = 0 (disabled). If sload is used, data[] must be connected.

OUTPUTS

Port Name	*Required*	*Description / Comments*
q[]	No	Data output from the counter. Output port LPM_WIDTH wide. Either q[] or at least one of the eq[15..0] ports must be connected.
eq[15..0]	No	Counter decode output Active high when the counter reaches the specified count value (AHDL only). Either the q[] port or eq[] port must be connected. Up to c eq ports can be used (0 <= c <= 15). Only the 16 lowest count values are decoded. When the count value is c, the, the eqc output is set high (1). For example, when the count is 0, eq0 = 1, when the count is 1, eq1 = 1. Decoded output for count values of 16 or greater require external decoding. The eq[15..0] outputs are asynchronous to the q[] output.
cout	No	Carry-out (borrow-in) of the MSB.

Parameters

Parameter	*Type*	*Required*	*Description*
LPM_WIDTH	Integer	Yes	The number of bits in the count, or the width of the q[] and data[] ports, if they are used.
LPM_DIRECTION	String	No	Values are "UP," "DOWN," and "UNUSED." If the LPM_DIRECTION parameter is used, the updown port cannot be connected. When the updown port is not connected, the default for the LPM_DIRECTION parameter is "UP."
LPM_MODULUS	Integer	No	The maximum count, plus one. Number of unique states in the counter's cycle. If the load value is larger than the LPM_MODULUS parameter, the behavior of the counter is not specified. This information is from the MAX+plus II help file. The software is available from the Atmel Web site: **www.Atmel.com**.

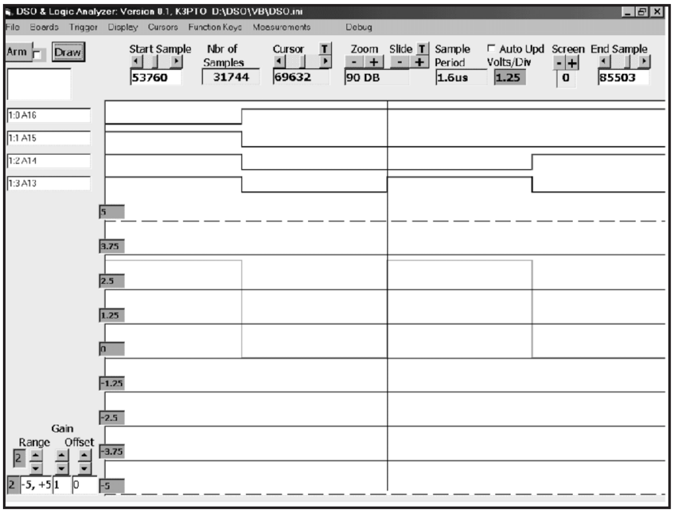

Fig 16—Four address bus signals as captured by an LA board as well as the A12 signal as captured by an A/D board.

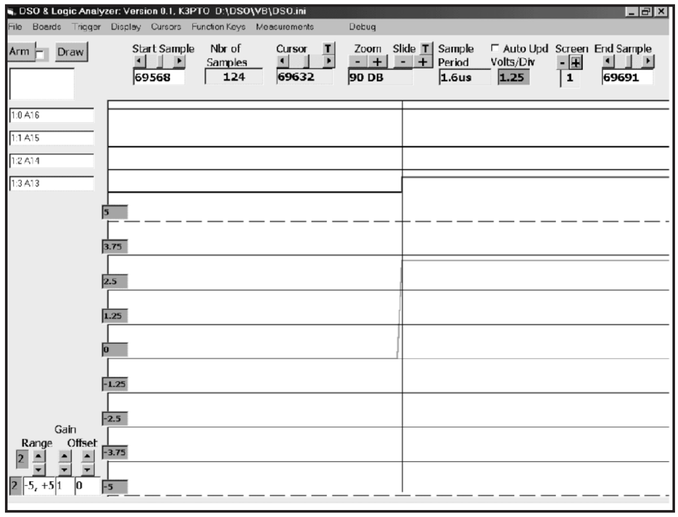

Fig 17—The same signals as Fig 16 but zoomed in.

believe them! The etchant I used, Sodium Persulfate, works best at about 110°F. I found that it does not work well at all below 100°F.

Looking closely at the photos, you may notice that the IC sockets look a little odd. I designed the boards for SMT ICs. However, I did use mostly normal DIP devices. I found IC sockets with the flat side of their pins parallel to their long edges. By bending the pins to the side and extending traces at least 0.2 inches beyond the socket sides, the socket pins can be soldered on top of the traces. I had to trim the leads on a few sockets, but this is quite easy.

Mount ICs on both sides of the boards where necessary.

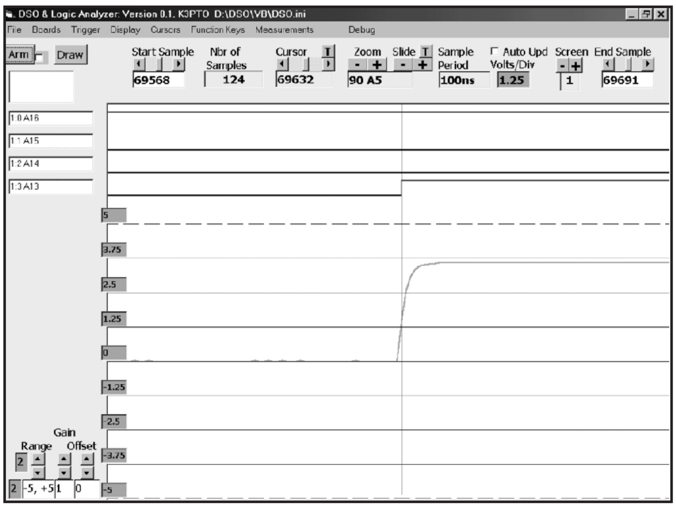

Fig 18—A view of A4 instead of A12. Also the time base has been changed from 1.6 µs per sample to 100 ns per sample. Notice that the signal fall-time can now be seen.

Some General Construction Information

Each board has several hand inserted feed-through wires and jumpers. All are labeled in copper. Each feed-through wire is labeled with an "F." The jumpers are labeled with the same lower-case letter at each end of the jumper. The silkscreen shows the locations of all resistors and capacitors. The leads of discrete resistors and capacitors often double as feed-through wires.

Be careful when soldering the board-to-board connectors. Do not get solder high up on the pin. If you do, it will be more difficult to connect to the board below.

The IC socket for the oscillator on the PLD board is the only one in the system mounted as a through-hole socket.

Cut each board the same size: 4.25×3.5 inches.

Insertion of the wires into the sockets for the right-angle connectors can be quite tedious, so I used wire removed from eight-conductor telephone cable. It is flexible and of eight different colors. At first, I soldered the wires after crimping them by hand, but sometimes the solder would wick up into the contact area. I did not solder the last several I wired, and they are holding up fine.

There are several connections from the Control board to the input boards. For several of these, I simply put heat-shrink tubing over the connector pin after crimping it rather than cut a housing for it.

Remember that you will loose a pin when you cut the board-to-board connectors to the appropriate size. File the cut side flat to make it look better.

Keep the main circuit functions on separate boards. This makes for a very modular system that can be easily customized. It also makes it easier to test the individual circuits. This was very important in the early designs, so that I could make changes. It is not quite as important now that most of the circuitry is in a PLD.

Install load resistors on selected inputs. This makes it easier to test the boards and protects CMOS devices, which can be damaged when their inputs float.

Install a few test points on each board—especially at least one ground. This makes debugging much easier! I even put a few test circuits into the PLDs of the first designs so I could monitor some internal signals.

Display Screens

Figs 16 through 18 are screen shots showing various features of the DSO/LA. Fig 16 shows four address bus sig-

Table 3—DSO/LA Parts, Listed by Board

Part	*Qty*	*Vendor*	*Part #*
Miscellaneous			
Cabinet, aluminum, 7.0×6.2×4.6 inches	1	Jameco	11893
Cable, 25 pin D, M-F, 5 feet	1	Jameco	163133
Connector, D Sub 25P, cbl, M	1	Mouser	156-1225
Connector, DIN, 5 pin F ch	1	Jameco	15843
Connector, DIN, 5 pin M cbl	1	Jameco	15878
Desoldering braid, 5 feet	1	Hosfelt	46-130
PW board developer	3	WebTronics	POSDEV
PW board: 12×12 inches, photosensitive	1	WebTronics	GD1212
PW board: etchant	1	WebTronics	
Rubber feet, $^1/_2$-inch square by $^1/_8$-inch high, 12 pcs	1	Hosfelt	85-109
Tubing, heat shrink, $^3/_{32}$, 10 feet	1	Hosfelt	33-131
Wire, #30 wire wrap, 100 feet, red	1	Jameco	22630
Wire, miscellaneous			
Control			
Capacitor, 0.001 µF, 50 V	2	Hosfelt	95-179
Capacitor, 0.22 µF, 50 V	3	Hosfelt	82-102
Capacitor, 33 µF, 25 V	1	Hosfelt	15-455
Connector D Sub 25P, M, rt angle, PCB	1	Mouser	152-3325
Connector header, 36 pin, M, rt angle	1	Jameco	103270
Connector housing, 36 pin	1	Jameco	103157
Connector pin, female for 103157	20	Jameco	100765
IC Digital, 74HC138, 3-to-8 line decoder	3	Jameco	45330
IC Digital, 74HC245, 8 bit xcvr	1	Jameco	45671
IC Digital, 74HC574, 8 D FF, 3-state	1	Jameco	46084
Resistor network, 47 kΩ, 10P, SIP, common	2	Mouser	266-47K
Socket, 35 pin, single row	1	Samtec	ESQ-135-14-T-S
Socket, IC, DIP 16, order increments of 10	3	Jameco	112221
Socket, IC, DIP 20, order increments of 10	2	Jameco	112248
PLD			
Capacitor, 0.001 µF, 50 V	2	Hosfelt	95-179
Capacitor, 0.22 µF, 50 V	3	Hosfelt	82-102
Connector housing, 36 pin	1	Jameco	103157
Connector pin, female for 103157	4	Jameco	100765
Connector header, dual row, 10-pin male, right angle	1	Jameco	203932
Connector header, 36-pin, M, strip header	1	Jameco	103270
IC, PLD, 84 pin, PLCC	1	Arrow	EPM7128SLC84-15
Oscillator, 20 MHz	1	Hosfelt	23-132
Socket, 35 pin, single row	2	Samtec	ESQ-135-14-T-S
Socket, 84 pin, PLCC, through hole	1	Arrow	PLC C-84P-T-SMT
Socket, IC, DIP 14, order increments of 10	1	Jameco	112213
LA			
Capacitor, 0.001 µF, 50 V	2	Hosfelt	95-179
Capacitor, 0.22 µF, 50 V	2	Hosfelt	82-102
Connector D Sub 9P, F, cbl	1	Mouser	156-1309
Connector D Sub 9P, M, right angle, PCB mount	1	Mouser	152-3309
Connector D Sub 9P, hood	1	RadioShack	276-1539
Connector header, 36 pin, M, right angle	1	Jameco	68339
Connector header, 36 pin, M, strip header	1	Jameco	103270
Connector pin, female for 103157	12	Jameco	100765
IC Dig, 74HC00, NAND, Q2	1	Jameco	45161
IC Dig, 74HC541, 8-buffer, 3-state	2	Jameco	46050
IC Dig, SRAM, 128×8, SOJ, 25 ns	1	Avnet	CY7C109B-35VC
Resistor network, 1 kΩ, 16P, DIP, isolated	1	Mouser	652-4116R-1-1K
Resistor network, 47 kΩ, 10P, SIP, common	1	Mouser	266-47K
Resistor, 10 kΩ, $^1/_4$ W, 5%	2		
Socket, 35 pin, single row	1	Samtec	ESQ-135-14-T-S

Part	Qty	Vendor	Part #
Socket, IC, DIP 14, order increments of 10	1	Jameco	112213
Socket, IC, DIP 20, order increments of 10	2	Jameco	112248
A/D			
Capacitor, 0.001 µF, 50 V	2	Hosfelt	95-179
Capacitor, 0.22 µF, 50 V	5	Hosfelt	82-102
Connector header, 36 pin, M, right angle	1	Jameco	103270
Connector housing, 36 pin	1	Jameco	103157
Connector pin, female for 103157	10	Jameco	100765
IC Digital, 74HC00, NAND, Q2	1	Jameco	45161
IC Digital, 74HC541, 8-buffer, 3-state	1	Jameco	46050
IC Digital, 74HC574, 8-D FF, 3-state	1	Jameco	46084
IC Digital, 74HC85, 4-bit comparator	1	Jameco	46172
IC Digital, SRAM, 128×8, SOJ, 25 ns	1	Avnet	CY7C109B-35VC
IC Linear, A/D Converter, 20-MHz, SOIC	1	DigiKey	ADS820U-ND
Socket, 35 pin, single row	1	Samtec	ESQ-135-14-T-S
Socket, IC, DIP 14, order increments of 10	1	Jameco	112213
Socket, IC, DIP 16, order increments of 10	1	Jameco	112221
Socket, IC, DIP 20, order increments of 10	2	Jameco	112248
Resistor, 10 kΩ, 1/4 W, 5%	3		
A/D Input Buffer			
Capacitor, 0.001 µF, 50 V	2	Hosfelt	95-179
Capacitor, 0.22 µF, 50 V	3	Hosfelt	82-102
Connector header, 36 pin, M, strip header	1	Jameco	103270
Connector housing, 36 pin	1	Jameco	103157
Connector pin, female for 103157	6	Jameco	100765
Connector, BNC, F, chassis	1	Hosfelt	952
Diode, 1N914, order increments of 10	2	Jameco	36311
IC Linear, op amp, 2× high speed, 1 Sup, SOIC	1	DigiKey	OPA2631U-ND
Pot, 500 Ω, 25 turn, 3/8-inch	1	Hosfelt	38-124
Resistor, 1 kΩ, 1/4 W, 5%	5		
Resistor, 1.7 kΩ, 1/4 W, 5%	1		
Resistor, 62 kΩ, 1/4 W, 5%	1		
Resistor, 47 kΩ, 1/4 W, 5%	1		

The quantities of some connector components will vary depending on the construction technique.

nals as captured by an LA board as well as the A12 signal as captured by an A/D board. Fig 17 shows the same signals as the previous screen shot but zoomed in. Fig 18 shows A4 instead of A12. Also the time base has been changed from 1.6 µs per sample to 100 ns per sample. Notice that the signal fall time can now be seen. Several more features appear in on screen, but some don't show in the B/W figures here:

- A different color for the A/D trace
- The analog voltage for the A/D channel is in the Status box near the upper left corner. The background color is the same as the one selected for the trace.
- There is another cursor on the screen. The system allows up to four more cursors in addition to the main one.
- Horizontal grid lines for the A/D signal along with the Volts/Div next to the Sample Period.
- The A/D Scale and Offset features

Larry has a BSEE from Drexel Institute of Technology and a Masters in Engineering Science from Penn State. He has worked at ZWorld in Davis, California, as a Technical Support Manager since March 2000. Before that, he worked for 30 years designing and developing automatic test equipment for automotive electronic subsystems.

Larry has been licensed since 1961, and currently holds an Advanced class license. He enjoys electronic hobbies, church and reading. □□

D-STAR: New Modes for VHF/UHF Amateur Radio, Part 1

Our friends in JARL have created a new digital communication standard. Let's look at their new system, and what's in it for hams.

By John Gibbs, KC7YXD

This article is the first in a three-part series describing and analyzing a new communication standard developed by the Japan Amateur Radio League (JARL). The first part focuses on the advantages of upgrading our VHF/UHF equipment to a new, more capable system. The second article in the series addresses the technical design considerations of a digital voice and high-speed data system in the VHF/UHF spectrum. The third, and final, article discusses the D-STAR standard and how it addresses the needs and technical issues raised in the two previous parts.

JARL has developed a new open standard for VHF/UHF digital radio called D-STAR. The system supports both digitally modulated voice transmission and data transmission, including Internet connections, at DSL rates.

At a time when the third-generation (3G) cell phone proposals for high-speed data have been severely delayed, D-STAR presents Amateur Radio operators with the opportunity to bring the Internet Age to mobile and portable operation.

I have been fortunate to be one of the first hams to see and use the prototype transceivers of this new Amateur communication system. Therefore, I would like to take this opportunity to share some of the knowledge and experience I have gained. In this article, I will present the objectives of the new JARL D-STAR system and provide a glimpse of the capabilities of this new system and the engineering tradeoffs that went into the system design. I hope you will find it interesting both in developing an understanding of this system and as an insight into the design process of a digital radio system.

One of the major goals of D-STAR is that it be an open system. This series of articles contains enough system details for a skilled ham to develop a homebrew D-STAR digital voice transceiver.[1]

If you are interested in this system, you may soon have a chance to try it yourself. Because the FCC encourages the Amateur Radio community to develop new digital modes, the US has the regulatory structure in place for hams to use an all-digital voice and high-speed data radio system without special licensing or permits. US hams will therefore be the first in the world with the opportunity to use the new D-STAR system illustrated in Fig 1.

Regular readers of *QEX* know that hams have been experimenting with digital voice.[2] In the US, the FCC encourages hams to continue such experimentation to demonstrate our stewardship of our spectrum. In addition to individual efforts, Amateur Radio organizations have also been promoting digital radio. For years, TAPR has focused exclusively on advancing the state of the art in Amateur Radio digital communications. The ARRL has increased its efforts in this area by sponsoring the establishment of Technology Task Force Working Groups on digital voice, high-speed multimedia and software radio.

In addition to the efforts of individual hams and their organizations, one manufacturer has already introduced a digital voice option to handheld VHF/UHF radios. Unfortunately, these

18225 69th Pl W
Lynnwood, WA 98037
kc7yxd@arrl.net

[1]Notes appear on page 34.

radios are of limited usefulness because the necessary repeater infrastructure for VHF/UHF digital voice operations with these radios does not exist. These radios will not work through existing analog repeaters and the necessary digital repeaters have not been developed. Early on in the D-STAR planning, the JARL recognized that developing VHF/UHF digital capabilities also requires developing new standards for digital voice repeaters and the links between repeaters.

D-STAR History

The D-STAR standard not only addresses the needs of VHF/UHF voice and data communications with mobile and handheld radios, but also provides the standards for repeater-to-repeater linking and Internet access. It was clear that developing and testing such a complex system would take many man-years of engineering and testing. The efforts that would be required to achieve this in a timely manner would far exceed any reasonable expectations of volunteer ham labor, no matter how dedicated. So, the JARL contracted with the Amateur Radio manufacturer ICOM to develop and evaluate D-STAR prototype hardware. D-STAR has been under development since 1998 and the system operation has been proven in lab and field tests. The result of all this development effort is about to bear fruit. The JARL expects to finalize the D-STAR standard this summer.

A D-STAR mobile transceiver called the ICOM ID-1 was used for field trials in the Tokyo area (see the cover photo on this issue) and shown at three US Amateur Radio shows: Dayton Hamvention 2002 and 2003 and the Digital Communication Conference (DCC) in Denver last fall. Since then, repeaters and microwave links have been developed and are currently available on a limited basis to application developers in the US. All these D-STAR compatible components will soon be shipping in quantity, and we expect that other manufacturers will be shipping D-STAR-compatible radios in the future.

Existing VHF/UHF System Properties

To replace any existing system with a new standard, there must be compelling reasons for incurring the expense of new equipment. So it is good to start the discussion of D-STAR with a look at the capabilities and limitations of our existing VHF/UHF Amateur communication systems in Tables 1 and 2. To do this, let us look at the capabilities of a representative voice repeater system that covers the Pacific Northwest and beyond: the Evergreen Intertie.

The Evergreen Intertie connects more than 23 repeaters by full-duplex UHF radio links that are transparent to the user. From my location, there are two main links in the system, a North-South link that connects Western Washington and Oregon and an East-West link that crosses the Cascade Mountains and connects to cities in Eastern Washington.

Users can control switches using DTMF tones to connect repeaters to the link. The way this particular system is configured, a minimum of three switches must be set by a user or control operator to connect two repeaters. In a more-extreme case, seven switches must be set to talk from Seattle repeater K7NWS to Portland repeater KJ7IY. Of course, each switch that connects to the next link may be already in use, so it can be difficult for a user to establish such links if the system is heavily used.

On a repeater link, only one contact can be held on a link at a time. That is, unlike the telephone system, there is no multiplexing on links. If a link is in use or out of service, there is no way to link the repeaters unless an alternate path is available.

Another difference from the telephone trunk system lies in how a link is established. In the telephone system, the system automatically picks the link based on the call destination and the trunk lines currently available. In the Evergreen Intertie, the user must determine the logical path through the repeater links and to know the DTMF codes for each of the switches.

Amateur Radio packet systems offer an analogous set of features through dedicated packet nodes (simplex repeaters.) Packet radio is used to transfer data (for example, computer files) and for keyboard contacts. It might even be possible to have a digital voice contact on a 9600-bps system. However, the system is packet-oriented, which means that real-time communications are not guaranteed. Unless the system was very lightly loaded, some of the voice packets would be unacceptably delayed.

Both the amateur voice repeaters and packet nodes are FM systems. Within the limitations of the existing analog FM technology, some very creative communication solutions have been developed. For instance, sub-audible tone codes are used to protect repeaters against accidental activation by interference. DTMF is used to control some repeater functions, activate a phone patch or for selective calling of amateurs.

Enterprising hams continually add new capabilities to the systems. A few

Table 1—Existing VHF/UHF Amateur Radio System Features

- Voice is FM, half duplex
- Data is FSK, simplex
- CTCSS protection
- DTMF control
- Linked repeaters
- 1200/9600 packet
- APRS
- Voice over Internet

Table 2—Existing VHF/UHF Amateur Radio System Limitations

- Spectrally inefficient
- Low speed data
- One QSO per link
- Difficult to establish links
- Cannot mix data and voice

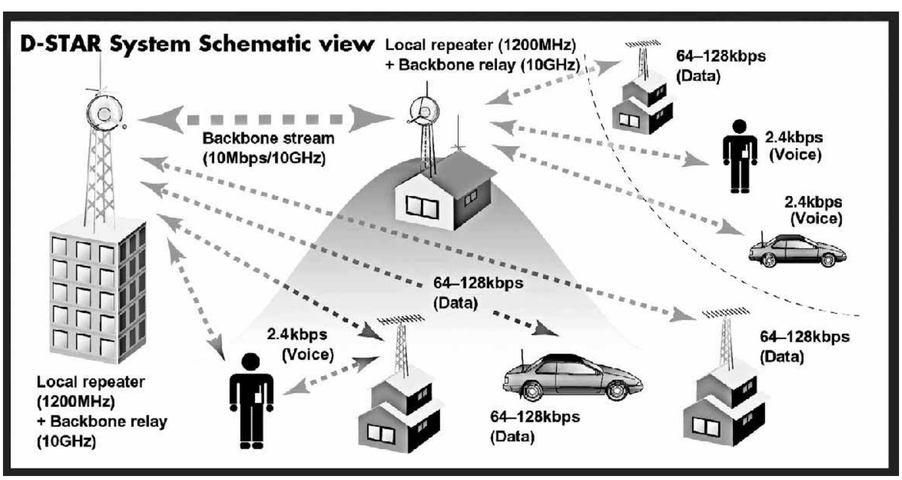

Fig 1—JARL's proposed D-STAR system offers digital voice and data communication on 1.2-GHz with repeaters linked on 10 GHz and Internet gateways.

examples that come to mind include satellite gateways, GPS-based location systems (APRS) and worldwide communications with VHF/UHF transceivers when voice-over-Internet-protocol (VOIP) is added to a repeater. Yet we are rapidly approaching the limit of what we can do with the existing infrastructure, as we can see by investigating the limitations of existing VHF/UHF Amateur Radio systems (see Table 2).

Spectral Efficiency

The first major limitation is spectral efficiency. The amateur community's VHF/UHF spectrum usage has not changed despite dramatic improvements in communication technology that have occurred in the last few years. The FCC views the radio spectrum as a finite resource that must be efficiently shared among many users. There are many new potential users appearing for the VHF/UHF spectrum, and they are often looking at the spectrum that has been allocated for Amateur Radio. A growing part of ARRL resources are being devoted to spectrum-defense.

However, defending our usage of these valuable frequencies will become more difficult because the current amateur FM system is not spectrally efficient. Today, the FCC only grants new licenses in Land Mobile services to users that meet reduced spectrum-occupancy requirements. The FCC calls this "refarming." The FCC has extended this principle to other radio services. For example, the existing GMRS spectrum was refarmed with FRS channels placed between the old GMRS channels. There is no reason why we should feel that the Amateur Radio Service would be exempt from the requirement for spectral efficiency.

As a matter of fact, the quest for spectral efficiency is increasing. Current Land Mobile services refarming is from 25-kHz channel spacing to 12.5 kHz. However, in the next few years, the FCC plans to repeat this process and force all new Land Mobile Service licenses to use equipment compatible with 6.25-kHz channel spacing. It is not clear that FM radios can be developed that will meet the stability and bandwidth requirements of such a system and be sold at an affordable price, so radios using other technologies may need to be developed. But what is certain from modulation theory is that as the deviation is reduced, the signal quality advantage of FM over AM systems (including SSB) quickly disappears.

Data Rate

A second limitation is the 9600-baud rate limitations of existing commercially available radios. In this data-intensive Internet age, this speed is woefully inadequate. Any new system should have the capability of supporting data transfers at speeds rivaling DSL.

Limited Linking

As mentioned above in the Evergreen Intertie example, a severe limitation of the current FM-analog repeater system is the number of contacts that can be handled by a link. An ideal repeater-to-repeater link would have much wider bandwidth than the existing links. This bandwidth would then be dynamically allocated between voice contacts and high-speed data users.

In addition, as we have seen, it is difficult for the user to establish links between repeaters. With today's low-cost computing power, a more automated method of calling a distant ham could certainly be developed.

Data and Voice

The final and very significant limitation of the existing systems is that repeaters can only handle voice or data, not both simultaneously. As we shall see later, there are many applications that could be opened to Amateur Radio operators if this feature could be incorporated in a new VHF/UHF system.

Desired Properties

Having considered the features and limitations of current analog FM systems, let us next consider what properties any new analog or digital systems should have. Ideally, any new system should solve the limitations of the existing systems without losing any of the features. In addition, any new system should have the properties described below and in Table 3.

Table 3—Desired Properties of New VHF/UHF Amateur System

- Compatible with regulations
- Worldwide standard
- Enables new applications
- Enhancement friendly
- Scalable
- Open standard
- Repeater operation
- Linking repeaters
- Simplex
- High speed data
- ANI
- Expandable
- Affordable

Compatible with Regulations

If a new system required changes in the FCC regulations, it might take years before it could be adopted. Fortunately, this is not necessary for digital voice and data transmissions in the US.

The FCC encourages the Amateur Radio community to develop digital voice and new digital data communication systems. One example is the FCC's attitude toward the new HF digital modes such as PSK31. There was some concern in the amateur community that the encoding used in PSK31, called Varicode, would be considered a form of encryption and hence barred by the Part 97 regulations. However, the FCC has clearly and repeatedly stated that encoding is not encryption and that as long as the encoding method is public there is no regulatory problem.

Where should digital voice transmissions occur in the current band plan? Again the FCC in its encouragement of digital radio has already decided that digital voice operations belong in the phone bands.[3]

What regulatory issues are there for new linked systems? William Cross, W3TN, of the FCC Policy and Rules Branch, made it clear at his presentation at Dayton last year that there are no rules specifically written for linked systems; the FCC regulates stations, not systems.

Finally, emergency operation is clearly one of the requirements for any Amateur Radio system to meet one of the Part 97 justifications for the Amateur Radio Service. Any new system must not only be available to support communication needs during an area-wide emergency, but an amateur must be able to break in and use the system during an accident or other local emergency.

A Worldwide Standard

Why is it desirable to be compatible with an international standard? The primary reason for all countries to share the same system architecture is to make the radios affordable. If the radios and the repeater infrastructure are not within the financial reach of the majority of the ham community, no amount of extra features will make a new system successful.

Radio costs are dramatically dependent on sales volume both because research and development costs can be spread over a larger number of radios and because manufacturing unit costs decrease as volume increases. Today North America accounts for about a third of the world's Amateur Radio licenses. Japan, with a far smaller population, has about another third. So if

Japan and the US agree on a single standard, the manufacturing volume could double, which would dramatically reduce radio costs for all amateurs. If the rest of the world also joined in the standard, further cost reductions would follow. As an example of what can happen when there is not a world standard, consider the 222-MHz band.

Because the band is not available worldwide, manufacturers offer a limited number of transceiver models. And we find that equivalent rigs (if even available) tend to be more expensive than the high-volume 2-meter rigs.

A second reason for a worldwide standard is that tying repeaters together via the Internet is becoming a popular feature of today's repeater systems. Any new system must support this trend for both voice and high-speed data. This could be done by specifying a protocol that two otherwise incompatible systems would use to exchange data; but due to the economic issues discussed above, this is a less-than-ideal solution.

New Applications and Enhancements

To take full advantage of the digital revolution in Amateur Radio, minimum standards will need to be established. Unlike a telecom system, which needs rigid standardization, an Amateur Radio system must have just enough standardization to allow communication, without inhibiting innovation.[4] This is a difficult balance and requires a great deal of work during the system design to properly blend these conflicting requirements.

Ideally, any new communication system would be a perfect "wireless cable." Of course, one of the things of interest to *QEX* readers is that no communication system is perfect. The study of the impairments and experimenting with ways to improve communications over an impaired channel are interesting areas of our hobby. Every system involves a great deal of compromise; that is a part of daily life for the communication-system design engineer. An ideal system for Amateur Radio would allow a great deal of experimentation that could be layered on top of a well-functioning, but not overly constraining, radio system.

A Scalable System

A cell-phone system will not work until the complete infrastructure is deployed in an area. Clearly this is not practical for Amateur Radio. Any new Amateur Radio VHF/UHF system must be able to work with only one repeater and even—within the limits of line-of-sight propagation—without repeaters at all. Multiple repeaters and the linking of repeaters can come later as the user base develops or as funds become available.

In addition, it is important to be able to communicate with other hams who have not upgraded to the new system. This can be done in two ways: The radios themselves could have analog FM capability, or the repeater can be capable of interfacing with the existing analog radio repeaters.

The system should also be scalable to facilitate emergency operation. Natural or man-made disasters can destroy both the commercial and amateur communication infrastructure. A new communication system should be able to work immediately without repeaters and be flexible enough so that spare transceivers can be connected to quickly form an emergency, temporary repeater.

An Open Standard

As this is an Amateur Radio system, the system should be available from more than one manufacturer. It is desirable to have competition between the radio manufacturers to keep prices low and encourage innovation within the framework of a new standard.

Yet it is at least as important to those of us with *QEX* leanings that the system technology is such that a ham with a sufficient technical background can make any part of the system, including radios, repeaters and repeater links. Because so much of leading-edge communication technology is the intellectual property (IP) of communication companies, the requirement that hams be able to develop and publicize equipment without violating patent rights becomes a system-design challenge.

Further Requirements

High-Speed Data

Fixed site-to-site data links at greater than 9600 bits/s are rare, but not unknown in Amateur Radio. Any new VHF/UHF system should support high-speed data, not only for these fixed links but also for mobile and portable operation. This means the system must tolerate channel impairments like multipath and Doppler shift.

To be able to interface into the vast array of low-cost hardware and software available today, the new VHF/UHF system should appear as a "wireless Ethernet cable" to a PC. You should be able to use any software that can interface with the IEEE 802.3 (10Base-T) Ethernet, connect a cable from the PC to the transceiver and use the computer just as if it was a wired connection. For example, if the other half of the RF link is connected to an ISP, then an Internet browser will work seamlessly and the Amateur world will have high-speed wireless Internet connections.

Repeater Operation

Because the FCC requires that the control operator is able to shut down the repeater and repeaters are often in remote locations, remote control of the repeater must be designed into any new system. With today's systems, shutting down the system is the only option available if a user abuses the repeater. A new system should have the ability to block offenders from repeater access while still allowing others to access the system.

Control over landlines is certainly required, but radio control operation is necessary for those sites without phone-line access. Of course, it is highly desirable that the control operator can use the data capabilities of the system to monitor the status of the system and control many other features.

Linking Repeaters

Any new Amateur Radio system must have a wide-bandwidth links capable of supporting multiplexed contacts. Multiple contacts are necessary because the system should support multiple repeaters at a single site as well as different pairs of sites using the link at the same time. The link must also support both voice and data so that we do not have to invest in two links. The best way to meet this need is for the link itself to be digital and the voice digitized for transmission over the link. Because more than one pair of repeaters is using the link at a time (multiplexed), the link must be full duplex.

Each site in the system repeats the high-speed link signal and extracts and adds the contacts that are appropriate for its site. Normally only one repeater in the system would broadcast the contact. The other repeaters ignore contacts that are not directed to them. Otherwise one contact would tie up the entire repeater system.

Most often, these repeater links would be microwave links. However, because of the distances involved, it may be more attractive to use Internet linking with some repeater systems. Any new VHF/UHF Amateur system should support both types of links.

Simplex

Any new system, no matter what benefits are available from repeater operation, must be able to work simplex without a repeater. And unlike typical fixed digital radio networks, it is critical that anyone tuning the bands can immediately listen in on a contact.

This requires two properties that are not available on many digital radio systems. First, the digital voice system must work without handshakes. That way it is possible to have one talker and many listeners. Second, it must not be necessary to wait for the start of a new transmission to acquire the carrier, frame and bit synchronization necessary to demodulate the contact.

Automatic Number Identification (ANI)

Any new Amateur system should support a higher level of automation in establishing a contact. An equivalent feature to what the commercial Land Mobile market calls "Automatic Number Identification" (ANI) needs to be developed. With this feature enabled, your radio opens squelch only when your call sign is received. Some hams do this today with a DTMF code rather than their call sign, but DTMF codes are not unique and DTMF signaling is very slow. If desired, the radio can beep when you are called or in mobile applications, the horn can sound.

This call-sign squelching principle should also be extended to repeaters. Repeaters today use CTCSS tones to keep from being opened accidentally by interfering signals. On any new system, you should use the repeater call sign to unambiguously and easily open the repeater. This would be followed by the call signs of the party you are calling and the repeater they use so that the system can route your call.

Affordabilty

The system must be designed to be tolerant of the performance limitations of reasonably priced components. Particularly with high-speed data at UHF, the frequency and time accuracy requirements of many modern digital radio systems are so great as to be prohibitively expensive for amateur usage.

Another reason for designing the system to be reasonably tolerant of component and system variations is to allow enterprising Amateurs the opportunity to homebrew their own D-STAR hardware.

Also to save user cost, the system should not be designed for full duplex operation. Full-duplex operation requires expensive isolation between the transmitter and the receiver. Half-duplex and simplex operations allow the sharing of many expensive components between the receiver and transmitter. Finally, radio amateurs almost always operate in these low-cost modes so there is no problem with conversion to new modes.

Advantages of Digital Modulation

In the next part of this series, we delve into the engineering design considerations that were made in developing D-STAR and the technical details of its implementation. Yet, let us conclude by investigating the advantages of a new system based on digital instead of analog modulation.

The first advantage of digital modulation is the ability to reduce occupied spectrum. To meet the regulatory pressures discussed above and to reduce the congestion on our bands, any new system must be spectrally efficient. One solution would be to stay with an analog FM system and reduce the deviation, as the FCC has required of the Land Mobile Service. However, doing so reduces the audio quality that is the major benefit of FM.

It is a better solution to change the modulation completely and transmit voice using digital modulation. However, without careful system design, switching to digital voice could actually increase the bandwidth required for voice communication because of the high bit rates required by uncom-pressed voice. For instance, pulse-code modulation (PCM), as used by the US telephone standard, requires a digital stream of 64,000 bits/s. Even with very elaborate modulation schemes, that high bit rate would require a much wider bandwidth than current FM voice radios.

The enabling technology for digital voice is digital signal processing (DSP). It has long been realized that the information in a voice signal is highly redundant and that it should be possible to establish good transmissions without sending the redundant information. Modern high-speed, low-cost signal processors and very clever algorithms can dramatically reduce the bit rate required to accurately reproduce a human voice in real time. We shall see that it is possible to get similar voice quality at only 2400 bits/s and therefore occupy far less spectrum than today's FM systems.

A second advantage of digital modulation is improved quality. With wide-band systems like HDTV and high-speed wireless Internet service, the most important advantage of digitizing transmissions is the ability to use DSP to correct for transmission errors. This results in improved performance over the vast majority of the operating area. In analog radio communication systems we have little choice but to live with the errors caused by propagation, noise and interference (both natural and man-made). We can sometimes increase the received signal-to-noise ratio by increasing transmitter power and/or using gain antennas. However the fading caused by multipath propagation is not improved by increasing the transmitted signal power. Particularly in mobile wide-band systems, multipath can be a serious problem. You have probably heard multipath impairment if you listen to FM broadcasts in your car. It is perhaps most noticeable if you are at a stop light and hear distortion but move a few feet and the distortion disappears.

But perhaps the greatest advantages of digital voice transmission are the added features that are possible when a digital data payload is added to a voice contact. The availability of simultaneous low-speed data transmission with voice transmissions opens up a whole world of new possibilities for Amateur Radio. Imagine sending still pictures, maps, small data files and GPS position *while* rag chewing. What would it be like to have "instant messaging" on your radio? What a great way to politely break into a contact!

Notes

[1]Remember, however, the D-STAR specifications discussed in this article have not yet been finalized.

[2]See for example "Practical HF Digital Voice," by Charles Brain, G4GUO, and Andy Talbot, G4JNT, *QEX* May/June 2000, pp 3-8.

[3]See, for instance, the editors preface and Paul Rinaldo's, W4RI, comments in a sidebar in "Practical HF Digital Voice," pp 3 and 4.

[4]See "Technical Standards in Amateur Radio," Doug Smith, KF6DX, *QEX* Mar/Apr 2003, p 2.

An Extra class license holder, John usually is found on the HF bands, primarily operating PSK31. At age 3, John exhibited early talents in electronics by "helping" his dad fix a TV. He plugged the speaker into a wall socket! Despite this traumatic start, he spent his youth building Heathkit and Eico equipment, repairing vacuum-tube radios and TVs and designing and building numerous homebrew projects including a Morse decoder high-school project built with resistor-transistor logic in the mid 1960s.

With BSE and MSEE degrees in control and communication theory, he has worked for Hewlett-Packard in the fields of spectrum and network analysis and frequency synthesis. He is currently the research department engineering manager at ICOM America, where his primary interests are digital communications and DSP. John has eight patents and is currently applying for four more. □□

Active Loop Aerials for HF Reception Part 1: Practical Loop Aerial Design

Should you consider a small loop antenna? Why? Can they be efficient?

By Chris Trask, N7ZWY

The performance of any receiving system is highly dependent on the first few stages. Very often the aerial itself is not given consideration as being a part of that system, let alone recognized as the stage that determines the minimum noise figure (*NF*) that can be realized. Aerials having poor efficiency or that are not properly matched to the receiving unit can cripple the ability of the operator to receive low-level signals. Electrically small aerials, regardless of their configuration, are especially vulnerable to low efficiencies and hence become the critical elements in their receiving systems where larger aerials with good efficiency are impractical. With many radio amateurs and shortwave listeners (SWLs) living in apartments or subject to property zoning restrictions, small aerials having good performance, both for transmitting and receiving, have become increasingly popular. This two-part series will describe the theory and practical design of a high-performance active receiving loop aerial.

Sonoran Radio Research
PO Box 25240
Tempe, AZ 85285-5240
ctrask@ieee.org

Active Aerials

Active aerials are often considered as being a viable option when the need for a small aerial arises. Many such aerials are available commercially, and most that are published for hobbyists fail to provide the operator with good performance for many reasons. The two most relevant are that the antenna itself is of poor efficiency, and the aerial amplifier has poor dynamic range, either with respect to *NF* or intermodulation distortion (*IMD*). Very often, it is both maladies.

Short vertical monopoles and dipoles are notorious for poor efficiency, and it does not help to follow a poorly designed aerial with a high-dynamic-range amplifier, regardless of how low the amplifier's *NF* may be. The aerial itself—or rather the aerial noise temperature—determines the minimum *NF* of the receiving system. This is somewhat contrary to the notion that the use of small tuned loops for receiving can be justified when taking the expected external noise into account.[1] To those having only basic skills who want to realize a small aerial with good efficiency, very few options are

[1]Notes appear on page 41.

as easily comprehended and constructed as the loop aerial. When properly designed and constructed, a loop aerial can easily exceed 80% efficiency. The low real impedance of the loop, usually less than an ohm, is in fact a highly desirable feature as exceptionally high tuning Q's can be realized. Loop aerials also have good directivity, whereas the vertical monopole is unidirectional.

The low impedances of loop aerials can be easily dealt with by way of suitable aerial amplifiers that are designed with due regard to matching these low impedances. The remaining necessary features of low *NF* and good *IMD* performance can be attained with equal ease. Remote tuning is also a desirable feature to accommodate the reactance of the loop aerial and to give some degree of selectivity at the earliest stage of the receiving system. The active loop aerial described here consists of three basic parts: the loop aerial proper, the aerial amplifier unit, which includes remote tuning and the aerial control unit.

Loop Aerials

Again, it does not help in any way to follow a poorly designed aerial with a high-dynamic-range amplifier regardless of how low the amplifier's *NF* may be. Therefore, it is necessary to look much more closely at the loop aerial. We should become familiar with the various design aspects and their effects on performance so as to arrive at a suitable design that focuses on the efficiency of the aerial, very likely at the expense of broadband operation.

Generally, two loop-aerial models are popular. The first of these, shown in Fig 1, consists of a signal voltage source, an inductance L_{ant}, a radiation resistance R_{ant} and a loss resistance R_{loss}. This model is suitable for loop aerials that are very small with respect to a wavelength, the guideline is that the enclosed area of the aerial should be much less than the operating wavelength squared. For this model, the inductance is easily determined by way of classical inductance formulas,[2] and it has been suggested that the radiation resistance of a loop aerial of any geometry can be determined by:

$$R_{ant} = 320\,\pi^4 \left(\frac{A}{\lambda^2}\right)^2 N^2 \quad \text{(Eq 1)}$$

where A is the area of the aerial and λ is the wavelength, both in the same units,[3,4] and N is the number of turns. This formula is convenient for frequencies that are much less than the first antiresonance frequency of the aerial, but it loses significance as the frequency is increased towards antiresonance and fails completely at antiresonance. Kraus notes (see Note 4) that Eq 1 is applicable only for very small loops where $A < (\lambda^2 / 100)$.

For small loop aerials, the loss resistance is primarily a result of skin effect and can be approximated by (see Note 4):

$$R_{loss} = \frac{L}{\sigma\,\pi\,d\,\delta} = \frac{L}{d}\sqrt{\frac{f\mu_0}{\pi\,\sigma}} \quad \text{(Eq 2)}$$

where f is the frequency in Hertz, μ_0 is the permeability of free space ($4\pi \times 10^{-7}$ H/m), σ is the conductivity of the material in S/m, L is the perimeter length of the aerial and d is the diameter of the conductor, both in meters. The quantity δ is referred to as the *depth of penetration* (see Note 4), and is defined as:

$$\delta = \frac{1}{\sqrt{f\pi\mu\sigma}} \quad \text{(Eq 3)}$$

where μ is the permeability of the material in H/m. From Eq 2, it can be seen that the loss resistance can be improved by increasing the size of the conductor. It might also be improved by the use of Litz wire; but because of irregularities in the stranding and capacitance between the strands, the effectiveness of Litz wire in reducing the loss resistance diminishes above 1 MHz.[5]

Power applied to the aerial is dissipated as electromagnetic energy by the radiation resistance and as heat by the loss resistance. The ratio of radiated power to total power is referred to as the aerial efficiency and is readily defined as:

$$Eff = \frac{R_{ant}}{R_{ant} + R_{loss}} \quad \text{(Eq 4)}$$

When we measure the terminal impedance of the antenna, we see these two resistances as the real part of the impedance. These resistances can be determined by measuring the terminal impedance and the efficiency of the aerial, the latter of which can be measured two methods,[6] both of which require test equipment beyond the means of most amateurs and hobbyists. For the purposes discussed here, an analytical approach is more desirable.

A more-exact model of the loop aerial is shown in Fig 2, where the inductance of the model in Fig 1 has been replaced with a λ/4 transmission line of impedance Z_0. This model holds true for loop aerials with balanced feeds, and it helps to explain the various antiresonances and resonances that are observed in practice. For loop aerials with unbalanced feeds, the transmission line becomes λ/2, which has serious consequences with respect to impedances and radiation patterns. These will be discussed later as the opportunities arise.

Using this model, an alternative method for approximating both the radiation resistance and reactance of single-turn loop aerials up to antiresonance for specific geometries was published by Awadalla and Sharshar.[7] There, the radiation resistance is shown to be closely approximated as:

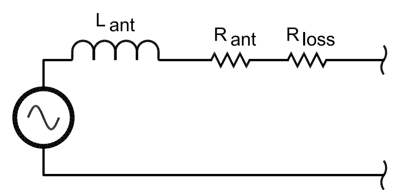

Fig 1—Loop aerial model (low frequency).

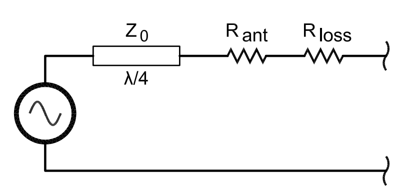

Fig 2—Loop aerial model (high frequency).

Table 1—Coefficients *a* and *b* for Equation 3

Configuration	*L/λ ≤ 0.2*		*0.2 ≤ L/λ ≤ 0.5*	
	a	*b*	*a*	*b*
Circular	1.793	3.928	1.722	3.676
Square (side driven)	1.126	3.950	1.073	3.271
Square (corner driven)	1.140	3.958	1.065	3.452
Triangular (side driven)	0.694	3.998	0.755	2.632
Triangular (corner driven)	0.688	3.995	0.667	3.280
Hexagonal	1.588	4.293	1.385	3.525

$$R_{ant} = a \tan^b \left(\frac{k_0 L}{2} \right) \quad \text{(Eq 5)}$$

The wave number k_0 is defined as:

$$k_0 = \omega \sqrt{\mu_0 \varepsilon_0} \quad \text{(Eq 6)}$$

where ω is the frequency in radians/second and ε_0 is the permitivity of free space (8.8542×10^{-12} F/m). The coefficients a and b are dependent on both the perimeter length and the geometry of the aerial, a list of values being shown in Table 1. Despite its convenience and favorable comparison to the moment-method (*NEC*) solutions, Eq 5 is only useful in approximating the radiation resistance for loops having a perimeter length of less than λ/2. It does not help in determining either the loss resistance or the aerial efficiency. Awadalla and Sharshar do, however, provide a useful approximation of the aerial reactance, wherein they approximate the characteristic impedance, Z_0, of the λ/4 transmission line in the model of Fig 2 as being:

$$X = j Z_0 \tan \left(\frac{k_0 L}{2} \right) \quad \text{(Eq 7)}$$

where Z_0 is the equivalent impedance of the transmission line, defined as:

$$Z_0 = 276 \log \left(\frac{4 A}{L r} \right) \quad \text{(Eq 8)}$$

where r is the radius of the wire or tubing. These equations are shown to compare favorably with method moment (*NEC*) simulations within the prescribed bounds (see Note 7) and are very useful in the design of single-loop aerials.

Resistances of Large Loop Aerials

The equations shown thus far are very useful in approximating the impedance of single-turn loop aerials and the efficiency of small loop aerials. They do not help in determining the resistances and the efficiency of a loop aerial that is large with respect to wavelength or has multiple turns, which is a much more complicated matter.

For this purpose, a more exact and comprehensive determination of the resistances and efficiencies for circular-loop aerials can be made by a series of equations developed by T. L. Flaig at the Electroscience Laboratory of Ohio State University.[8,9] From these reports, the radiation resistance for a circular multiturn loop can be determined as:

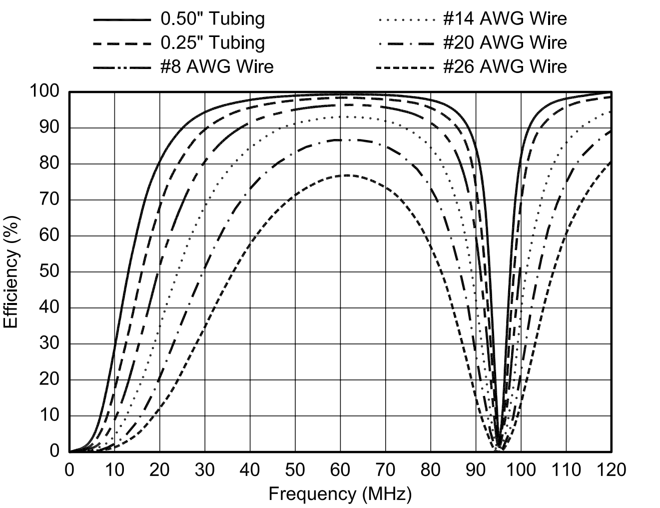

Fig 3—Aerial efficiency versus wire diameter.

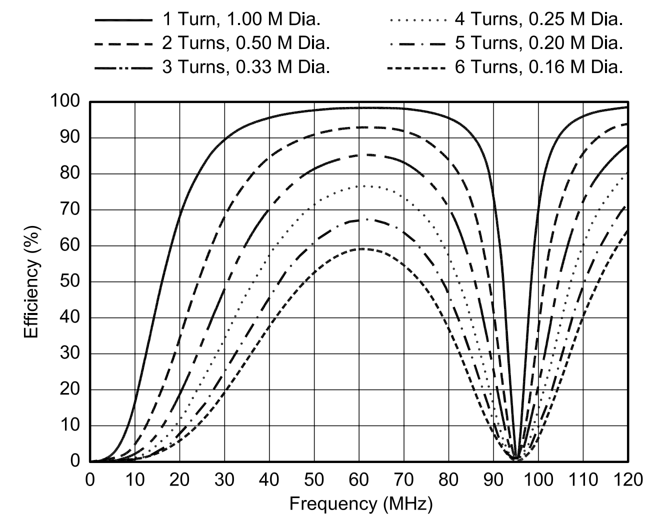

Fig 4—Aerial efficiency (constant wire length, 0.25-inch-diameter tubing).

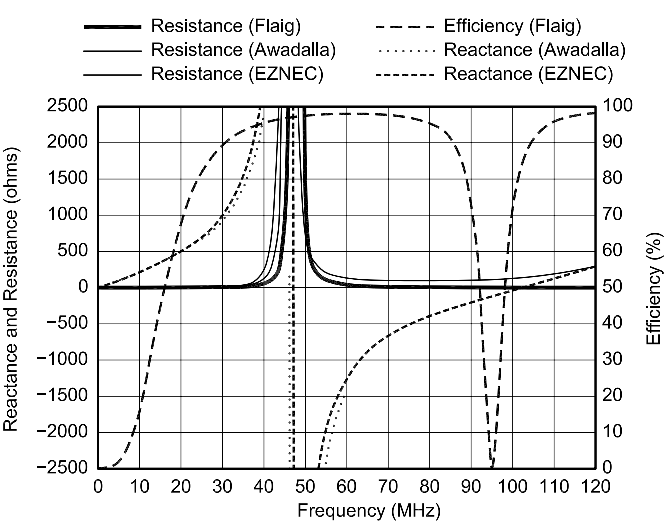

Fig 5—Aerial efficiency and impedances (analytical versus *EZNEC* free-space model).

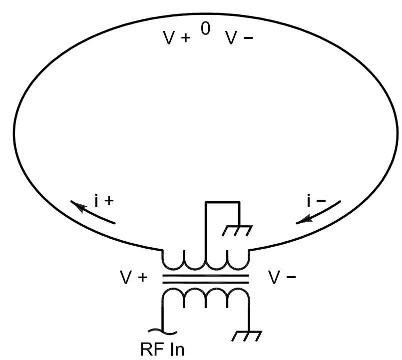

Fig 6—Loop aerial with balanced feed.

$$R_{\text{ant}} = \frac{8\,\pi^2\,F^2\,R^2}{9 \times 10^3} \tan^2(N\pi\,k_0 R) \qquad \text{(Eq 9)}$$

where F is the frequency in megahertz, R is the mean radius of the aerial and N is the number of turns in the aerial. Next, the loss resistance (for copper material) is determined by:

$$R_{\text{loss}} = \frac{4.16 \times 10^{-5}}{r} \frac{N\pi\,R\sqrt{F}}{\cos^2(N\pi\,k_0 R)} \left[1 + \frac{\sin(2N\pi\,k_0 R)}{2N\pi\,k_0 R}\right] \qquad \text{(Eq 10)}$$

where r is the radius of the wire or tubing. By combining Eqs 4, 9 and 10, the efficiency of a circular loop aerial made with copper wire or tubing can be determined by:

$$Eff = \frac{\sin^2(N\pi\,k_0 R)}{\sin^2(N\pi\,k_0 R) + \dfrac{0.374N}{8\pi\,R\,rF^{1.5}} \left[1 + \dfrac{\sin(2N\pi\,k_0 R)}{2N\pi\,k_0 R}\right]} \qquad \text{(Eq 11)}$$

More rigorous solutions for the resistances and reactance are available,[10, 11, 12] but are not as convenient as those presented by Flaig. As such, Eqs 9, 10 and 11 are well suited for analysis by way of spreadsheets such as *Excel*.

Analytical Evaluation

With suitable equations available, we can now embark on an analytical evaluation of the efficiencies and resistances of circular loop aerials. We begin the evaluation by first examining the effects that the size of the conductor has on the efficiency. Using Eq 11, the efficiency of a single-turn circular loop aerial having a diameter of 1 meter and a variety of conductor diameters ranging from #26 AWG to ¼ inch (6 mm) was evaluated. The results of this initial evaluation are shown in Fig 3. Notice that the peak efficiency of this aerial decreases significantly as the wire diameter decreases. Also notice that the efficiency decreases rapidly below 20 MHz, becoming less than 5% for the 80-meter band. Now, consider what the efficiency of your 24-inch diameter commercial loop might be at 80 meters. (Think of a number less than 2%.)

We might want to consider making the aerial smaller

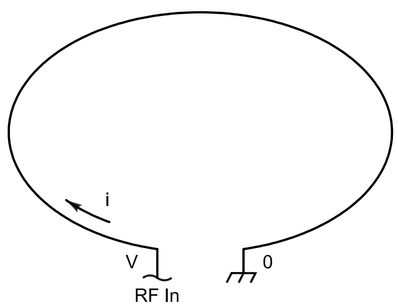

Fig 7—Loop aerial with unbalanced feed.

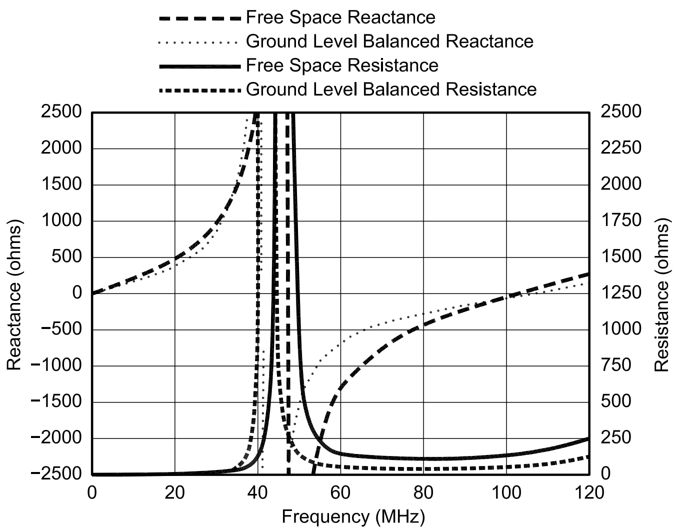

Fig 8—Free space versus ground environment impedances.

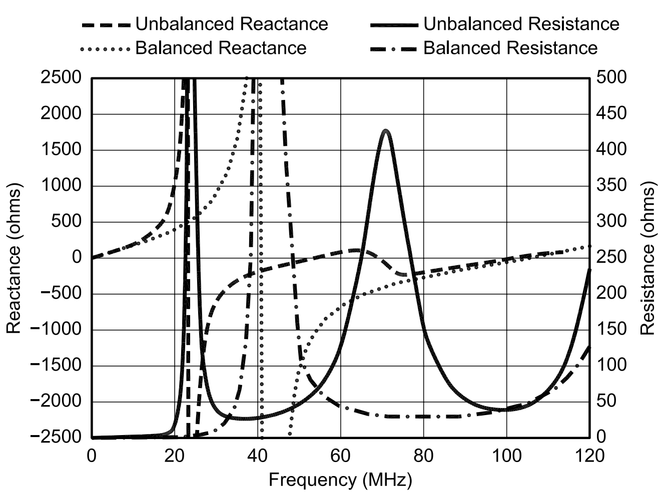

Fig 9—balanced versus unbalanced impedances.

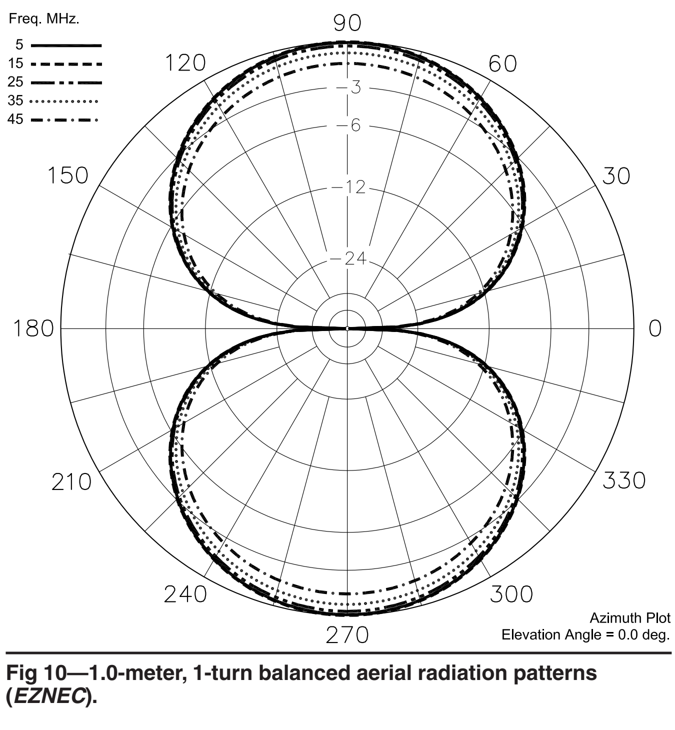

Fig 10—1.0-meter, 1-turn balanced aerial radiation patterns (*EZNEC*).

by increasing the number of turns while keeping the length of wire constant so as to retain the antiresonance and resonance characteristics. Might we make an efficient aerial of the same diameter while decreasing the antiresonance and resonance frequencies? Such an evaluation is shown in Fig 4, where increasing the number of turns actually degrades the efficiency in much the same manner as decreasing the wire diameter. This is not to say that multiturn loop aerials are impractical or that they should not be considered, but rather it is necessary to examine the consequences of making the aerial more compact by increasing the number of turns. The lower efficiencies of multiturn loop aerials can, in most circumstances be compensated to some degree by using larger diameter wire or tubing.

NEC Simulation

To gain some confidence in the analytical approaches described so far, it is useful for us to evaluate loop aerials with an *NEC* based simulation program, such as *EZNEC*. This will also allow us to evaluate aerials in proximity to ground, as the equations used so far are for free space and do not account for images or ground loading. At the same time, we need to recognize that *NEC* solutions will not give us any idea of the loss resistance, so we need to use the *NEC* modeling and the analytical solutions together to form a suitable basis for design.

To begin, a model for a single-turn loop aerial was formed and refined by comparison with the analytical equations and measured prototypes, the construction of which will be discussed later. This first model is a 1-meter diameter 12-sided polygon, similar to the first prototype when using wire, having a wire diameter of 6-mm (approximately 1/4-inch). The segmentation was adjusted at various frequency ranges to remain well within the guidelines that give good results.

The free-space *EZNEC* results for resistance compare very well with the radiation resistances obtained from Eqs 5 and 9 and are shown in Fig 5 along with the efficiencies derived by Eq 11 and the reactance derived by *EZNEC*. The resistances show that all three methods are in good agreement, the frequency of the antiresonance differing by less than 5% between them. From this and the comparisons that Flaig and Munk show for measured versus calculated efficiencies (see Notes 8 and 9), we can now have confidence in the radiation resistance and efficiency derived by their equations as well as the equations from Awadalla and Sharshar. We can do a more detailed analysis using *EZNEC* with good confidence that the efficiency will remain associated with the antiresonance frequency as the effects of ground proximity are brought into play.

Balanced versus Unbalanced Loop Aerials

The equations from both Flaig and Adawalla are meant for an aerial in free space, just as the model used so far in *EZNEC*. In free space, the aerial has no reference to ground and is thus balanced (assuming a single source is used in the *EZNEC* model). When the aerial is placed in a more realistic environment where a ground is present, we have the opportunity to examine the differences in performance between a balanced and an unbalanced aerial.

Let's begin by looking at the two configurations to better understand their differences. A balanced loop aerial is shown in Fig 6, in which the load (or source) is coupled to the aerial directly by way of a transformer having a center-tapped secondary winding, often referred to as a hybrid transformer or simply hybrid. With the secondary tap connected to ground, the aerial is now fed with two equal but opposite voltages and currents, the consequence of which is that the very top, or center of the aerial is a virtual ground. This is the property of the loop aerial that allows Awadalla and Sharshar to make their approximation by considering it to be a shorted transmission line having a length that is equal to one half the aerial perimeter (see Note 7).

An unbalanced loop aerial is shown in Fig 7. Here, the signal is coupled to the aerial at one end while the opposite end is grounded. The result of this configuration is that there is no longer a virtual null at the center, which negates the quarter-wave approximation of Awadalla and Sharshar. Instead, the loop aerial is now $\lambda/2$ long, which has

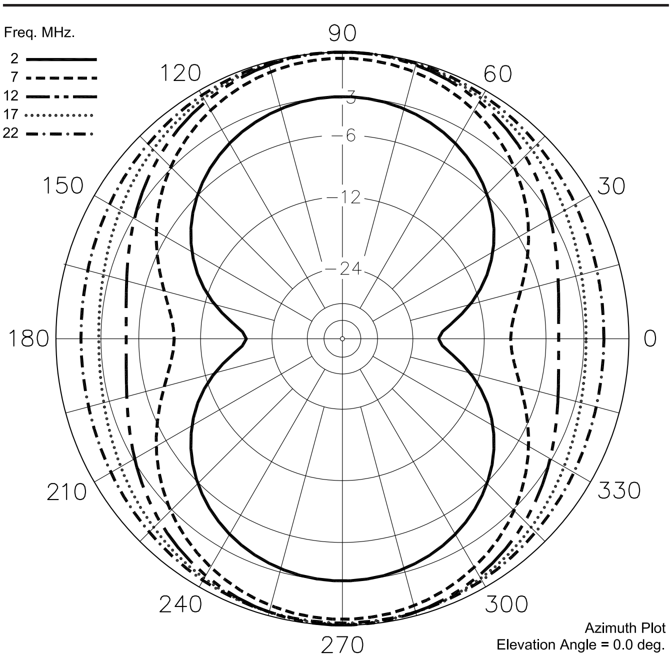

Fig 11—1.0-meter, 1-turn unbalanced aerial radiation patterns (*EZNEC*).

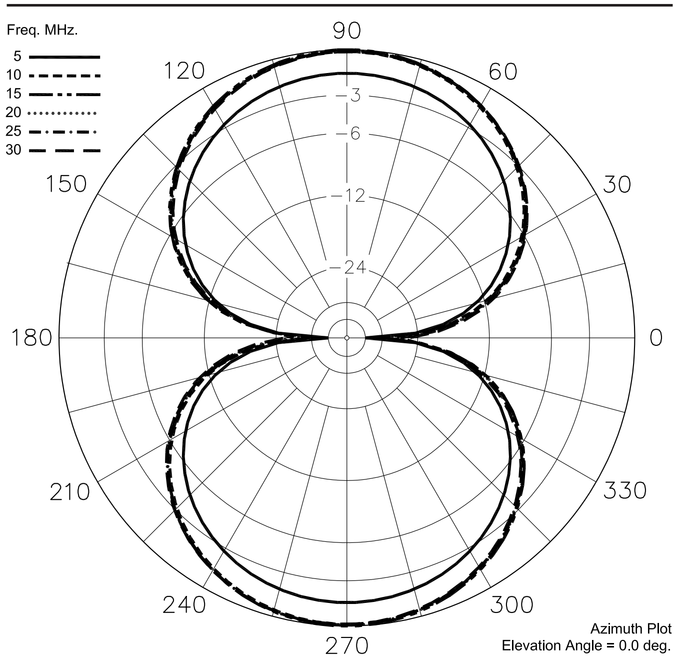

Fig 12—0.5-meter, 2-turn balanced aerial radiation patterns (*EZNEC*).

serious consequences on the impedance and the radiation pattern, as we are about to see.

By way of *EZNEC*, the loop aerial model used earlier is now placed in an environment having a perfect ground, with one end of the aerial connected to the ground, representing a worst-case application. This is not entirely unrealistic, as in the application of a compact aerial such as this we can easily anticipate that some users will mount the aerial in very close proximity to ground. For the balanced aerial, two sources of equal and opposite amplitude are used with the common point connected to ground. The result of this configuration is shown in Fig 8, where it is compared with the earlier free-space results, showing that the antiresonance frequency is shifted downward slightly as is the resonant frequency, as should be anticipated by virtue of parasitic loading to ground.

For the unbalanced aerial, one of the sources is removed, leaving the aerial with a single source on one side and the other side grounded, as described in Fig 7 earlier. In Fig 9, the results are compared with the balanced aerial results of Fig 8. It is clear that the antiresonant and resonant frequencies of the unbalanced aerial are now half of what they were for the balanced aerial, confirming that the unbalanced aerial is twice as long electrically as the balanced aerial. The low Q of the second antiresonance shows that the Q of the unbalanced aerial degrades with increasing frequency.

A comparison of the radiation patterns further reveals the degree to which unbalanced loop aerial operation degrades performance. The radiation patterns for the balanced loop aerial are shown in Fig 10, where the direction of the pattern is parallel with the plane of the aerial. Here we can see that the balanced loop aerial exhibits the deep, sharp nulls perpendicular to the plane of the aerial that are a characteristic of loops and make them popular for direction finding. The gain of the aerial degrades slightly as the frequency approaches antiresonance, but the quality of the nulls remains.

The radiation patterns for the unbalanced loop aerial are shown in Fig 11. The imbalance in the currents has led to a severe degradation in the quality and usefulness of the aerial, where the pattern nulls disappear rapidly at a low frequency and the aerial becomes virtually unidirectional as the frequency approaches antiresonance.

A subsequent model for a two-turn loop aerial was formed and used to evaluate the consequences of making a more compact aerial for the same range of frequencies. This second model is a 0.5-meter diameter 12-sided polygon having the same 6-mm wire diameter, the turns being spaced 30 mm apart, acknowledging the guidelines for minimizing the proximity effect given by Smith.[13, 14] The exact center of the aerial, at the bottom immediately adjacent to the feed points, is grounded to ensure exact balance. The radiation patterns are shown in Fig 12, and except for a slight reduction in the peak gain, this aerial remains suitable for consideration where circumstances dictate that a smaller aerial be used.

Construction Practices

Before we begin an experimental evaluation of circular loop aerials, notice that none of these equations nor any of the *NEC* programs (*EZNEC* included) account for the proximity of adjacent wires (in multiturn loop aerials) or the dielectric loading of the supporting structure, if any. We are all familiar with the effects that closely wound wires have on inductors, and the same is true here. The result of moving the wires closer together in a multiturn loop aerial is that the antiresonance frequency decreases but the resonance frequency remains virtually unaffected. We shall see this later, when we compare experimental results with those of *EZNEC*. Further, closely spaced conductors in multiturn loop aerials dramatically increase the loss resistance, and a spacing of at least five times the wire radius should be used to prevent this effect (see Notes 13 and 14). Hint: Do not use computer ribbon cable.

Since loop aerials have very high impedances at antiresonance, any dielectric loading from the supporting structure will effect the antiresonance frequency. Therefore, take care in the mechanical design, use insulating materials such as wood or plastic with low dielectric constants, and keep use of such materials to a minimum. Avoid metallic materials such as screws and nails. Rely instead on good woodworking joinery practices and proper adhesives. (Hint: Attaching copper tubing to a solid piece of plywood using EMT clamps with sheet metal screws is a bad idea.)

Larger diameter conductors, such as 1/4-inch (6-mm) or 1/2-inch (12-mm) copper tubing require less supporting material. Be mindful here that soft flexible copper tubing may contain lead, which greatly increases the bulk resistance. Large-diameter copper electrical wire and refrigeration tubing have good resistance characteristics and are therefore preferable materials. Rigid copper pipe is ideal if you can find some way of bending it into a uniform circle without collapsing it in the process.

Because of the low impedance of loop aerials, it is essential that all solder connections be done thoroughly and properly, using a good acid-free flux to ensure good wetting and preferably using a solder containing silver to avoid any lossy connections.

Experimental Results

With all of this analytical and mod-

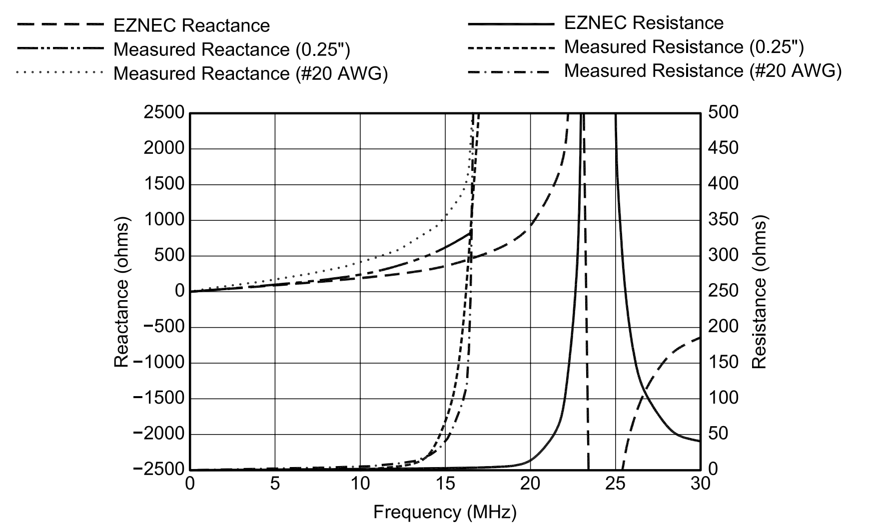

Fig 13—*EZNEC* and measured impedances for 1-meter, 1-turn unbalanced aerial at ground level.

eling information available, it is now safe to construct and test a prototype. For demonstration purposes, a single-turn aerial having a diameter of 1 meter was constructed using both #20 AWG wire and 1/4-inch refrigeration tubing. The supporting frame was made with a 24-inch-diameter circle of 3/4-inch-thick plywood to which arms made from 1/2-inch-thick plywood were attached at 30° intervals. The arms were glued to the disk and held in place with screws, which were later removed to reduce any parasitic loading.

Impedance measurements were made using a GR-1606A bridge and an HP-8407A vector network analyzer, and then comparing the two methods to correlate the results. This was necessary because of the low impedances at lower frequencies and the high impedances as the antiresonance is approached. Care was taken to ensure that the measurements were not affected by nearby objects. The presence of nearby AM broadcast stations made repeated measurements necessary to ensure accuracy.

Initial tests were made for the unbalanced aerial using #20 AWG wire for the conductor for later comparisons. The conductor was then replaced with more desirable 1/4-inch copper tubing. These test results are shown in Fig 13 along with the *EZNEC* simulation results for the unbalanced aerial model. Here we can see that the antiresonance frequency has been lowered by almost 25%, most of which can be attributed to the dielectric loading caused by the supporting frame. There is little difference in the antiresonance between the two conductors, and the sharp knee in the resistance is similar to that from the *EZNEC* simulation, showing that the aerial Q has not suffered appreciably from the loading.

In Fig 14, the Q of the aerial is calculated and compared between the two conductor materials, the 1/4-inch copper tubing having a Q almost twice that of the #20 AWG wire, especially at the lower frequencies. This verifies the earlier finding from Kraus' Eq 2 and Flaig's Eq 9 and 10 regarding the effect of the wire diameter on the resistances. This effect is well known in practice, and it is reassuring to know that an analytical method is available to aid in the design process.

Finally, the prototype aerial was configured for balanced feed using a three-winding hybrid transformer, the exact details of which will be covered in the design of the antenna amplifier/tuner in Part 2 of this series. The results in Fig 15 show that the antiresonance has been reduced by 32%, which is reasonably consistent with the reduction noticed for the unbalanced aerial test.

These tests confirm that an unbalanced loop aerial feed effectively reduces the resonance frequency to half that of the same aerial with a balanced feed, thereby verifying the *EZNEC* simulations used in the design process. To this degree, we can now have confidence in using the equations from the two analytical methods in conjunction with the simulation of *EZNEC* in the design of loop aerials.

Synopsis

Loop aerials are viable options when compact antennas are being considered. The results described here show that it is not unreasonable to construct such an aerial with design efficiencies in excess of 80% provided that certain design rules are given proper attention:

1. The diameter of a single-loop aerial should be approximately $\lambda/20$ to $\lambda/10$.
2. Use the fewest turns possible, preferably no more than two. If using two turns, ground the center to ensure good balance.
3. For multiturn loop aerials, separate the turns by no less than five times the conductor radius to minimize proximity effect.
4. Use the largest diameter conductor available, such as 1/4 or 1/2-inch copper tubing. Do not use tubing that is a copper/lead alloy.
5. Solder all junctions properly, preferably using silver solder to accommodate the low impedances.
6. Minimize support material to avoid parasitic loading.
7. Use a balanced feed.

With due attention to these details, it is easy for those having a good understanding of the mechanical aspects of aerial construction to make a loop aerial having good efficiency. In Part 2, we will cover the theory, design and operation of the antenna amplifier/tuner and the control unit.

Notes

[1] A. Boswell, "Loop Antennas in the 3-30 MHz Band," *Eighth International Conference on HF Radio Systems and Techniques*, 2000, pp 33-36.

[2] "Radio Instruments and Measurements," National Bureau of Standards Circular C74, 1937.

[3] A. J. Henk, "Loop Antennas: Fact, Not Fiction," *Radio Communication*, Sep 1991, pp 51-53 and Oct 1991, pp 47-50.

[4] J. D. Kraus, *Antennas*, 2nd ed. (New York: McGraw-Hill, 1988).

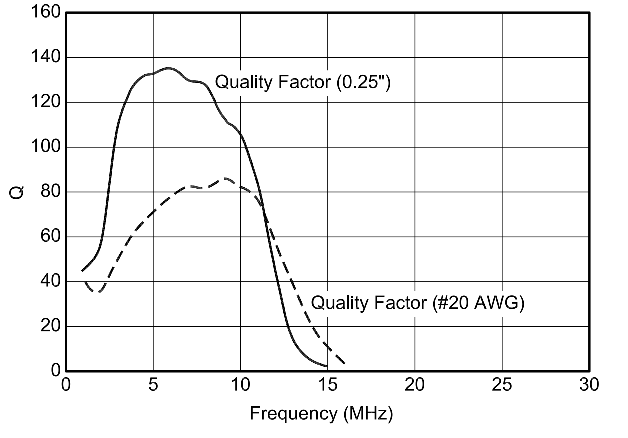

Fig 14—1-meter, 1-turn unbalanced antenna quality factor versus wire diameter.

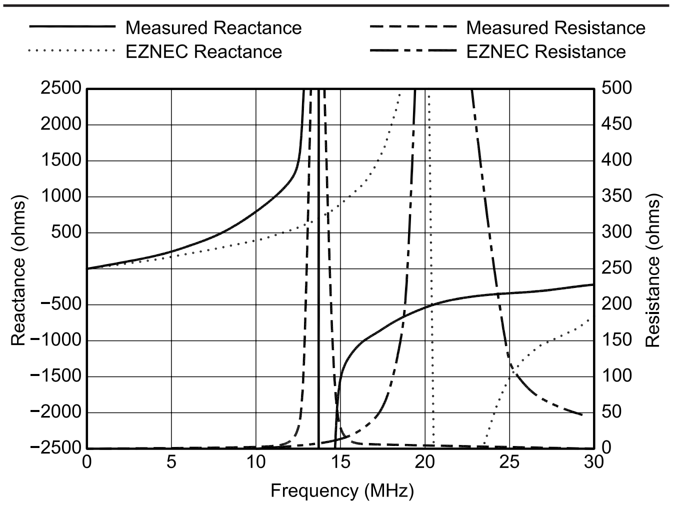

Fig 15—*EZNEC* and measured impedances for 1-meter, 1-turn balanced aerial at ground level.

[5]F. E. Terman, *Electronic and Radio Engineering*, 4th ed, (New York: McGraw-Hill, 1955).
[6]E. H. Newman, P. Bohley and C. H. Walter, "Two Methods for the Measurement of Antenna Efficiency," *IEEE Transactions on Antennas and Propagation*, Vol 23, No. 4, Jul 1975, pp 457-461.
[7]K. H. Awadalla, and A. A. Sharshar, "A Simple Method to Determine the Impedance of a Loop Antenna," *IEEE Transactions on Antennas and Propagation*, Vol 32, No. 11, Nov 1984, pp 1248-1251.
[8]T. L. Flaig, "The Impedance and Efficiency of Multiturn Loop Antennas," *Electroscience Laboratory Technical Report 2235-3*, Ohio State University, 3 Apr 1968.
[9]B. A. Munk and T. L. Flaig, "Radiation Resistance and Efficiency of Multiturn Loop Antennas," *Electroscience Laboratory Technical Report 2235-4*, Ohio State University, 1 May 1968.
[10] C. D. Taylor and C.W. Harrison, "On Thin-Wire Multiturn Loop Antennas," *IEEE Transactions on Antennas and Propagation*, Vol 22, No. 3, May 1974, pp 407-413.
[11]J. E. Storer, "Impedance of Thin-Wire Loop Antennas," *Transactions of the AIEE*, Pt 1, Vol 75, No. 11, Nov 1956, pp 606-619.
[12]R. W. P. King and C. W. Harrison, *Antennas and Waves: A Modern Approach*, (Cambridge, Massachusetts: MIT Press, 1969) Chapters 9 and 10.
[13]G. S. Smith, "Radiation Efficiency of Electrically Small Multiturn Loop Antennas," *IEEE Transactions on Antennas and Propagation*, Vol 20, No. 9, Sep 1972, pp 656-657.
[14]G. S. Smith, "Proximity Effects in Systems of Parallel Conductors," *Journal of Applied Physics*, Vol 43, No. 5, May 1972, pp 2196-2203.

Special Properties of 45° (λ/8) Networks

Some antenna matchers are easier to tune than others. Which is easiest to tune and why?

By Grant Bingeman, KM5KG

Why is Shortwave Radio Important?

In this age of satellite communication, broadband fiber optics, point-and-click computer operating systems and high-definition television, why is old radio technology still vitally important? The answer is pretty obvious: It relates to the areas of security, backup, emergency, independence, preparedness, and so forth. In other words, what happens when the lights go out? Well, there are a lot of Amateur Radio operators who have immediate access to small battery-powered QRP transceivers that regularly communicate over thousands of miles using a large variety of modulation methods. There are military installations that maintain shortwave, medium-wave and long-wave communication capabilities as listening posts or as emergency communication posts. There is a surprising amount of clandestine message traffic from foreign intelligence-gathering agents living in the United States that relies on old-fashioned ionospheric radio propagation—and the list goes on.

1908 Paris Ave
Plano, TX 75025
DrBingo@compuserve.com

Why is Impedance Matching Important?

1. To radiate an RF signal, it is necessary to deliver RF power to an antenna;
2. Radiated RF signal intensity (oscillating electric and magnetic fields) is proportional to the square-root of the amount of power absorbed by the radiating antenna from the transmitter (almost anything can radiate, but some antennas are better than others);
3. Maximum practical available RF power is delivered by a real-world transmitter to a radiating system when the impedance seen by the transmitter is equal to its nominal design load value as specified by the manufacturer (50 ohms resistance, no reactance is typical);
4. System power losses and reflected power are minimized when the antenna impedance is matched to the nominal design load impedance;
5. A variety of methods exist to provide impedance transformation: lumped-parameter **L**, **T** and π networks, transmission line stubs and transformers, antenna dimension adjustment, etc.

In other words, to obtain maximum transmitted and received RF signal intensity, a correct impedance match must exist between the transceiver and the antenna. Remember that the Law of Reciprocity tells us that when we have a good impedance match, we have created two good situations at the transceiver location:

1. When transmitting, maximum transmitter power will be delivered to the antenna, and
2. When listening at the same frequency, maximum antenna signal will be delivered to the receiver.

Throughout this article, keep in mind that the *RF system* consists of four blocks: a transceiver, a transmission line, an antenna coupler network and an antenna. In the context of this article, an RF *network* is simply a configuration of resistances and reactances. A load impedance is defined to be what a transmitter would see looking towards the radiating antenna. This article will show you how to simplify impedance matching network adjustment, taking this often seat-of-the-pants process out of the realm of trial-and-error. A logical understanding of matching network design will reduce your chances of burning up components inside and outside of the network, especially if you have an auto-tuner. A class of networks that eliminates interaction between *reactance* and *resistance* adjustment will be introduced. Relationships among network Q, bandwidth, phase shift, resistance transformation ratio, component stress, adjustability and load resonance will be discussed. In-line impedance measurement at high power will be mentioned. The physics or *magic* of electromagnetic radiation, displacement current, Maxwell, Lorentz, Hertz, Poynting and all the unsung heroes are beyond the scope of this article, but are certainly worth a little Web surfing. Special coupled devices may be covered in a future article.

Study the graphs in this article carefully and take your time perusing the material. Also, get a practical understanding of the orthogonal and polar representations of impedance before attempting to apply the design concepts discussed. Remember that the subject matter is RF, not dc, so there is always a reactance term to consider in addition to a resistance term.

Many Amateur Radio operators prefer to think of RF impedance matching networks (also called *couplers*) simply in terms of forward and reflected power, whereas an RF designer may think more in terms of Q, R_{in} and Z_{load}. In the case of an antenna, Z_{load} consists of an antenna *resistance* term, R_{ant}, and a *reactance* term, X_{ant}. In many cases, X_{ant} is resonated or *tuned out* at the feed-point of the antenna. Or X_{ant} may not be resonated until a transmission line or other devices have transformed it. In any case, the function of impedance matching is to provide optimal RF-power transfer from the transmitter to R_{ant} over a wide range of frequencies, without overheating network components, exceeding voltage ratings of components or losing much power in the network.

Please notice that there are two separate and distinct things going on in any impedance matcher, and it is important not to confuse the two, even though the functions may ultimately be combined in a single network leg:

1. Resistance transformation (*loading* the transmitter power amplifier), and
2. Reactance cancellation (resonating or *tuning* the transmitter load).

When we say a load or antenna is *resonant* it means that its reactance has been reduced to zero ohms. At a specific frequency, resonance can be attained by adjusting the physical dimensions of an antenna, or by adding a series or a shunt reactance at the input to the antenna. A shunt reactance will also transform the load resistance, which can complicate the adjustment process. This is why T networks are sometimes easier to adjust than π networks, since the output series leg of a T network provides resonance simply by inserting a reactance of the opposite sign but same magnitude as the load reactance. (In the ideal, loss-less case, such a series reactance does not affect resistance). For example, assume a load impedance of $46 + j67\ \Omega$. Resonance is achieved by inserting a series capacitor of $-j67\ \Omega$, which would be about 330 pF at 7.1 MHz, according to Ohm's Law.

Impedance Matcher Design

Sometimes a network is designed for a desired phase shift without regard to a specific Q, such as in some phased antenna arrays, where individual network Q is simply desired to be low. At other times, such as in a filter, a high specific Q may be the primary design target. In either case a specific *resistance transformation ratio* is desired. A transmitter tube power amplfier may want to see 1000 Ω,

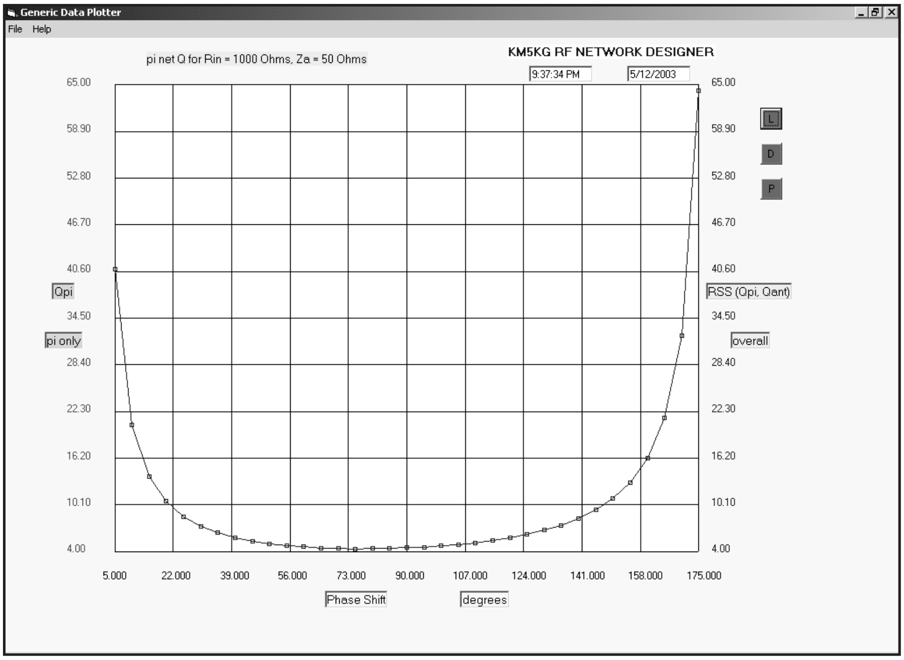

Fig 1—T and π-network Qs are typically highest for very low and very high values of phase shift.

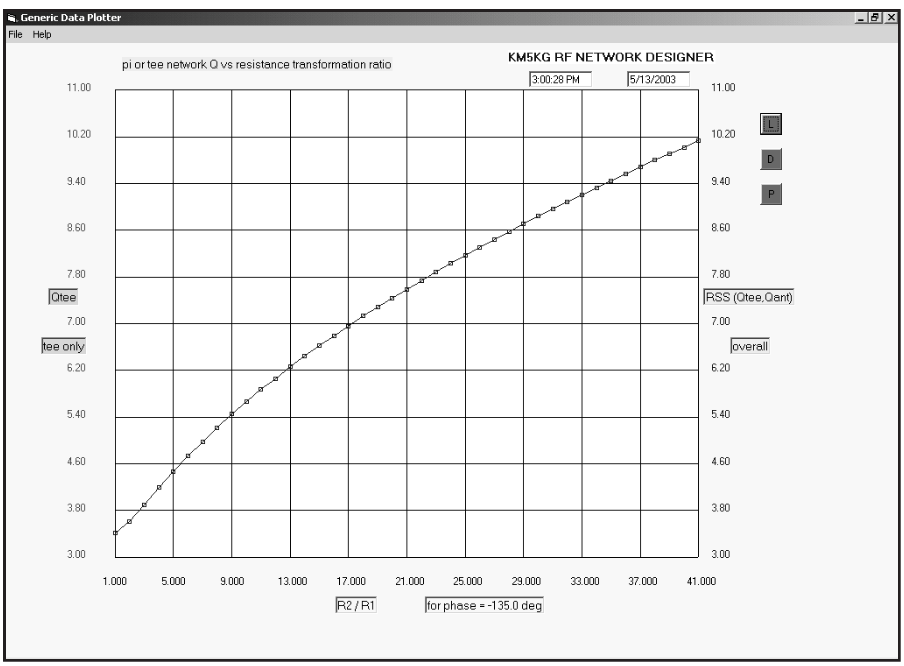

Fig 2—T and π-network Qs increase as the resistance transformation ratio increases.

resonant, when operating into a 50-Ω transmission line, in which case the transformation ratio is 1000:50 = 20. We will define resistance transformation ratio as the greater of R_{in}/R_{load} and R_{load}/R_{in}. In fact, the network Q is the same for transformation ratios of 2 and 0.5, or 5 and 0.2, or 10 and 0.1, etc. In this network context, $R_{in} + j0$ is the impedance seen looking into the network when the network is terminated in an impedance of $R_{load} + j0$.

T and π network Q and component stresses are related to network phase shift. For this article, I define *phase shift* as the time delay of the current passing through a network, not the delay of a voltage across a network, although in some cases they are the same. For example, a 20-foot length of transmission line may be 60 electrical degrees long at a particular frequency where the load impedance is equal to the line's characteristic impedance. We could then say that the current leaving the line lags the current entering the line by 60°, or the phase shift through the line is –60° or λ/6.

Notice that in all cases, the L network phase shift produces the lowest network Q. You can think of an L network as a degenerate form of T or π network. However , keep in mind that L network phase shift is not independent of resistance transformation ratio, whereas T and π network phase shifts are independent of transformation ratio. Fig 1 shows that T and π network Qs are typically highest for very low and very high values of phase shift. Fig 2 shows that T and π network Qs increase as the resistance transformation ratio increases. Network Q is minimum when the transformation ratio = 1.0. Notice that the Q of the resonated antenna is separate and distinct from the Q of the network.

This article assumes that the network Q is determined when the network is terminated in a flat load resistance, or when the antenna has a Q of zero. We will call this the *isolated case*.

This article will not explicitly address antenna Q or component Q, to reduce confusion among the three Qs (network, load and component). Do keep in mind that network Q and antenna Q can sometimes partially cancel each other over a certain frequency band, so a system viewpoint is ultimately needed. It is also true that component losses improve bandwidth. It should be clear to the reader, however, that each individual part of the system needs to be understood first in its isolated form. Then through careful design, synergy can produce a system Q that is less than the individual Qs across a specific frequency sub-band, at the expense of higher SWR outside that sub-band.[1]

The effects of variable load impedance on the performance of a network optimized for easy adjustment will be considered. In other words, what can be said about a network designed for an ideal flat load impedance compared with that same network operating into a typical antenna at the end of a random length of mismatched transmission line? Can the interaction between resistance adjustment and reactance adjustment be kept at some minimal value, regardless of the impedance excursions of the load beyond the design center frequency or load impedance? Is there an explicit technique that can be used to match any antenna impedance to a value that keeps the transmitter happy and minimizes interaction between adjustment of R and X? What tools are required to do this?

Mathematics

Please refer to the built-in help text in the *RF Network Designer* demonstration, for the many design equations that apply to the subjects of this article. The demonstration can be downloaded from **www.qsl.net/km5kg**.

A little math derived from the Q of an L network designed to match R_p to R_s can relate the phase shift and Q of T and π networks, each of which is simply two L networks back-to-back. Starting from the definition of L network Q

$$Q = \left|\frac{X_s}{R_s}\right| = \left|\frac{R_p}{X_p}\right| = \sqrt{\frac{R_p}{R_s} - 1} \qquad \text{(Eq 1)}$$

we know that the phase shift across an L network is $\tan^{-1}(Q)$. Notice that in an L network, R_p is always greater than R_s, and the sign of X_p (the shunt component reactance) is always opposite that of X_s (the series component reactance). Q is not related to the sign of the phase shift or the signs of the reactances (see Fig 3). Valid values for Q are always positive in passive systems.

The effective Q of a T or π network is the RSS (square root of the sum of the squares) value of the input and output L network Qs. A frequency sweep of any network would also show that:

$$Q = \frac{f_0}{f2 - f1} \qquad \text{(Eq 2)}$$

Where f_0 is the band center frequency and $f2–f1$ is the 3-dB bandwidth. Per Fig 4, the effective Q of the example π network is:

$$Q = \sqrt{7.3^2 + 1.4^2} = 7.4 \qquad \text{(Eq 3)}$$

[1]Notes appear on page 51.

and the 3-dB bandwidth is 7100/7.4 = 960 kHz or ±480 kHz. Thus the 3-dB bandwidth is from 6620 to 7580 kHz. The input reactance and resistance to a network are typically equal at the 3-dB band edges.

For example, if the input impedance to a network were 1000 + j0 Ω at band center, then the input impedance would be about 1000 ± j1000 Ω at the 3-dB band edges, which are also called the *half-power points* in the case of an ideal RF source. This equates to a band-edge SWR of 3:1, which is really not a suitable load for a typical transmitter. Some impedance matcher adjustment must be provided at the band edges, even though the SWR is a perfect 1.0 at the band center.

The effective system Q is the RSS of the network and the resonated antenna Qs, with the caveat that sometimes the two Qs can oppose one another to produce a better frequency bandwidth over a limited range. Remember that the basic definition of Q is that of a series-resonant R-L-C triad or a parallel-resonant R-L-C triad. A more general definition of Q is the band-center frequency divided by the 3-dB bandwidth of a network and antenna combination. And as always, when in doubt, measure!

You can save adjustment time by exploiting the mirror-image symmetry of matching networks. For example, in Fig 4, the left-to-right transformation is 1000:50, and the right-to-left transformation is 50:1000. In other words, you can terminate the right port in 50 Ω and adjust for 1000 Ω at the left port. Or you can terminate the left port in 1000 Ω and adjust for 50 Ω at the right port. If you need to tune out a reactance, X_{load}, at the right port, then you would simply adjust for $50 - jX_{load}$ at that port, the complex conjugate impedance, when the left port were terminated in 1000 Ω.

Independent *R* and *X* control

A T, π, L network or transmission line that has a phase shift of an odd multiple of 45° (±45°, ±135°, etc), has the unusual quality of allowing *independent* resistance and reactance adjustment as seen at the input to the network. This is a highly desirable feature when tuning an RF power amplifier, for example. Consider a –135° π network that matches a 50-Ω load to the 1000 Ω that a particular tube power amplfier wants to see. Adjusting the input shunt leg of the π network (*X1*) affects mostly the reactance seen by the power amplifier, which is a process we normally call power amplifier *tuning* where we adjust for minimum power-amplifier DC current. Adjusting the output shunt leg

($X2$) of the π network affects mostly the resistance seen by the power amplifier, which is a process we normally call power amplifier *loading*, where we adjust for a particular power output from the transmitter.[2] When these adjustments are independent and do not interact, it is not necessary to jump back and forth very often between controls, as would be required with a 90° network, for example. There is a lesser tendency for a transmitter operator to tune by the "seat of the pants" and overstress network components or the power amplifier tube when interaction between the tuning and loading controls is reduced.

Fig 4 is a design for a 40-meter band, –135° lossy π network.[3] The loaded Q at the power amplifier is about 7.3. Notice that the currents and voltages are CW RMS values for 1 kW. Most of the heating losses occur in the coil, which has a Q of 300. The capacitors have Qs of 900. Table 1 shows the results of a sensitivity analysis, where the input and output capacitors are adjusted by changing the reactances in the $X1$ and $X2$ boxes of Fig 4. Notice that there is only a small amount of interaction between the controls. $X1$ does indeed mostly affect tuning, and $X2$ does indeed mostly affect loading. Per Table 1, $X1$ changes input reactance by 9% when input resistance changes only 1%. $X2$ interaction between resistance and reactance is similar. But interaction between input resistance and reactance is bad when $X3$ is the control arm. Therefore $X3$ would only need to be adjusted when the load varies from the design center value. Since this particular π network is built into the transmitter, an external impedance-matching network needs to take up the slack, producing a resonant load of 50 Ω when frequency or antenna are changed.

A –90° π Network Example

We can compare the adjustment interaction of the –135° π network with a common –90° π network (see Fig 5), to verify the odd-multiple-of-45° theory. The –90° π network has a loaded Q of only 4.4, so will not filter the power amplifier harmonics and spurious signals very well, but this is not critical to our adjustment-sensitivity comparison. Table 2 tells us that $X1$ and $X2$ act as input reactance controls, and $X3$ affects both R_{in} and X_{in}, with greater effect on the reactance. So there does not appear to be an independent resistance control in this –90° network. Much trial and error is required to adjust this network, or an RF generator and impedance bridge to set each branch perfectly at the start of the matching process.

The ugly reality of HF lumped-parameter tuning means that stray shunt capacitance, coupling between components and the metal housing, tubing and strap inductance, losses and self-resonances are often compensated for by a haphazard design, installation and adjustment approach. Careful component placement and connection are important considerations, and an accurate impedance meter is worth its weight in gold when adjusting any network.

A –45° L Network Example

Assume you want to match your transmitter to a 100-Ω transmission line. Notice that an L network designed to match 50 to 100 Ω has a phase shift of ±45° per Fig 6. The shunt leg of any L network is on the higher resistance side. So, in this case, the shunt-leg reactance ($X2$) would affect mostly the input resistance to the L network, and the series-leg reactance ($X1$) would affect mostly the input reactance (see Table 3). In fact, any L network where R_{HI}/R_{LO} = 2 has a phase shift of ±45°.

A –135° T Network Example

Fig 7 and Table 4 show a –135° T network designed to transform 50 to 100 Ω, where the input coil ($X1$) provides reactance control, and the output coil ($X2$) provides resistance control. If this were a +135° T network, the input and output arms would be

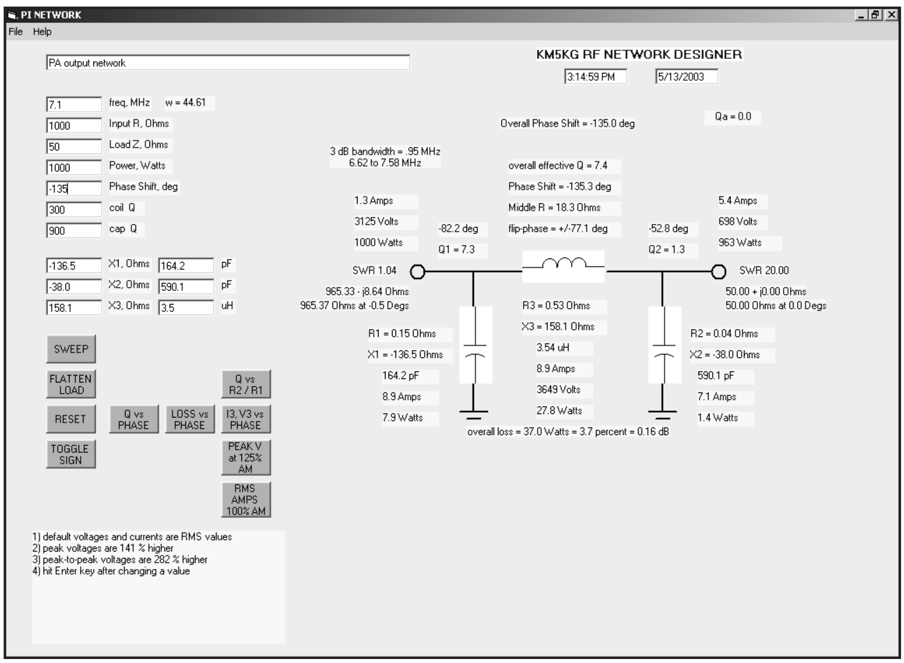

Fig 4—A –135° π network transforming 1000 Ω to 50 Ω designed for the 40-meter band.

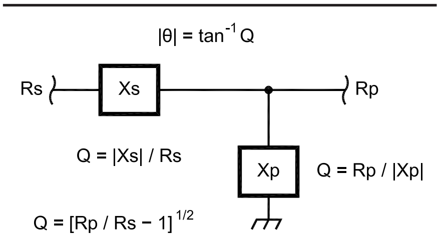

Fig 3—Q is not related to the sign of the phase shift or the signs of the reactances.

Table 1— –135° π-Network Adjustment Sensitivity

X1 *(Ω)*	X2 *(Ω)*	X3 *(Ω)*	*Network* Z_{in} *(Ω)*	*Comments*
–136.7	–37.0	158.1	998 + *j*0	Design center
–135.0	–37.0	158.1	990 –*j*91	*X1 reactance* control
–138.4	–37.0	158.1	990 + *j*89	
–136.7	*–35.0*	158.1	1075 –*j*5	*X2 resistance* control
–136.7	*–39.0*	158.1	934 + *j*0	
–136.7	–37.0	*156.0*	957 + *j*104	*X3 mixed* control
–136.7	–37.0	*160.0*	1015 –*j*102	

variable capacitors, but this would constitute a high-pass network, which would not help to attenuate harmonics. So, you don't see too many leading phase-shift networks used in transmitter output networks. The leading network is more likely to be used in phasing and coupling equipment design, where it is assumed that the harmonics have already been filtered to a reasonable level.

A Transmission-Line Example

The special case of 76 feet of Cablewave 50-Ω LDF4-50A transmission line, which has a phase shift of –225° at 7.1 MHz when perfectly matched, can be assessed by changing the reactance in the load impedance box of the transmission line model per Fig 8. In other words, if the termination of this line consisted of a 50-Ω resistor, a series-resonant variable coil and a fixed capacitor of |30 Ω| reactance each, a knob on the coil would allow excellent resistance control at the transmitter end of the line, per Table 5. The same type of series-resonance circuit could provide reactance control if placed at the input to the transmission line. Or the termination resistance could be varied to produce a similar effect.

A Stub Example

At frequencies above the 10-meter band, it is practical to replace some of the lumped parameter coils and capacitors with shorted or open lengths of transmission line that produce the desired reactance at their inputs. Coaxial line stubs sometimes have an adjustable plunger short-circuit that an operator can slide up and down the inner conductor. Of course such a stub has an air dielectric and no support for the inner conductor other than the plunger. Ladder lines have a jumper that can be moved along the line.

Assume that you had a requirement similar to the –135° π network of Fig 3, but your operating frequency was 144 MHz. You would still need the same reactance values in each of the three π-network branches, but stubs would avoid many of the self-resonances, stray reactances and other problems associated with discrete coils or capacitors and their connections.

We want *X1* to be –137 Ω, *X2* to be –37 Ω and *X3* to be 158 Ω. According to Fig 9, if we use 50-Ω line with a velocity factor of 0.99, a short-circuited length of about 25 inches would work for *X1*, about 32 inches for *X2* and about 16 inches for *X3*. It is interesting to note that the reactance of a stub is not significantly affected by the loss of the line. The important consider-

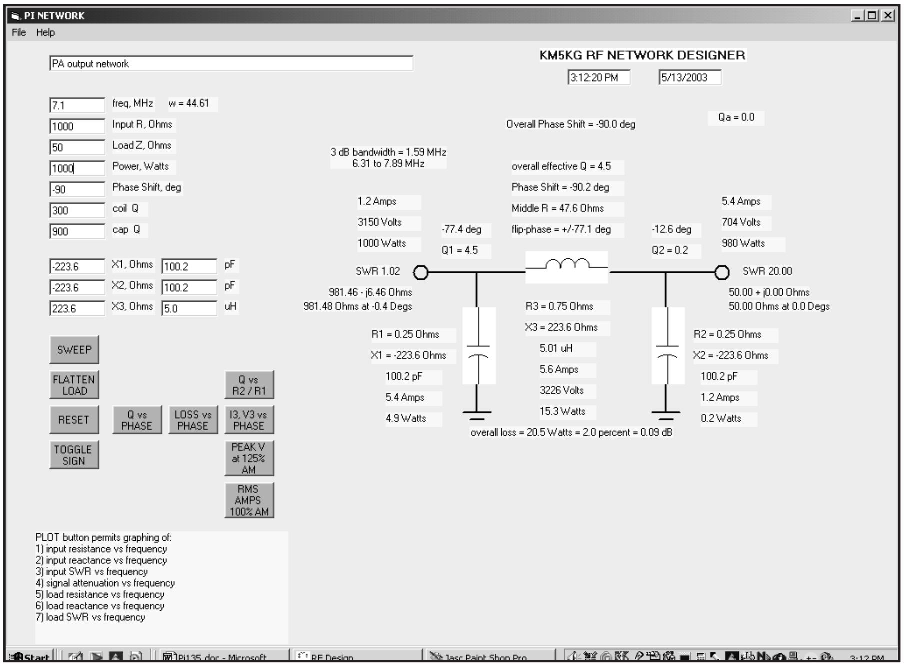

Fig 5—A –90° π network transforming 1000 Ω to 50 Ω designed for the 40-meter band.

Table 2— –90° π-Network Adjustment Sensitivity

X1 *(Ω)*	X2 *(Ω)*	X3 *(Ω)*	*Network* Z_{in} *(Ω)*	*Comments*
–226	–223	225.8	1001 + *j*0	Design center
–231	–233	225.8	992 + *j*95	*X1* reactance control
–221	–233	225.8	991 –*j*99	Strong
–226	–154	225.8	1001 –*j*103	*X2* reactance control
–226	–410	225.8	1001 + *j*99	Weak
–226	–233	231	1036 –*j*103	*X3* mixed control
–226	–233	220	940 + *j*99	

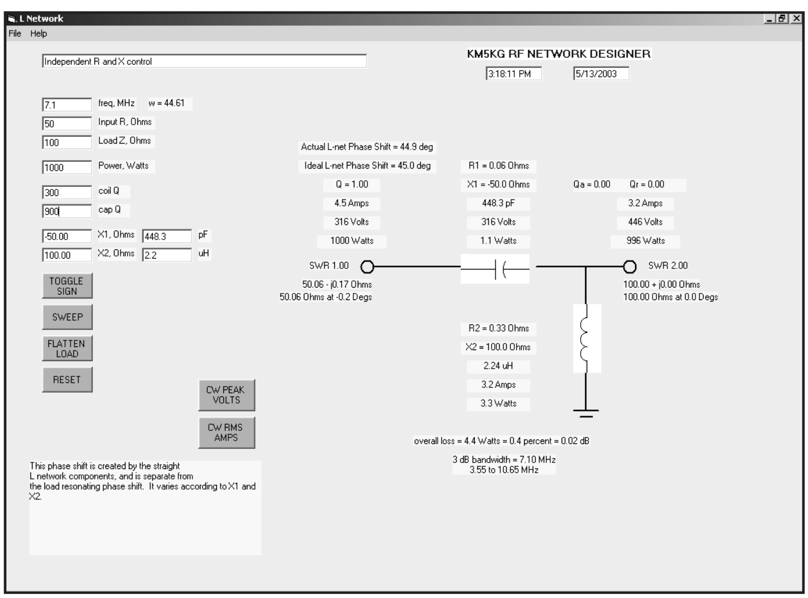

Fig 6—A –45° L network transforming 1000 Ω to 50 Ω designed for the 40-meter band.

ation is the impedance of the stub termination: How close to ideal is it? If you have some resistance and inductance in your short-circuit, or some capacitance in your open-circuit, it is a good idea to add this to your model.

Fig 10 shows what to expect if the stub termination impedances are 0.1 + $j0\ \Omega$ and a small inductor (essentially a short length of wire at 144 MHz) is used in place of *X3*. The input impedance to this π network is quite sensitive to the coil value, which is obtained with about 0.174 µH and an inductor *Q* of 600.

Remember that some stubs may require both conductors to be above ground potential. Thus in the case of coaxial transmission line, the insulation or lack thereof on the outer braid or conductor can affect placement of the stub. It is possible for the outer-conductor to be *hot*, or at some RF voltage potential above the reference or ground value. As such, the stub may also radiate RF, thereby becoming a part of the antenna.

Since most of the stored energy in this high-*Q* transmitter output network can be found in the first shunt leg, adjustment of stub 1 is touchy. As you can see in Table 6, a change in the stub-1 length of only about 1/16 inch creates a big change in the impedance seen by the power amplifier at this relatively high frequency of 144 MHz. Adjusting such a device could be a very frustrating experience unless a vernier of some kind is provided. That might be a disk attached to a fine-thread screw and lock nuts forming an adjustable shunt capacitor.[4] This still sounds like a pain to adjust with a screwdriver, so a knob would be helpful.

Adjustment when Load Varies

Assume that a load impedance can exist anywhere within the 5.82 SWR circle (3-dB bandwidth) on a Smith Chart and that our reference impedance is 100 + $j0\ \Omega$. When the load resistance is held at 100 Ω, this means that the load reactance can vary from –100 to +100 Ω. When the load reactance is held at 0 Ω, the load resistance can vary from 38 to 267 Ω. A frequency range must also be selected, since the matching-network component reactances are a function of frequency, and most amateurs want to operate on more than one frequency.

Fig 7 shows the design values for a –135°, 50:100-Ω T network. Specific inductor and capacitor values are shown for 7.1 MHz. Resonating the load reactance is a simple matter of adjusting *X2* over the expected reactance range of 100 to –100 Ω. T-network phase shift is not affected by using *X2* to resonate the load.

One way to provide this adjustment range for *X2* is by placing an inductor and capacitor in series. Either one or both of the components may be adjusted for the network reactance that provides resonance and ultimately the desired resistance transformation. A short-circuit or *shunt* across each component may be switched in or out depending on the load impedance.

For resistance transformation only, the reactances required in the three legs of the –135° T network over a load resistance range of 38 to 267 Ω are in Table 7.

If we use a –45° T network, the required leg reactances would not require as large an adjustment range compared to the –135° T network, but there is a sign change required of *X2* as shown in Table 8.

Let us not forget that *X2* must also handle the load reactance, so the required adjustment range of *X2* in a –45° T network is actually 124 to –204 Ω. Similarly the required adjustment range of *X2* in a –135° T network is then 0 to 530 Ω for the given load-impedance excursion. This is about 12 µH at 7.1 MHz.

The adjustment range of π-network components, as opposed to T-network

Table 3— –45° L-Network Adjustment Sensitivity

X1 *(Ω)*	X2 *(Ω)*	*Network* Z_{in} *(Ω)*	*Comments*
50	–100	100 + *j*0	Design center
40	–100	50 –*j*10	*X1* reactance control
60	–100	50 + *j*10	
50	–120	59 + *j*1	*X2* resistance control
50	–80	39 –*j*1	

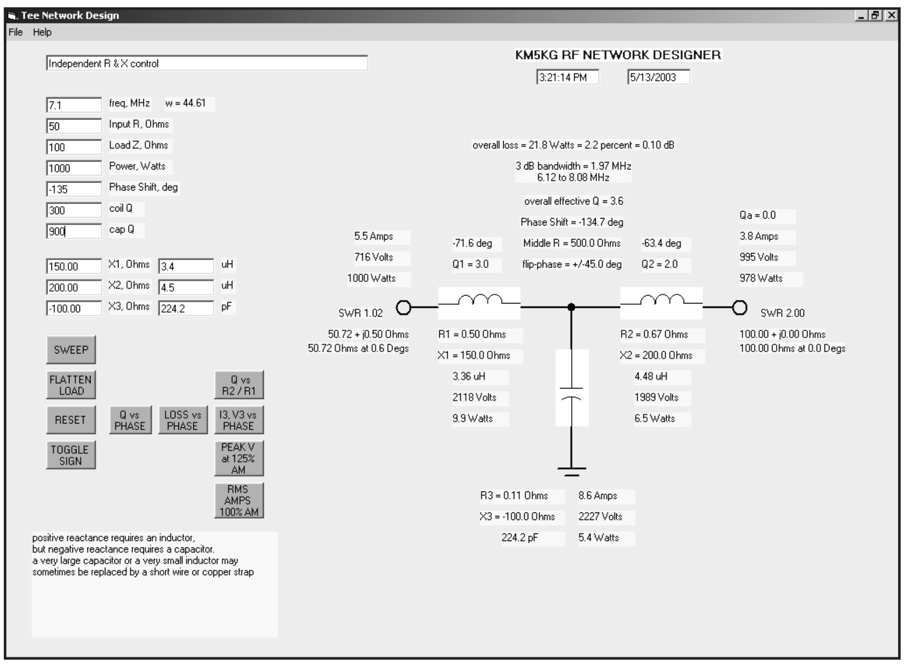

Fig 7—A –135° T network designed to transform 50 to 100 Ω for the 40-meter band

Table 4— –135° T-Network Adjustment Sensitivity

X1 *(Ω)*	X2 *(Ω)*	X3 *(Ω)*	*Network* Z_{in} *(Ω)*	*Comments*
150	200	–100	51 + *j*1	Design center
140	200	–100	51 –*j*9	*X1* reactance control
160	200	–100	51 + *j*11	
150	225	–100	40 + *j*2	*X2* resistance control
150	180	–100	62 + *j*2	
150	200	–95	44 + *j*10	*X3* mixed control
150	200	–105	59 –*j*9	

components, is complicated by the load resonance using the output shunt leg of the network, which forces a change in the load resistance. For the case of a –135° π network designed to cover the same load *R* and *X* range as the T network above, the required leg reactances are shown in Table 9. Will a –45° π network fare any better? Not according to Table 10.

This suggests that a middle phase shift, such as –90°, might be the answer; but notice in Table 11 that the input shunt leg must still change sign, requiring both an inductor *and* a capacitor or an adjustable transmission-line stub with a switchable open/short circuit termination.

Other than compromising the phase shift, the problem encountered by the odd-multiple-of-45° π networks can be eliminated if the load reactance is resonated in series rather than parallel. Yet this means that we have a component count of four instead of three. My preference for using T instead of π networks for antenna matching is based on the complication shown above and the fact that T network behavior is easier for me to predict and intuit during actual hands-on adjustment.

The advantage of adjusting your network to have a phase shift that is an odd multiple of 45° is simply the inherent independence of the resistance and reactance adjustments. The catch-22 here is that you must start with unknown load impedance, unless you have an in-line impedance bridge or meter (for details of a hot impedance meter, contact me). Assuming that each control has a calibrated dial and a means to convert from dial position to reactance, the desired three branch values can be calculated and set. Thus, you know the exact component stresses (assuming the effects of strays are small). During the adjustment process, once you are in the ballpark, you can switch to full power, and use the input arm of the network to touch up the reactance, and the output arm of the network to touch up the resistance.

Keep in mind that component voltage and current ratings should never be exceeded for any of the load impedance possibilities described above, so RF power output from the power amplifier may have to be reduced in some cases to avoid voltage breakdown. Short of having an RF ammeter in each leg and an RF voltmeter across each leg of a matching network, it is difficult to follow component stresses during the adjustment process. When expensive vacuum variable capacitors are at stake, however, in-line current and voltage samples provide a lot of security,

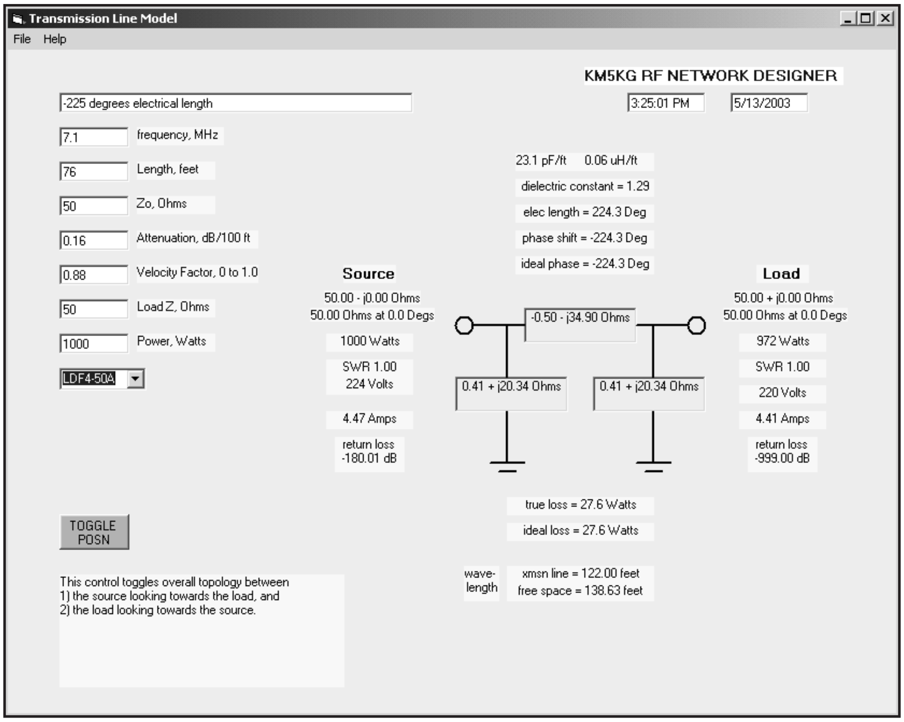

Fig 8—The special case of 76 feet of Cablewave 50-Ω LDF4-50A transmission line is assessed by changing the reactance in the load-impedance box of the transmission line model.

Table 5— –225° Transmission-Line Termination Adjustment Sensitivity

R_t *(Ω)*	X_t *(Ω)*	*Line* Z_{in} *(Ω)*	*Comments*
50	0	50 + *j*0	Design center
40	0	49 + *j*11	R_t reactance control
60	0	49 –*j*9	
50	–10	41 –*j*1	X_t resistance control
50	+10	61 –*j*1	

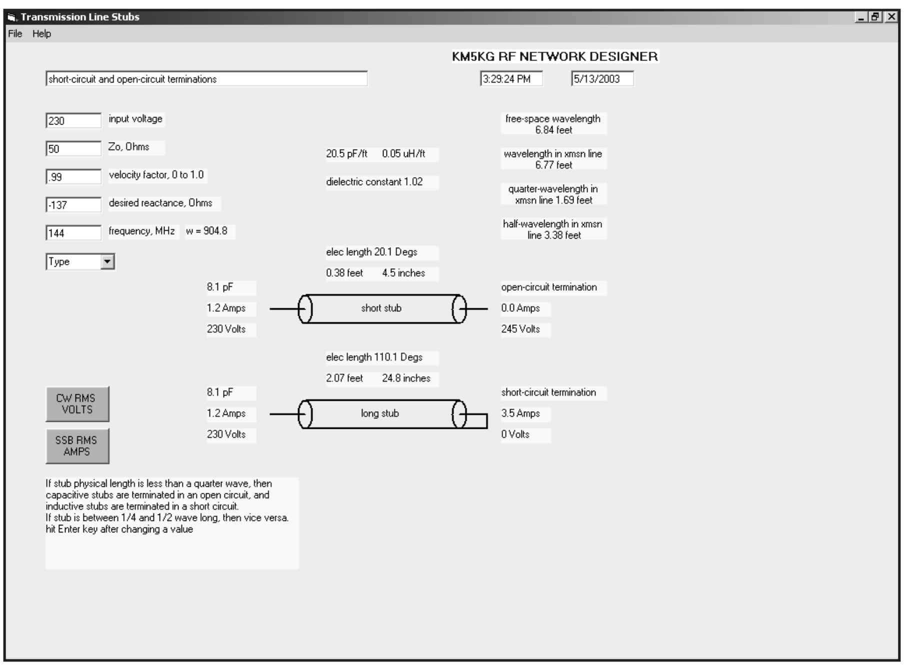

Fig 9—If we use 50-Ω line with a velocity factor of 0.99, a short-circuited length of about 25 inches would work for X1.

and an arc gap set to flash over below the component voltage rating is mandatory. Ultraviolet detectors make great arc sensors, and sometimes an RF-proof temperature sensor is useful as well.

A working knowledge of the math specifically associated with matching networks is always helpful. For example Eq 4 is rarely mentioned in the literature, but can be used to determine the phase shift across a T network if the shunt-leg current and some additional parameters are known (Fig 11). An easier method is to use Eq 5, a dimensionless version of Eq 4. This lends itself to uncalibrated, home-made loop sampling of the currents in the network branches.

$$2\cos\theta = \sqrt{\frac{R2}{R1}} + \sqrt{\frac{R1}{R2}} - I_3^2 \frac{\sqrt{R1 \bullet R2}}{P} \quad \text{(Eq 4)}$$

where

θ = phase shift across T network
R1 = input resistance, ohms
R2 = load resistance, ohms
P = input power, watts
I_3 = shunt-leg current, amperes

$$2\cos\theta = \frac{I1}{I2} + \frac{I2}{I1} - \frac{I_3^2}{I1 \bullet I2} \quad \text{(Eq 5)}$$

where

I_1 = input current
I_2 = load current

The π network dimensionless analog of Eq 5 is composed of voltage ratios:

$$2\cos\theta = \frac{V1}{V2} + \frac{V2}{V1} - \frac{V_3^2}{V1 \bullet V2} \quad \text{(Eq 6)}$$

where

V1 = voltage across input leg
V2 = voltage across output leg
V3 = voltage across series leg

It should be clear that it is difficult to create a universal impedance matching network that maintains a constant *Q*, phase and input impedance, and no interaction between resistance and reactance adjustment controls, over a large frequency range and a large load impedance range. That is generally why a separate transmitter output network is built into the transmitter, and one or more external impedance matching networks are used to transform the antenna impedance to some value that the transmitter can handle, usually 50 Ω.

The ultimate matching-network tool is a hot or in-line impedance meter that can be used to measure operating impedance during the adjustment process. A sensor head consisting of a voltage sample and a current sample can be installed at both the input and the output of the network, and the operator can simply switch the impedance meter between the two heads. It is easy to make an in-line impedance meter by adding an analog-to-digital card to a PC [see K3PTO's article in this magazine—*Ed.*], and applying a little math to obtain impedance, SWR, forward and reflected power, peak voltage, RMS current and so forth. For details, contact me at **DrBingo@compuserve.com**.

Conclusion

Independent resistance and reactance control as seen by a transmitter power amplifier or other RF source can be obtained by using a network having a phase shift that is an odd multiple of ±45°. The input arm of this generalized network affects mostly reactance, while the output arm affects mostly resistance.

Thus it is possible to reduce the interaction between resistance and reactance adjustments, thereby reducing the number of iterations needed to obtain some desired impedance at the point where the RF power is generated in a transmitter. This allows quicker tune-up of a transmitter after frequency or antenna changes, as long as the load impedance is reasonably close to the expected value. For large impedance changes, a hot (or *operating*) load impedance meter is very helpful.

It is important to understand that impedance matching is best considered as two separate steps:

1. Resonating or tuning out the reactance of the load, and
2. Transforming the load resistance to the desired resistance.

Ultimately the required network output-leg reactance can be combined

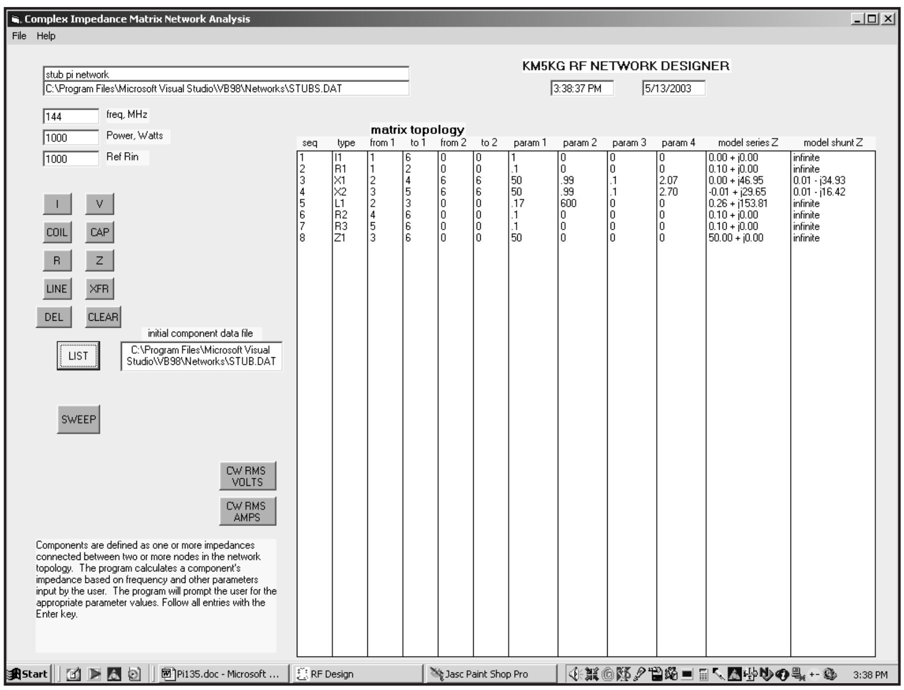

Fig 10—What to expect if the stub termination impedances are 0.1 + *j*0 Ω and a small inductor (essentially a short length of wire at 144 MHz) is used in place of X3.

Table 6— –135° Stub-π-Network Adjustment Sensitivity at 144 MHz

Length 1 (ft)	X1 (*Ω*)	*Length 2 (ft)*	X2 (*Ω*)	*Network* Z_{in} (*Ω*)	*Comments*
2.07 ft	–134.5	2.70	–37.5	967 + *j*21	Design center
2.065	–138.5	2.70	–37.5	953 + *j*118	*X1* reactance control
2.075	–136.5	2.70	–37.5	961 –*j*77	
2.07	–134.5	2.69	–38.6	944 + *j*20	*X2* resistance control
2.07	–134.5	2.71	–36.1	992 + *j*21	

Table 7—Reactances Required in a –135° T Network for Loads from 38 to 267 Ω

R_{in} (Ω)	R_{load} (Ω)	X1 (Ω)	X2 (Ω)	X3 (Ω)	Q
50	38	112	100	–62	3.4
50	267	213	430	–163	4.6

Table 8—Reactances Required in a –45° T Network for Loads from 38 to 267 Ω

R_{in} (Ω)	R_{load} (Ω)	X1 (Ω)	X2 (Ω)	X3 (Ω)	Q
50	38	12	24	–62	0.7
50	267	113	–104	–163	2.3

Table 9—Reactances Required in a –135° π Network for Loads from 38 to 267 Ω

R_{in} (Ω)	R_{load} (Ω)	X_{load} (Ω)	X1 (Ω)	X2 (Ω)	X3 (Ω)	Q
50	38	0	–19	–17	31	3.4
50	267	0	–31	–63	82	4.6
50	100	–100	impossible to obtain desired phase shift			
50	100	100	–100	–67	100	3.0

Table 10—Reactances Required in a –45° π Network for Loads from 38 to 267 Ω

R_{in} (Ω)	R_{load} (Ω)	X_{load} (Ω)	X1 (Ω)	X2 (Ω)	X3 (Ω)	Q
50	38 ohms	0	–80	–163	36	0.7
50	267	0	129	–118	44	2.3
50	100	–100	–100	–200	100	1.1
50	100	100	impossible to obtain desired phase shift			

Table 11—Reactances Required in a –90° π Network for Loads from 38 to 267 Ω

R_{in}	R_{load}	X_{load}	X1	X2	X3	Q
50	38 ohms	0	–44	–44	44	1.4
50	267	0	–116	–116	116	2.4
50	100	–100	–29	–71	71	3.3
50	100	100	171	–71	71	2.8

with the load reactance required for resonance, of course. When the load impedance is known, independent adjustment of the resistance and reactance seen by the transmitter can proceed via the design process outlined in this article.

When unknown load impedances need to be matched to a particular value, such as 50 Ω resonant, desired at the output of a transmitter, some method of component stress monitoring should be employed in the matching network other than WTBS (what's that burning smell?). Shielded toroidal current sampling transformers, capacitive voltage dividers and other devices can be used so long as they do not significantly alter the impedance transformation through insertion or proximity effects. Also, it is always a good idea to make sure that the sampling device ratings show a large safety factor relative to operating stresses.

The very best tool for improving the hands-on impedance-matching process is a remote impedance meter at the transmitter driven by a *complex* voltage sample and a *complex* current sample from the output of the matcher or the input to the antenna. These samples may be distributed anywhere throughout the RF system for the convenience of the designer or operator.

Glossary

λ: Greek letter lambda stands for wavelength

Antenna System: A transceiver, transmission line(s), network(s) and radiator(s).

Complex: Containing both resistive and reactive terms (applies to voltage, current, impedance).

Phase Shift: The time delay in angular units of a complex voltage or current from one node or branch in a network to another node or branch in that network.

Power: The real delivered power is defined as the RMS current magnitude squared multiplied by the load resistance, which is also equal to the forward power less the reflected power at the load.

RMS Current: The effective or heating value of a current.

RF: Radio frequency, or alternating current and voltage as opposed to dc.

Wavelength: the length of one electromagnetic oscillation (one cycle), which can be presented in units of physical length or time (360° per cycle).

Notes

[1]G. Bingeman, KM5KG, "A Flat Impedance Bandwidth for any Antenna," *QEX*, Sep/Oct 2001, pp 12-17.

[2]This method for independent R and X control has been around for at least 40 years, as used by commercial broadcast transmitter manufacturers.

[3]You can download a free demo copy of the RF Network Designer software that produced all the figures above by visiting **www.qsl.net/km5kg**. Refer to the built-in help text of the program for the explicit design equations and theory for the networks discussed in this article. Many of the demonstration functions are locked, but the full help text is still available for all functions.

[4]G. Bingeman, KM5KG, "Phased Array Adjustment for Ham Radio," *Communications Quarterly*, Summer 1998, available at **www.qsl.net/km5kg**.

Grant Bingeman has been a radio amateur since 1962. He has a BSEE from the University of Virginia, and is a registered Professional Engineer in the State of Texas. He has worked in the broadcast industry for 30 years.

Energy Conversion in Capacitors

Not all the energy involved in charging a capacitor goes into the capacitor. Come find out why not.

By Doug Smith, KF6DX

The first law of thermodynamics says, in effect, "You can't get something for nothing." The second law of thermodynamics says, "You can't even get your money's worth." Here are some examples of those laws in action.

Work is Done When Moving Charge

Imagine a closed system consisting of two capacitors. See Fig 1. One capacitor, C1, is charged to voltage V; the other, C2, has no charge. The capacitors are equal in value: C1 = C2. At time t = 0, the conditions are that capacitor C1 has potential energy:

$$E1 = \frac{C1 \times V^2}{2} \quad \text{(Eq 1)}$$

225 Main St
Newington, CT 06111
kf6dx@arrl.org

Capacitor C2 has zero energy. The total potential energy of the system is therefore that of C1 alone. A time t = 1, the switch is closed and current naturally flows from C1 to C2.

Some time later, the charges on the two capacitors will have equalized. The voltage across each capacitor will be V/2, since each has half the charge. The potential energy then stored in C1 is:

$$E1' = \frac{C1\left(\frac{V}{2}\right)^2}{2} = \frac{C1 \times V^2}{8} \quad \text{(Eq 2)}$$

The energy in capacitor C2 is identical, so the total potential energy in the system is:

$$E = \frac{2C1 \times V^2}{8} = \frac{C1 \times V^2}{4} \quad \text{(Eq 3)}$$

That is only half the starting energy! Where did the other half go?

Well, it did work on the charge as it moved from C1 to C2. The work done on some charge q moving through a potential difference ΔV is defined as $W=q\Delta V$. Since $q=C\Delta V$, the work done in moving that charge from C1 to C2 is:

$$\begin{aligned} W &= (C \times \Delta V)(\Delta V) \\ &= C \times \Delta V^2 \\ &= C\left(\frac{V}{2}\right)^2 \\ &= \frac{C \times V^2}{4} \end{aligned} \quad \text{(Eq 4)}$$

That work is the energy used transferring the charge. Work and energy take identical units, such as watt-seconds or joules.

Thus, charging a capacitor from zero to some positive potential energy involves significant energy conversion. But conversion to what form?

The charge itself is obviously accelerated and decelerated during its journey over some physical path of length d. That results in radiation. The path resistance, as low as it might be, dissipates heat during the transfer. Additionally, electrons have mass and their acceleration involves expenditure of energy. In fact, a maximum of half the charging energy is stored in the electric field of the capacitor after it is charged from zero to some level. Radiation and heat are the only forms known for the other half.

That example is held up as evidence that certain switched-capacitor power converters or capacitive charge pumps cannot achieve efficiencies greater than 50%.[1] It seems to say that half the energy used in charging a capacitor is always lost as radiation or heat. The trouble is that we know bridge rectifiers and capacitors transfer energy efficiently from the power mains to a load in a traditional power supply circuit, even though the charge on the capacitors does work most of the time. How can we reconcile what seems to be a paradox?

Adding Charge to an Already-Charged System

The answer comes in the form of a charge source that differs very little in voltage from that of the capacitor. The work $W = q\,\Delta V$ done transferring charge from source to capacitor is minimized when ΔV is minimal. A capacitor charged through diodes, as shown in Fig 2 for example, may be quite efficient. Note that ΔV is the difference between the source voltage and the capacitor voltage during charging—not necessarily the increase in capacitor voltage.

Clearly, adding some charge q to capacitor C already having voltage V requires a source voltage greater than V by some amount ΔV. The potential energy of charge q at the source is $q(V+\Delta V)$. The work done moving the charge from source to capacitor is $q\Delta V$. As shown above, only half that work is available to add energy to the capacitor. Energy efficiency is therefore:

$$\begin{aligned}\eta &= 1-\frac{q\times\Delta V}{2q(V+\Delta V)}\\ &= 1-\frac{\Delta V}{2(V+\Delta V)}\end{aligned} \qquad \text{(Eq 5)}$$

V is the capacitor voltage before charging begins. When V is large and ΔV is small, η approaches unity; but when V starts at zero, η= 0.5.

[1]Notes appear on page 54.

Energy Efficiency in Capacitor Discharge

Just as energy is expended charging a capacitor, it is expended discharging it because moving charge through a potential difference does work. In this case, however, all the energy goes to the load, except for the amount that is radiated.

For an example, refer to Fig 3. A 1-farad capacitor at 1 V has a charge of 1 coulomb and energy of 0.5 joules. Were all the charge removed by a constant current of 1 A for 1 s, very nearly 0.5 joules would be expended in the load.

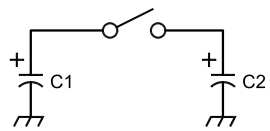

Fig 1—A closed system of two capacitors. Before the switch is closed, C1 is charged to voltage *V* and C2 is uncharged.

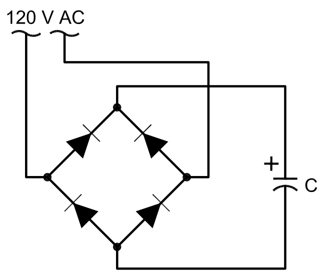

Fig 2—A capacitor charged through diodes.

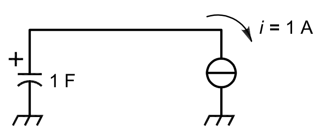

Fig 3—A 1-F capacitor discharged at a constant current of 1 A.

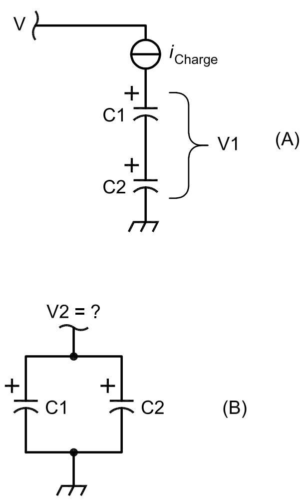

Fig 4—(A) Two capacitors in series charged to voltage *V*. (B) The capacitors of A are placed in parallel.

A Precision Voltage Divider

Here is another funny thing about capacitors. Refer to Fig 4A. Take two similar capacitors—they do not have to be identical—and hook them in series. Charge the series combination to some voltage *V1*. Then separate them and hook them in parallel, as in Fig 4B. The voltage across them will be *V1*/2 to a very high degree of precision.[2]

Why is that? When you charge the series combination, each capacitor receives an identical charge, q, because the capacitors are in series. Now separate them and hook them in parallel. What is the voltage across the capacitors?

Well, one thing we know: Charge is conserved. When the capacitors are in series:

$$V1 = \frac{q(C1+C2)}{C1\times C2} \qquad \text{(Eq 6)}$$

When they are in parallel, we have twice the charge across the sum of the capacitances:

$$V2 = \frac{2q}{C1+C2} \qquad \text{(Eq 7)}$$

The ratio of the voltages is therefore:

$$\begin{aligned}\frac{V1}{V2} &= \frac{\left[\dfrac{q(C1+C2)}{C1\times C2}\right]}{\left[\dfrac{2q}{C1+C2}\right]}\\ &= \frac{(C1+C2)^2}{2C1\times C2}\\ &= \frac{C1^2+2C1C2+C2^2}{2C1\times C2}\\ &= \frac{C1}{2C2}+1+\frac{C2}{2C1}\end{aligned} \qquad \text{(Eq 8)}$$

That ratio is very close to two even if the capacitors are quite different in value. For example, let them differ by about 20%: C1 = 1.1 µF and C2 = 0.9 µF. Then we have:

$$\begin{aligned}\frac{V1}{V2} &= \frac{1.1}{(2)(0.9)}+1+\frac{0.9}{(2)(1.1)}\\ &\approx 2.02\end{aligned} \qquad \text{(Eq 9)}$$

Even when the ratio of capacitances

is 1.1 / 0.9 = 1.22, the voltage divider produces an accuracy of about 1%. The voltage across the parallel combination of 1.1 + 0.9 = 2.0 µF is 2.02^{-1} V = 0.495 V. Did energy get converted?

Well, yes, it did! When charged in series, the smaller capacitor acquired a larger voltage than the larger capacitor. When connected in parallel, current naturally flowed from the smaller capacitor to the larger until the voltages equalized. That involved the expenditure of energy.

The potential energy in the series combination of 0.495 µF was (0.495 $V1^2$) / 2 = 0.2475 J. The potential energy of the parallel combination is (2)(0.495 $V1$)^2 / 2 = 0.2450 V1. The difference in energies was caused by having to do work moving charge through a potential difference.

That fact has led to switching power-supply topologies that transfer energy between capacitors only when their voltages are nearly identical. Such charge pumps are efficient because they avoid connecting capacitors whose voltages differ much. Claims of accuracy better than that indicated by Eq 8 are clearly unfounded (such as in the example in Ref 2).

One Final Quirk

It may seem odd, but the units of capacitance are units of length! That is readily shown by the classic equation for an air-spaced, two-plate capacitor:

$$C = \frac{A}{4\pi d} \qquad \text{(Eq 10)}$$

where the numerator is a plate area in cm^2 and the denominator contains a plate spacing in centimeters. Eq 10 results in a capacitance in the centimeter-gram-second (CGS) unit of capacitance: the cm!

It may seem like folly, but it is possible to equate meter-kilogram-second (MKS) units of capacitance (farads) to CGS units (cm) using a conversion factor. As it turns out, 1 cm ≈ 1 pF.[3]

Summary and Acknowledgement

The upshot of the above discussion is that capacitive charge pumps can be most efficient only if they pump charge when the potential difference between source and load is small. That is, when ΔV is low with respect to V. It may be somewhat ironic, but a lack of potential difference between capacitors does not necessarily encourage charge to flow! Finally, switched capacitors can form a precision voltage divider with little regard to matched capacitor values.

Notice that the equations I presented are independent of both the amount of charge transferred and the capacitance involved. They therefore hold wherever charge is supplied by a source to a load, regardless of whether capacitors are part of the act. Check out the references for further information.

Thanks to Lee Jones, WB4JTR, for reviewing my manuscript.

Notes

[1]C. K. Tse, S. C. Wong, and M. H. L. Chow, "On Lossless Switched-Capacitor Power Converters," *IEEE Transactions on Power Electronics*, Vol 10, No. 3, May 1995, pp 286-291.

[2]**www.linear.com/pdf/lt1044.pdf**, LTC1044 data sheet, Linear Technology Corp, Fig 9.

[3]E. Purcell, *Electricity and Magnetism* (New York: McGraw-Hill, 1965).

RF

By Zack Lau, W1VT

A 2-Meter Transmitter

Here is a 2-meter SSB/CW transmitter as an IF radio for satellite and microwave work. It is designed to produce a clean 10-mW 2-meter signal. It features RF clipping to improve the peak-to-average ratio and adjustable output power. SSB transmitters are somewhat difficult projects. While it is not difficult to build any of the circuits—getting everything to work well as a system can be a challenge. Gain distribution is important—a poor design can make it difficult to keep the unwanted carrier from leaking back into the signal.

Fig 1 is a block diagram of the transmitter. A low-impedance 600-Ω dynamic microphone puts out only 10 mV—an amplifier with a low-impedance output is needed to drive the doubly balanced diode modulator, which produces a double-sideband suppressed-carrier signal. A 2.7-kHz wide filter is used to select the upper sidebands. The RF clipper is used to improve the low peak-to-average ratio of voice signals. It also helps to establish a peak level so that the following stages are not overloaded. Another 2.7-kHz wide filter removes the out-of-band distortion created by the clipping process. Thus, while the third-order distortion at 10-mW PEP output is –26 dBc, the higher-order distortion products fall off quite rapidly, due to the extra attenuation provided by the crystal filter. At 3-mW PEP output, the third- order IMD is –40 dBc, when measured using a two-tone test. A 4 to 22 dB variable IF attenuator is used to select the desired output power. Thus, the power can be varied over an 18-dB range. The IF signal is then upconverted and amplified to 145 MHz. The 145-MHz signal is band-pass and low-pass filtered for a clean signal. Mini-Circuits MAR-3 and MAV-11 provide linear amplification up to the 16-mW or +12-dBm power level. The carrier, harmonic and spurious signals are at least 50 dB down. The mixing spurs are at least 54 dB down. For CW or data work, an FSK signal generator is substituted for the SSB generator.

The microphone amplifier is designed for 600-Ω microphones, but can be used with high-impedance 50-kΩ microphones by removing the 620-Ω resistor R1, possibly with a SPST switch. Like Rick Campbell's phasing exciter, it uses an emitter follower to drive the low-impedance doubly balanced diode modulator.[1] I used half an NE5532 instead of a NE5534—not only is it easier to find, but it is internally compensated for unity gain. The NE5534 has a pin for a compensation capacitor, if you want gain less than three. The *Art of Electronics*, by Horowitz and Hill, has an excellent chapter on "Feedback and Operational Amplifiers," if you want to study the topic of frequency compensation. C1 and C5 of Fig 2 are selected for a fairly

225 Main St
Newington, CT 06111-1494
zlau@arrl.org

[1]Notes appear on page 61.

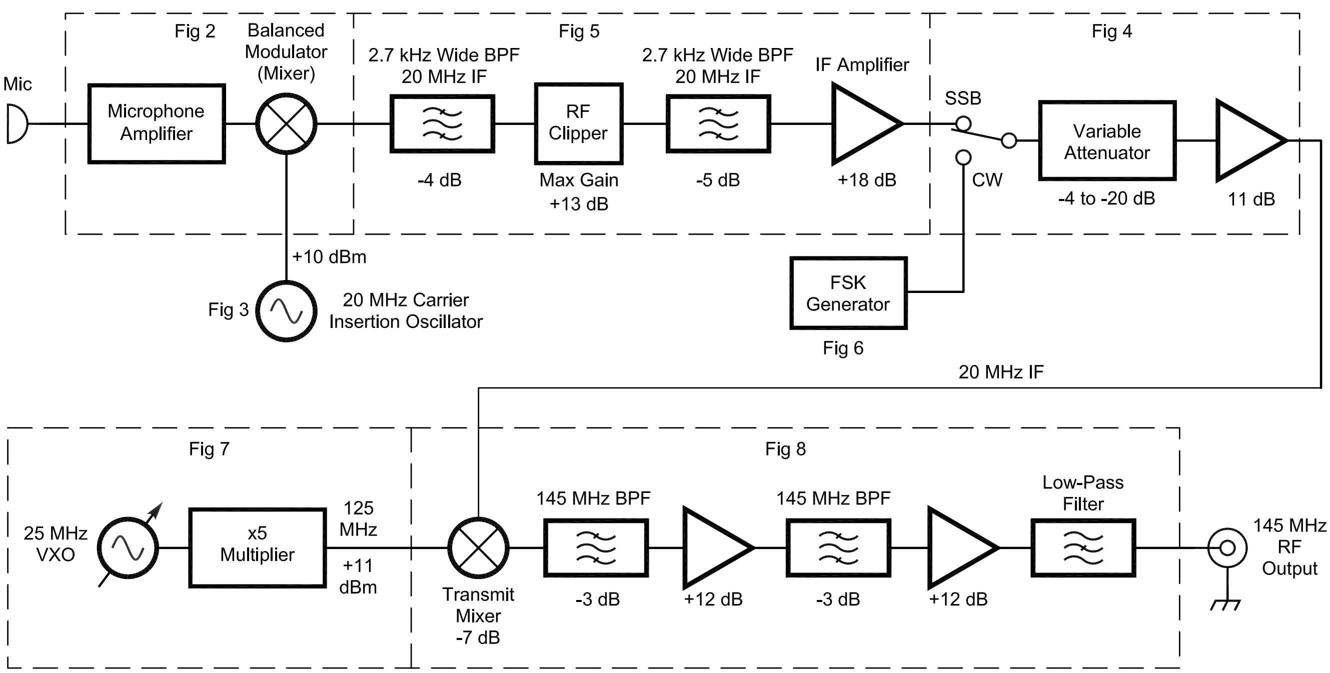

Fig 1—2-meter SSB/CW transmitter block diagram.

low high-pass cutoff frequency, as the crystal filters will add some low-audio frequencies. I measured a –3-dB cutoff of 55 Hz. They can be made smaller to raise the cutoff frequency, if you are using crystal filters with sharper skirts. The crystal filters add 6 dB of attenuation at 300 Hz. Setting the carrier-insertion oscillator to provide less attenuation would reduce the carrier suppression.

A Mini-Circuits SBL-1 doubly balanced mixer is used to generate the DSB suppressed-carrier signal. I've used a number of SBL-1 mixers as DSB modulators with good results—none of them required nulling adjustments.

However, a carrier-null adjustment can be added to the SBL-1. Instead of grounding IF pins 5 and 6, they can be raised above ground with a 250-Ω potentiometer. The wiper of the potentiometer provides an adjustable path to ground. A significant improvement was seen on a damaged SBL-1 that had been repaired with unmatched 1N4148 diodes. The SBL-1 is tack welded together—it isn't too hard to remove the metal cover. This mixer showed a LO to RF isolation improvement from 46 to 56 dB. The LO was +10 dBm at 20 MHz. *The ARRL Handbook* has details on the wiring of typical commercial DBMs.[2]

The carrier-insertion oscillator (CIO) is shown in Fig 3. If you want both USB and LSB, I recommend building two CIOs and switching them, using the PIN-diode switch shown in Fig 4. Two independent oscillators are much easier to align than a single VXO, as stray capacitance often makes the tuning adjustments interactive. The latter approach does have merit if you need to use expensive crystals. The biasing for the MAR-3 is a little unusual—I just used two low-value resistors and a bypass capacitor. Normally, this is not done, as it reduces the output by 2 dB, compared to an ideal RF choke that is properly bypassed. However, real RF chokes radiate, a significant problem with a suppressed carrier SSB system that does not use extensive shielding. Thus, this cheap design actual works better, on a system level. The output amplifier has more than enough output to drive the mixer, so the loss of power isn't significant.

The crystal filters use inexpensive 20-MHz clock crystals. They seem to be getting even cheaper, while custom crystals become ever more costly. I'd buy twenty crystals and select the eight closest in frequency for the crystal filters. They should be within 270 Hz of each other. I'd also set aside the crystals lowest in frequency for the USB carrier-insertion oscillator. The crystals highest in frequency are useful for an LSB carrier-insertion oscillator. The center frequency was cleverly chosen to minimize impedance-matching difficulties—a reasonable SSB bandwidth is obtained with 50-Ω terminations. The filters have measured –3-dB bandwidths of 2.5 and 2.7 kHz. The pair provides a –3-dB bandwidth of 1.7 kHz and a –6-dB bandwidth of 2.7 kHz. A lower frequency would raise the optimum impedance but would also increase the difficulty of filtering out spurious signals. The use of two separate filters allows the simple implementation of an RF clipping circuit. The clipping circuit is a little unusual—I transformer coupled two clipping diodes to the RF choke of a low-level transmit amplifier. This reduces the signal level required for the diodes to conduct. It provides about 12 dB of clipping, as shown in Table 1. A π attenuator, R1, R2 and R3, of Fig 5, is used to reduce the impedance variation presented to the second crystal filter. Another MAR-1 amplifier boosts the power to about –2 dBm—about 16 dB below the third-order intercept point—distortion isn't a problem. There may be some concern about the long-term stability of cheap high-frequency clock crystals. An early prototype measured in September 1996, had –6-dB points of 20.00025 and 20.00268 MHz. In February 2003, the frequencies changed

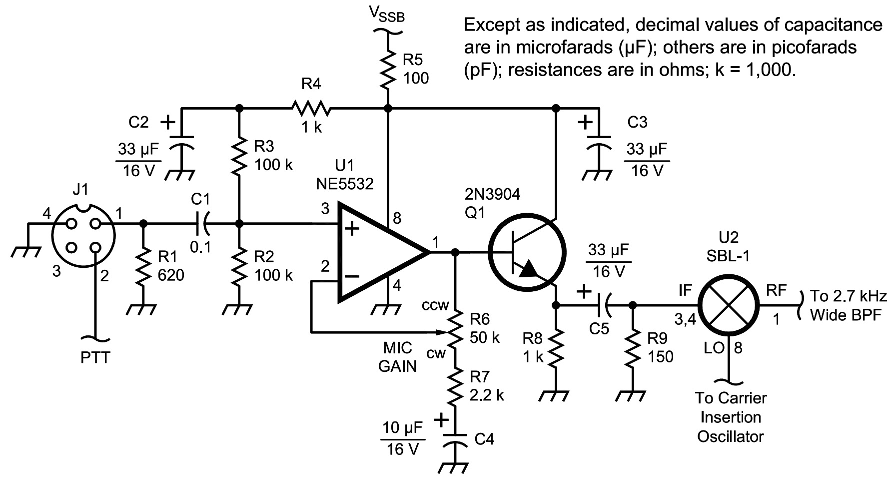

Fig 2—Schematic of the microphone amplifier and balanced modulator.

C1—0.1 µF metal-film, see text (Digi-Key P4525).
J1—4-pin mic connector, see text.
U1—Phillips NE5532 dual op amp.
U2—Mini-Circuits SBL-1 doubly balanced diode mixer.

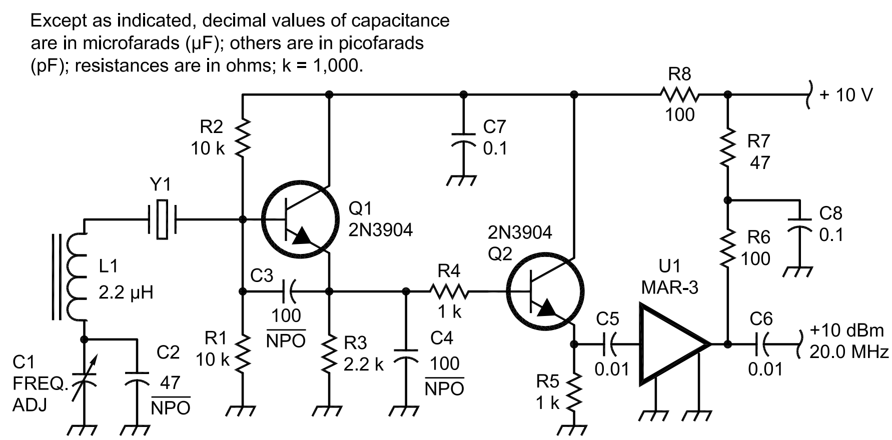

Fig 3—20-MHz carrier-insertion oscillator schematic.

C1—Xicon 9-50 pF ceramic trimmer capacitor (Mouser 24AA024 or 24AA074[SMT]).
L1—2.2-µH ferrite-core inductor (Digi-Key M7817; J W Miller 78F2R2K).
U1—Mini Circuits MAR-3 MMIC.
Y1—20-MHz clock crystal (Mouser 520-HCU-2000-S).

to 20.00024 and 20.00262 MHz. As an upper-sideband filter, the drift of 10 Hz is quite acceptable. If the filter were used for lower sideband, some degradation in speech quality would be noticed until the carrier oscillator were reset.

I used 1N4007 rectifier diodes to switch between the SSB generator and the FSK generator—they have an intrinsic layer just like expensive PIN diodes. This helps reduce distortion, compared to ordinary rectifier or switching diodes. Lower loss is possible with better diodes, but this isn't important in this application. The switch feeds an adjustable π attenuator that sets the power output of the transmitter. This is quite useful in satellite operations, where inconsiderate users running too much power degrade the usefulness of the satellite. Soldering the shield leads to the case of the potentiometer provides adequate shielding. The 18-dB range can be lowered to 14.5 dB by using a 500-Ω potentiometer, instead of the 1 kΩ specified.

Why use an FSK generator for on-off keying? The answer is flexibility. If you have a receiver with a 20-MHz IF, it may be quite important that you offset the signal during receive, to minimize interference. Turning the oscillator on and off may not be a simple exercise—not only may the signal chirp, but there may be a significant delay. If desired, the circuit may be easily adapted for FSK data work. FSK is obtained by switching out the variable capacitor, C3 of Fig 6. The switching circuit provides some basic sequencing—it switches fast but has a bit of a delay when switching back. Shaping the dc power to the 145-MHz amplifiers shapes the keyed CW signal. Since the signal is weak when the FSK occurs, you should not hear any chirp at the transmitter output. The rise and fall times may be adjusted by changing C14. With 0.1 and 0.43 µF of capacitance, the times were 0.5 and 2.0 ms, respectively. The advantage of changing the capacitor is symmetry—the rise and fall times remain similar. A small amount of wave shaping is also

Table 1—Power gain of the RF clipper shown in Fig 5

Input Power (dBm)	*Output Power (dBm)*	*Gain (dB)*
–40	–18	22
–30	–9	21
–20	–5.5	14.5
–10	–2.8	7.2
–6	–2	4.0
–4	–1.7	2.3
–3	–1.3	1.7

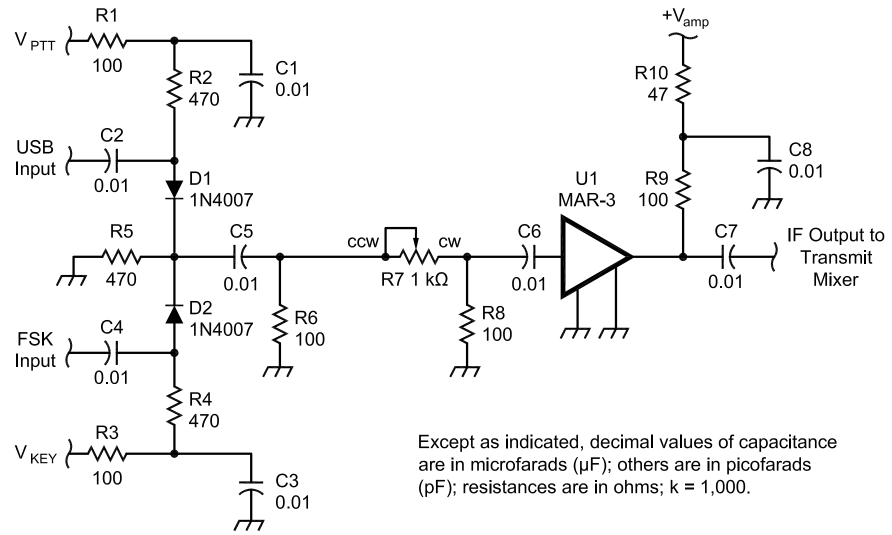

Fig 4—Variable Attenuator and 11-dB amplifier schematic.

R7—1-kΩ audio potentiometer (Mouser 31VJ301).

U1—Mini Circuits MAR-3 MMIC.

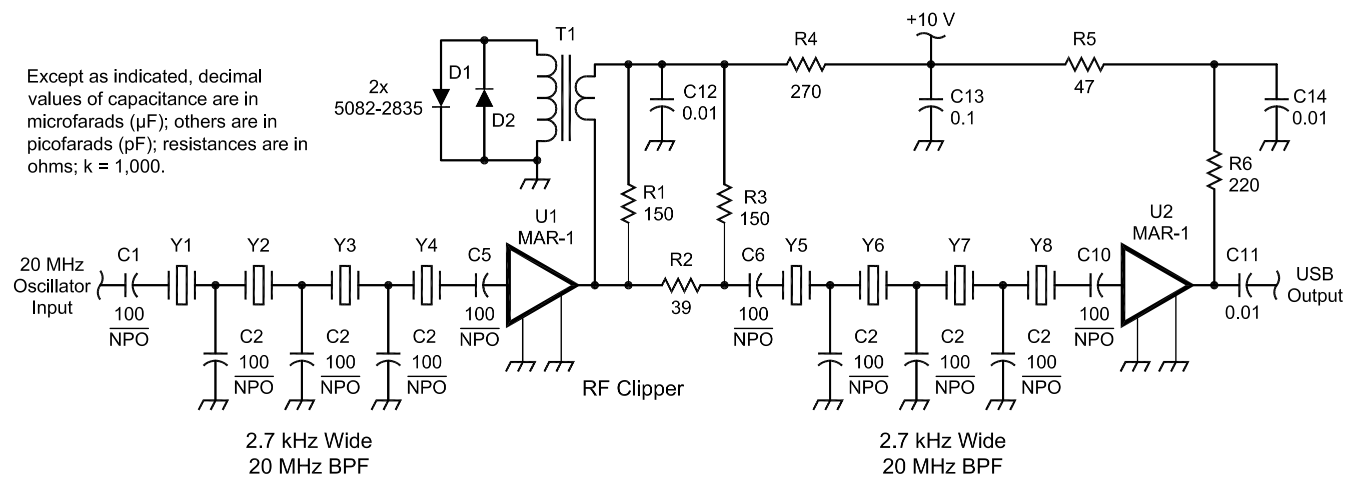

Fig 5—20-MHz crystal filters and RF clipper schematic.

D1, D2—Agilent 5082-2835 Schottky diodes.
T1—Toroidal transformer: 12-turn primary, 2-turn secondary #28 AWG enameled wire, on a FT-37-43 core; primary inductance 46 µH at 796 kHz.

U1, U2—Mini Circuits MAR-1 MMIC.

Y1-Y8—20-MHz clock crystals (Mouser 520-HCU200-S. The crystal frequencies should be within a 200-Hz range).

done on SSB, to avoid generating a signal outside the desired transmit passband. Yes, poor switching circuitry can generate interference to nearby channels that is impossible to filter out.

Conversion of the 20-MHz sideband signal to 145 MHz requires a 125-MHz local oscillator. I used a cheap clock crystal in a Colpitts VXO (see Fig 7). A 2.2-µH molded inductor in series with a HC-6 cased crystal provided a tuning range of 125.000 - 125.045 MHz. A 4.7-µH inductor increased the tuning range from 45 to 84 kHz, but the coverage, from 124.932 to 125.016 MHz, may actually be less desirable for some applications. A 2.24-µH toroidal inductor wound on a T-37-7 core resulted in a tuning range of 125.004 to 125.047 MHz. This core material generally provides the best temperature stability of readily available ferromagnetic materials—winding your own inductor should be considered if the radio is to be used in adverse weather. The miniature CA301 crystal may also be useful—it provided 36 kHz of tuning range with the 2.2-µH series inductor. Custom crystals often provide several times as much tuning range, but at a significantly higher cost. It is even possible to order crystals optimized for VXO applications.

A MAR-1 silicon MMIC is used to multiply the 25-MHz signal by five. The high harmonic content of the oscillator may help its effectiveness. A pair of two-pole band-pass filters clean up the signal. The loss of each filter is approximately 2.5 dB, according to a computer model with capacitor *Q*s of 300 and inductor *Q*s of 80.

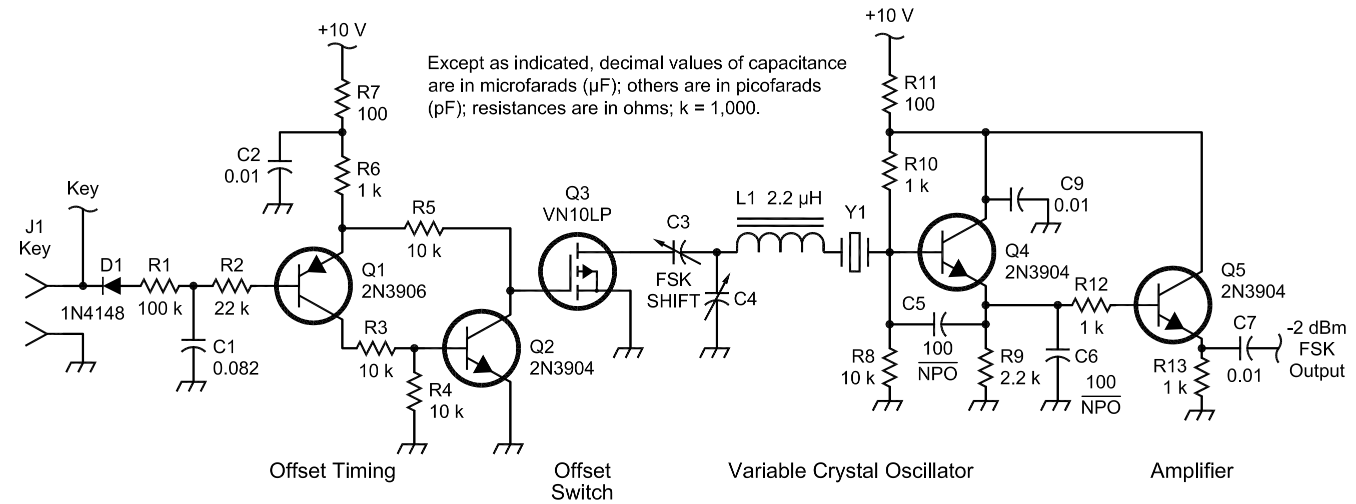

Fig 6— FSK generator schematic

L1—2.2-µH ferrite-core inductor (Digi-Key M7817; J W Miller 78F2R2K).

Q1—2N3906 PNP transistor.
Q2, Q4, Q5—2N3904 NPN transistor.
Q3—VN10LP.

Y1—20-MHz clock crystal (Mouser 520-HCU-2000-S).

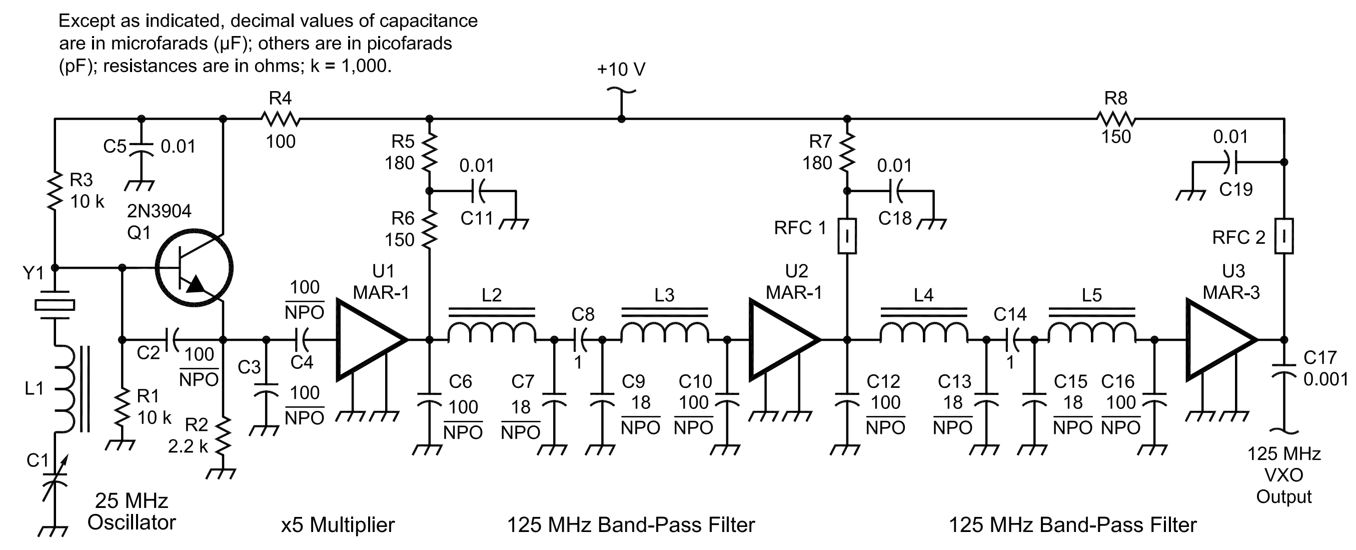

Fig 7—125-MHz VXO schematic.

C2-C4, C6-C10, C12-C16—NP0 or silver-mica capacitors may be used.
L1—2.2-µH ferrite-core inductor (Digi-Key M7817; J W Miller 78F2R2K). For enhanced temperature stability, use 25 turns of #28 enameled wire on a T-37-7 iron powder core.

L2-L4, L5—7-mm tunable coil, 108-nH nominal inductance value (Digi-Key TK-2804-ND; Toko E528NAS-100075).
RFC1, RFC2—Fair-Rite EMI Z=220 Ω @ 100 MHz (Mouser 623-2743009112).

U1, U2—Mini Circuits MAR-1.
U3—Mini Circuits MAR-3.
Y1—25-MHz crystal, see text (Digi-Key CTX093-ND).

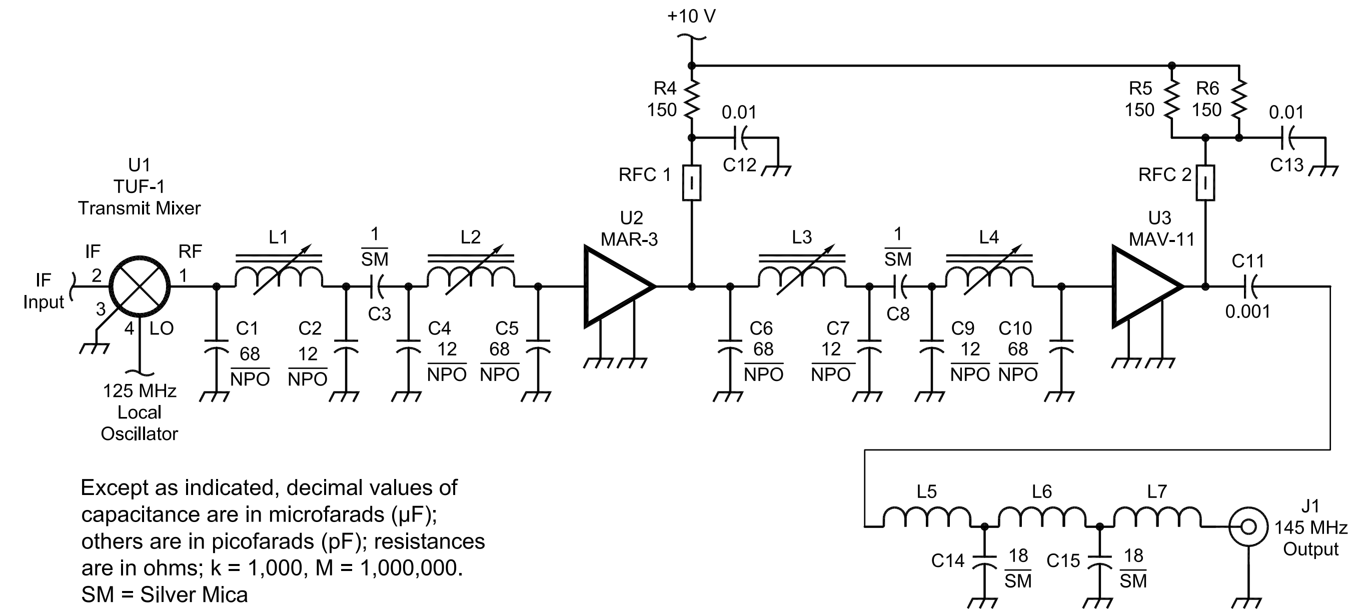

Fig 8—2-meter RF-section schematic.

C1-C10—NP0 or silver-mica capacitors may be used.
J1—Amphenol 31-203-RFX (Digi-Key ARFX1062).
L1-L4—7-mm tunable coil, 111-nH nominal inductance value when tuned. (Digi-Key TK-2804-ND; Toko E528NAS-100075).
L5, L7—32-nH, 3 turns #24 AWG enameled wire close wound on 0.125-inch air core. The coil length is 0.07 inches, not inclusive of the 0.1-inch leads.
L6—69-nH, 5 turns of #24 AWG enameled wire close wound on 0.125-inch air core. The coil length is 0.11 inches, not inclusive of the 0.1-inch leads.
RFC1, RFC2—Fair-Rite EMI Z=220 Ω @100 MHz (Mouser 623-2743009112).
U1—Mini Circuits TUF-1 mixer.
U2—Mini Circuits MAR-3 MMIC.
U3—Mini Circuits MAV-11 MMIC.

The 125 and 145-MHz band-pass filters use shielded tunable coils. They were optimized for amplifier stability. They are essentially coupled low-pass filters—to ensure that there is a minimum of high-frequency spurious responses. This is much better than typical helical filters, which often have significant responses near odd multiples of the designed passband frequencies. This is important when cascading very wide-bandwidth MMICs—you can easily get oscillations at microwave frequencies if you aren't careful. You might not even notice a strong oscillation at 1 GHz, except that you can't seem to achieve the rated power output. You might even use these filters to build sun-noise amplifiers. You should be able to cascade a half dozen MMICs if you use three shielded enclosures—putting a pair of MMICs in each enclosure. Putting more gain in a single box is tough—you need to eliminate unwanted waveguide feedback paths, and typical box sizes often look like low-loss microwave waveguide! The filters are designed for 50-Ω input and output impedances. This modular approach simplifies alignment if RF test equipment is available. You can hook the input to a 50-Ω signal generator and look at the output on a 50-Ω power meter or spectrum analyzer. The ideal test instrument is a network analyzer that

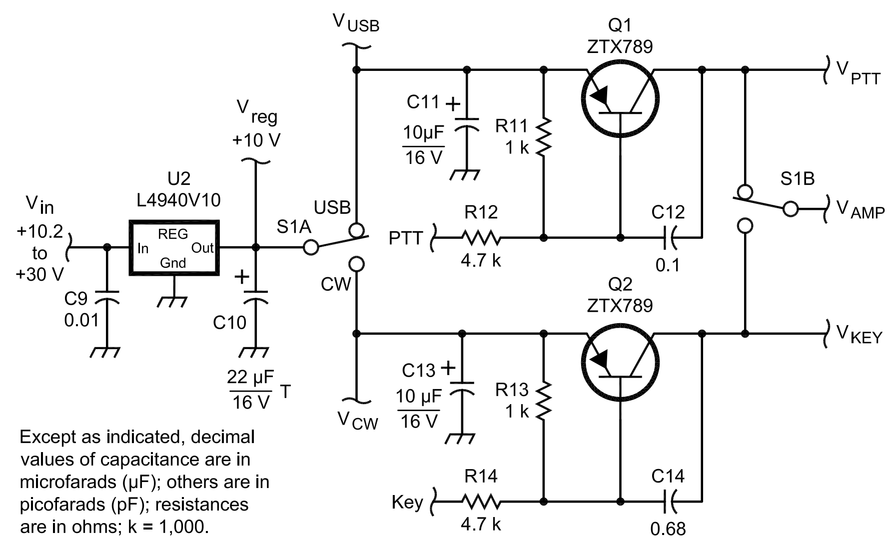

Fig 9—Power supply and control circuits schematic.

C10—22-µF tantalum, 16 V see text.
C12—0.1-µF metal-film (Digi-Key P4525).
C14—0.68-µF metal-film (Digi-Key P4673).
Q1, Q2—Zetex PNP switching transistors (Digi-Key ZTX-789A).
S1—DPDT toggle switch.
U2—STMicroelectronics L4940V10 10-V low-dropout regulator.

will simultaneously display return loss and transmission loss. Such a display makes tuning remarkably easy.

As the power levels approach or exceed 0 dBm or 1 mW, one should not be too casual about amplifier distortion. Thus, I used MAR-3 and MAV-11 amplifiers (see Fig 8), even though it may appear that lower-power devices would be adequate. An excellent book for studying intermodulation distortion is the *VHF/UHF DX Book*, edited by Ian

White, G3SEK. It shows how to calculate the intermodulation of cascaded stages. However, the equations can be optimistic—I've seen the intercept point of a MAV-11 drop from +32 to +27 dBm, as the output power of the MAV-11 was increased from +18 to +20 dBm.[3]

If more power than 10-mW is required, I suggest using an MRF 581 transistor based amplifier to get up to the 100-mW level. A good design appears in the March 1994 "RF" column. The May 1996 "RF" column describes how to get up to the 10-W level with a Mitsubishi $58 M57713 hybrid module.[4]

A STMicroelectronics L4940V10 is used to provide a regulated 10 V for the transmitter circuits—it works well with just a few tenths of dropout voltage. It can handle as much as 30 V with a proper heatsink. A TO-220 case can't handle 6 W without a heatsink. Bolting the case to the back of an aluminum chassis should be adequate. It is also reverse polarity protected to –15 V. This feature is quite useful for portable battery operation, where accidents are common. The tantalum capacitor, C10 of Fig 9, is required for stability. It may be increased in capacitance. An ordinary electrolytic may be substituted if cold-weather performance is not required. National Semiconductor suggests the use of tantalums below –25°C, as many aluminum electrolytics freeze at –30°.[5]

Construction

I built my version for portable operation—I put all the connectors and controls on the front panel (see Fig 10). It is easier to check whether everything is connected properly when nothing is hiding. I used a four-pin mic connector because I have several 600-Ω microphones from old ICOM portable SSB radios. Eight-pin connectors are much more common with modern radios. Don't forget that many of the newer microphones have built-in amplifiers that require the radio to supply power. The controls are the main tuning knob, a USB/CW mode switch, and a power adjustment. I used a two-pin Molex for dc power, a four-pin mic connector for the microphone, a two conductor 1/8-inch mini-stereo jack for the CW key, and an Amphenol 31-203-RFX BNC jack for the antenna. This BNC jack is similar to the UG-290A—instead of #3-56 threaded holes it has 1/8-inch mounting holes. The threaded holes are impractical for most hams—#3-56 screws are difficult to find, so they are usually tapped for #4-40 threads or drilled out into 1/8-inch mounting holes.

I bent a 2.5×7×5.5-inch (HWD) aluminum box out of 0.032 and 0.050-inch 5052-H32 aluminum sheets. Small sheets are available from Enco.[6] It is a little small—I had to stack the IF switching and output amplifier board above the RF circuit with a pair 3/8-inch spacers. The size was chosen to match my 2-meter receiver. The variable capacitor already has a reduction drive, so it only needed a pointer and a dial scale. I used 1/16-inch Lexan sheet to protect the scale. I found it difficult to cut thin acrylic without cracking, so I also made the pointer out of Lexan. A thin line is cut into the pointer with a metal scribe. I used a 0.5-mm pencil to mark the paper scale—I don't see too much benefit in using a computer to generate the scale, given that it's not linear.

I used decals to mark the panel. An excellent tutorial on making decals can be found online at **www.tangopapadecals.com/** [Go to the "Decal Paper" page and follow the "Make your own decals 101" link.—*Ed.*]. After printing the decals with an Alps MD-1000, I clear coated them with Future floor wax. They were then cut from the decal paper, quickly dunked in water, and transferred to the painted panel. I decided not to clear coat the entire panel. This makes it easier to optimize the radio for better ergonomics—actual use may suggest that the controls be changed in size or type.

The transceiver is assembled using ground-plane construction. The parts are assembled over five small pieces of unetched circuit-board material. Single-sided board is actually preferred, to prevent unwanted electrolytic corrosion with the copper chassis, but double-sided board is cheaper and easier to find as surplus. The small boards hold just a few circuits each, making circuit revision much easier. I used small Teflon coax for the RF connections between the boards. RG-178B/U and RG-196A/U are just 75 and 80 mils in diameter, respectively. The hookup wire also has Teflon insulation. This makes it much easier to modify the circuit without damaging the existing wiring.

Capacitor C1 of Fig 2 should not be a ceramic capacitor, as they are often piezoelectric, which makes the audio amplifier vibration sensitive. Capacitors using plastic-film dielectric are a much better choice. The J W Miller inductors were chosen for ease of construction. If better temperature stability is desired, replace them with toroidal inductors wound on Micrometals type-7 iron-powder cores. Type-6 material is easier to find, but has slightly less temperature stability.

The cases of the crystals are easily soldered to the circuit board, substantially improving the stop-band performance of the filters. Similarly, shields of the coax to the variable attenuator should be soldered to the potentiometer case.

Testing

I built the 25-MHz VXO first. It will answer the biggest uncertainty about this project for most builders—will the cheap crystals cover the desired tuning range or will I need another

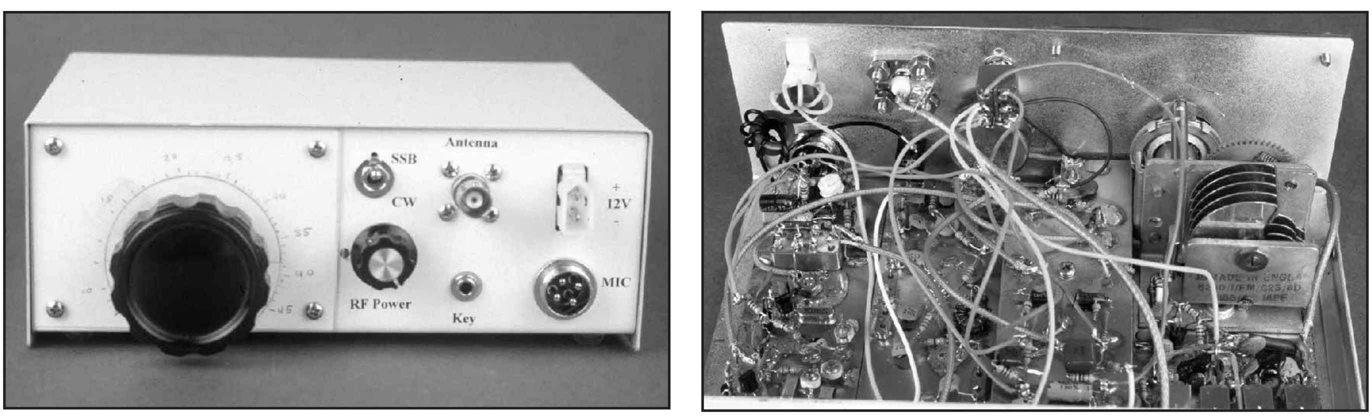

(A) (B)

Fig 10—(A) 2-meter SSB/CW transmitter front panel. (B) interior view of the transmitter looking from top rear toward back of the front panel.

approach? Once you have a VXO that covers the desired tuning range, you should be able to use your experience to get the other oscillators tuned to the desired frequencies. It may be necessary to experiment with different series inductors—more inductance will generally widen the tuning range, while lowering the center frequency. There is a limit, however, as too much inductance will seriously affect temperature stability. It is something of an art—there are tricks like using several smaller inductors in series to obtain more tuning range. However, it should be quite easy to get 40 or 50 kHz of tuning range at 2 meters with cheap crystals—and perhaps four times that with better crystals.

The next step is to tune the ×5 multiplier. The Toko coils should already be pretty close to the right inductances—you just need to maximize the output power. Digi-Key sells an inexpensive plastic alignment tool, the TK9003, for adjusting Toko 7KM and 10K adjustable inductors. A carefully shaped piece of unetched circuit board also makes a good alignment tool.

You should be able to measure about +10 dBm out of the 20 and 125-MHz oscillators that feed the SBL-1 and TUF-1, respectively. I generally look for anything between +7 and +13 dBm, although the Mini Circuits data book indicates acceptable performance at +4 dBm for the SBL-1 and TUF-1. The FSK generator should put out around –2 dBm.

If you build the FSK generator, it is a simple matter to adjust the 145-MHz filters with the CW signal. Again, the coils should be pretty close to the right inductance. If you intend to build a SSB-only transmitter, you can feed the 20-MHz carrier oscillator directly into the variable attenuator and then proceed to adjust the band-pass filters.

Adjusting the exact frequency of the carrier-insertion oscillator can be difficult. I generally set it 300 Hz below the –6-dB point of the cascaded filters. This is a compromise between audio quality and carrier suppression. Setting it is much easier with a spectrum analyzer, but few hams have access to one. If you figured out how to set the CIO for a receiver with an audio spectrum analyzer, you may be able to do the same with this transmitter. The balanced modulator works in reverse, so you can set it up as a receiver if you bypass the RF clipper and MAR-1 amplifiers. Some audio amplification may be needed, depending on the sensitivity of the audio spectrum analyzer.

I set the FSK generator so that the low frequency matches the carrier-insertion oscillator frequency. This makes it easier to calibrate the main tuning dial—this signal mixed with the VXO is the suppressed-carrier frequency. This is the standard used by amateurs to describe the frequency of a voice SSB signal.[7] This standard isn't universal, some services specify the center frequency of the transmit signal.

The last step is calibrating the main tuning dial. This is easily done if you built the FSK generator and set the off state to match the carrier insertion oscillator. If you temporarily disconnect the frequency shift, the CW signal will coincide with the carrier frequency. This is easily measured with a receiver or frequency counter. A counter is preferred—it eliminates having to determine the frequency offset that may be introduced by a receiver.

Notes

[1] R. Campbell, KK7B, "A Multimode Phasing Exciter for 1 to 500 MHz," *QST*, Apr 1993, pp 27 to 31.

[2] *2003 ARRL Handbook for Radio Communications*, (Newington, Connecticut: ARRL, 2002) Figure 15.25, p 15.18.

[3] Z. Lau, W1VT, "A VHF Driver for Hybrid Power Modules," RF, *QEX*, Mar 1994, pp 29-31.

[4] RF Parts Co, 435 S Pacific St, San Marcos, CA 92069; tel 800-737-2787, 760-744-0700, fax 888-744-1943, 760-744-1943; tel 1-800-737-2787, 1-760-744-0750; **www.rfparts.com**. RF Parts is a small-quantity source.

[5] Application Hints for the National Semiconductor LP2952.

[6] Enco, 400 Nevada Pacific Hwy, Fernley, NV 89408; tel 1-800-873-3626, fax 1-800-965-5857; **www.use-enco.com**.

[7] *2003 ARRL Handbook for Radio Communications,* p 12.4. □□

Next Issue in QEX/Communications Quarterly

We are fortunate to have several good series going; one or more of them will continue in the Sep/Oct 2003 issue. John Gibbs, KC7YXD, will have some technical details of D-STAR in his Part 2 of 3. If you haven't already done so, check out his introductory segment in this issue.

The number and quality of articles you submitted this year to *QEX* have been outstanding. Quite a few more standouts are on the horizon. Please remember that your friends who are working or retired engineers or scientists, students or generally technical types might like to know we exist. Why not loan them your copy or request a sample? □□

Letters to the Editor

A Subscription Issue (Mar/Apr 2003)

Dear Doug,

Today I received the Mar/Apr issue of *QEX*. The address label, which said something like "Mar/Apr 2003," caught my eyes and I suspected that my subscription was about to run out. A phone call confirmed it. As to the latter, a 16-digit number and expiration date fixed that.

The question remains, however, that I think I should have gotten a renewal notice *before* the last issue was sent. This may be true for USA subscriptions, but it certainly is not true for overseas as this issue apparently was my last and I have not seen a notice. With the logistics of foreign payments, you may want to consider giving people a timely notice.

I realize that *QEX* membership numbers are critical for the survival of the magazine. Making people expire their membership does not help, hence my comment.—*Geert Jan de Groot, PE1HZG, Hendrik Staetslaan 69, 5622 HM, Eindhoven, Netherlands;* **pe1hzg@arrl.net**

Hi Geert,

Thank you for your message. Our records indicate you have another year left for *QEX*. The "Mar/April 2003" on your label indicates that's the label for the March/April 2003 issue of *QEX*. I'm sorry if you were informed differently when you called. We've recently converted to a new computer system and we're still working out the kinks. The individual you spoke with would have had no idea where to look for your current subscription, as it wasn't where it was supposed to be.—*Kathy Capodicasa, N1GZO, ARRL Customer Service/QEX Circulation Manager;* **kcapodicasa@arrl.org**

***Linrad* (Mar/Apr 2003)**

Hi Doug,

The address for *Linrad* needs to be in all lower case. This works: **antennspecialisten.se/~sm5bsz/linuxdsp/linrad.htm.**—*Ron Skelton, W6WO, 4221 Gull Cove Way, Capitola, CA 95010-2025;* **ron-skelton@charter.net**

The 17-M Ragchewer (May/Jun 2003)

Dear Editor:

The 17-m Ragchewer transceiver would be a very interesting and useful project, but additional information is needed to build one. This includes printed-circuit board etch-pattern layouts (especially important with RF amplifier circuits), part numbers and suppliers for some of the harder-to-find parts and software listings (or sources to obtain them by mail or online) for both the internal Basic Stamp controller and for the computer used to operate the radio.

One thing I feel the Amateur Service needs to adopt is a nationally recognized HF frequency (or small band of frequencies) devoted to technical discussions and experiments. Perhaps the 17-m band would be a good place for this. Some of us, like myself, own older HF rigs that lack the 17-m band, so a single-band dedicated radio that could be easily home-built, or even available in kit form, may be a good starting point for this.—*Michael Kiley, WA9ZPM, 5445 W 137th Pl, Crestwood, IL;* **60445mikejkiley@juno.com**

Doug,

Over the years, I've noticed a major change in the ham community makeup. When I first entered the hobby back in the '50s, avid home-brewers constituted the majority. Only a relative few could afford the commercial gear of the day. In recent years, the balance has shifted completely the other way. To be sure, today's technology has frightened off many would-be homebrewers, but I think the spirit still lies latent in many minds and might be helped along if there was a "gathering place" for technical discussion and interchange. I think Mr. Kiley is onto something and I for one would love to see a part of the 17-m band devoted to this.

How about converting the entire band to SSB and allocating, say, the bottom 10 kHz to serious technical chit-chat? I don't hear much CW in the bottom of the band anyway.

As an individual, making the 17-m Ragchewer available as a kit is probably beyond my capability, but I would certainly be willing to work with a commercial concern toward that end.—*Rod Brink, KQ6F, 25950 Paseo de los Robles, Salinas, CA 93908;* **rodbrink@redshift.com**

On Regenerative Receivers

Dear* QEX*:

I have recently increased the frequency range of a simple regenerative receiver I built about five years ago, which incorporates a bifilar coupling transformer and diode bridge detector. This modified receiver has been a surprising success, and it has led me to suspect that self-resonance of the bifilar coupling transformer driving the diode bridge detector results in increased "smoothness" of regeneration control in regenerative receivers of this type.

I suspected—and have now confirmed with a dip meter—that the bifilar transformer in my receiver exhibits a "dip" or resonance very near 17 MHz. This dip is present with power on and with power off. Regeneration control of this receiver is smoother near 17 MHz than anywhere else within its tuning range, although the 19-m band above 15 MHz is almost as good. The 22-m band just below 14 MHz is noticeably worse, as is the 13-m band just below 22 MHz. This result, if it's correct, seems to agree with the information published in my article "A Mathematical Model for Regenerative RF Amplifiers," pp 53-54, *QEX*, July/Aug 2001. Self-resonance would result in increased impedance, which in turn would result in improved control. I further suspect that if self-resonance were occurring in this case, the only reason the stage weren't oscillating uncontrollably would be the diode-bridge load on the secondary of the bifilar transformer.

The most obvious application of the self-resonant bifilar transformer is in a regenerative intermediate amplifier stage as part of a superheterodyne receiver. The gate tuned circuit and the bifilar transformer could be made resonant at a chosen frequency and left there. Designing such a receiver may not be straightforward, though. Arranging for optimum coupling between a doubly or triply balance mixer and the regenerative IF stage would require some thought.

Or, it may be possible to establish self-resonance of the bifilar transformer at the upper end of the tuning range of a regenerative receiver and switch small fixed capacitors across the primary of the bifilar transformer to extend resonance across the rest of the tuning range. I'm sure, though, that there's a limit to how far the *Q* of the bifilar transformer can be increased without loss of regeneration control.—*Bill Young, WD5HOH, 343 Forest Lake Dr, Seabrook, TX 77586;* **blyoung@hal-pc.org** □□

QEX

QEX Subscription Order Card

ARRL
225 Main Street
Newington, CT 06111-1494 USA

QEX, the Forum for Communications Experimenters is available at the rates shown at left. Maximum term is 6 issues, and because of the uncertainty of postal rates, prices are subject to change without notice.

For one year (6 bi-monthly issues) of **QEX**:

In the US
- ☐ ARRL Member $24.00
- ☐ Non-Member $36.00

In the US by First Class mail
- ☐ ARRL Member $37.00
- ☐ Non-Member $49.00

Elsewhere by Surface Mail
(4-8 week delivery)
- ☐ ARRL Member $31.00
- ☐ Non-Member $43.00

Canada by Airmail
- ☐ ARRL Member $40.00
- ☐ Non-Member $52.00

Elsewhere by Airmail
- ☐ ARRL Member $59.00
- ☐ Non-Member $71.00

Subscribe toll-free with your credit card **1-888-277-5289**

☐ Renewal ☐ New Subscription

Name_________________________ Call ____________

Address_________________________________

City_______________ State or Province ________ Postal Code __________

☐ Payment Enclosed to ARRL

Charge:

☐ MasterCard ☐ VISA ☐ American Express ☐ Discover

Account #____________________________ Good thru________

Signature________________________ Date__________

Remittance must be in US funds and checks must be drawn on a bank in the US.
Prices subject to change without notice.

06/01